The influence of fold and fracture development on reservoir behavior of the Lisburne Group of northern Alaska

Fifth semi-annual report

Reporting period: June, 2001 to January, 2002

Principal investigator
Wesley K. Wallace

Co-principal investigators:
Catherine L. Hanks
Jerry Jensen[1]
Michael T. Whalen

Other contributors:
Joseph Brinton
Thang Bui[1]
Michelle M. McGee

Report date: September, 2003

Department of Energy Award DE-AC26-98BC15102

Submitting organization:
Geophysical Institute
University of Alaska
Fairbanks, Alaska
99775-5780

[1]**Department of Petroleum Engineering and Department of Geology and Geophysics, Texas A&M University, College Station, Texas 77843-3116**

10/14/03

Disclaimer

Abstract

The Carboniferous Lisburne Group is a major carbonate reservoir unit in northern Alaska. The Lisburne is detachment folded where it is exposed throughout the northeastern Brooks Range, but is relatively undeformed in areas of current production in the subsurface of the North Slope. The objectives of this study are to develop a better understanding of four major aspects of the Lisburne:

1. The geometry and kinematics of detachment folds and their truncation by thrust faults.
2. The influence of folding on fracture patterns.
3. The influence of deformation on fluid flow.
4. Lithostratigraphy and its influence on folding, faulting, fracturing, and reservoir characteristics.

The Lisburne in the main axis of the Brooks Range is characteristically deformed into imbricate thrust sheets with asymmetrical hangingwall anticlines and footwall synclines. In contrast, symmetrical detachment folds characterize the Lisburne in the northeastern Brooks Range. The Continental Divide thrust front separates these different structural styles in the Lisburne and also marks the southern boundary of the northeastern Brooks Range. Our 2001 field studies were in various locations in the northeastern Brooks Range, as well as in the vicinity of Porcupine Lake, immediately south of the Continental Divide thrust front.

The Wachsmuth, Alapah, and Wahoo Formations of the Lisburne Group were described in detail in five partial stratigraphic sections measured in the Porcupine Lake area during the summer of 2001. The Wachsmuth Limestone includes a crinoid limestone member, a middle member, and a banded limestone member and appears to be gradational with the underlying Kayak Shale and overlying lower Alapah. The lower Alapah is resistant and light colored, the middle Alapah is darkest-colored and recessive, and the upper Alapah is resistant and lithologically similar to the Wahoo Limestone in the north. Cycles in the Alapah shallow upward from mudstones or wackestones to packstones, grainstones, or rudstones. The Wahoo Limestone is thin in the study area due to non-deposition or, more likely, to subsequent erosion associated with formation of the unconformity beneath the overlying Sadlerochit Group.

Field work during the summer of 2001 documented several characteristics of the upright and symmetrical detachment folds in the Lisburne of the northeastern Brooks Range, north of the Continental Divide thrust front. Where shortening is relatively low, multiple closely spaced folds form local culminations that likely reflect amplification at the preferred wavelength of the entire competent unit. Where shortening is moderate to high, folds typically display an upward decrease in parasitic folding and in the amount of shortening apparently accommodated by folding. This likely reflects an overall upward increase in competency and suggests an upward increase in the proportion of shortening that is accommodated by layer-parallel shortening. In one place, a fold that has been truncated and displaced by a thrust fault displays a geometry very similar to that of the thrust-truncated asymmetrical folds south of the Continental Divide thrust front. Typical upright and symmetrical detachment folds that have not been cut by thrust faults exist in the same mechanical stratigraphy nearby.

Field work in the Porcupine Lake area during the summers of 1999 to 2001 identified several characteristics typical of the thrust-truncated asymmetrical folds in Lisburne south of the

Continental Divide thrust front. The dominant structures are asymmetrical anticlines that have been cut and displaced over thrust faults. Forelimbs typically are overturned to the north and commonly are thickened by parasitic folding and minor bulk strain. Hinge zones commonly display minor thickening, especially in less competent intervals. Thrust faults follow bedding low within or below the lowermost Lisburne in backlimbs and cut across forelimbs at a high angle. The geometry of thrust-truncated anticlines commonly has been modified by gentle antiformal folding of the underlying thrust faults. Fold asymmetry likely is the critical characteristic that accounts for the folds south of the Continental Divide thrust front being broken through by thrust faults, in contrast with the unbroken upright and symmetrical detachment folds to the north.

The distribution, character and relative age of fractures in detachment-folded rocks of the Lisburne Group and the overlying Sadlerochit Group provide important clues to the thermal and deformational sequence in the northeastern Brooks Range. Paleo-thermal indices in the host rock limit the conditions of folding to temperatures $\leq$280°C, but field and petrographic relationships suggest that different fracture sets formed at different times during the deformational history of the rocks. These rocks probably initially entered the oil generation window (100-150°C) during Early Cretaceous formation of the Colville basin due to thrust loading by the Brooks Range to the south. Regional fractures formed at this time as a result of high pore fluid pressures and low in situ differential stresses. These rocks began to experience shortening related to the advancing northeastern Brooks Range fold-and-thrust belt at ~80 Mybp. Early phases of detachment folding were by flexural slip, with associated fracturing. Continued shortening and growth of detachment folds resulted in structural thickening and deeper burial of the bottom portion of the deforming wedge. Early fold-related fractures were overprinted by penetrative strain during peak folding at temperatures $\leq$280°C. Continued shortening resulted in uplift and unroofing, and late fold-related fractures formed at ~150°C. Subsequent uplift of the thickened wedge through 60°C occurred after 25 Mybp. Late pervasive extension fractures formed at relatively shallow depths and low temperatures because of unroofing and/or regional stresses and overprinted all the earlier fractures and penetrative structures.

Field evidence and statistical analysis suggest that a significant population of fractures formed either late during or after detachment-folding of Lisburne Group carbonates. Both pre-fold fractures and penetrative strain associated with peak folding are overprinted by late- and post-fold fractures. The late-fold fractures strike parallel to fold axes and are consistently overprinted by pervasive late extension fractures that strike perpendicular to fold axes. Both the late- and post-fold fracture sets have similar average and median spacing. Statistical analysis of fold interlimb angle and fracture spacing indicates that the spacing of both fracture sets increases by a factor of two to three and becomes slightly more variable as the folds tighten. This is opposite from what is expected if the fractures were closely related to folding and suggests that the two sets are similar to each other and only weakly affected by the folding. The weak genetic relationship between folding and formation of the most obvious and open fractures serves as an important example with major consequences for reservoir modelling. Complex genetic and timing relationships between fractures and folds may result in several fracture sets, each having different characteristics. Unless recognized, genetically disparate fractures may be combined into one or a few sets to produce a reservoir model with fracture properties that do not apply to any of the sets. This could result in inappropriate wellbore placement or inaccurate productivity and recovery estimates.

Table of contents

List of figures

Part A: Introduction and geologic setting

Part B: Baseline stratigraphy of the Lisburne Group

Part C: Characteristics of detachment folds and thrust-truncated asymmetrical folds in the eastern Brooks Range

List of tables

Introduction and geologic setting

by Wesley K. Wallace, Geophysical Institute and Department of Geology and Geophysics, University of Alaska, Fairbanks, Alaska 99775-5780

Definition of problem and objectives

Carbonate rocks of the Carboniferous Lisburne Group are found throughout a vast region of northern Alaska, including the subsurface of the North Slope and the northern Brooks Range. The Lisburne is a major hydrocarbon reservoir in the North Slope: It was the original target at Prudhoe Bay and is the reservoir currently producing in the Lisburne oil field. Folded and thrust-faulted Lisburne has been a past exploration target in the foothills of the Brooks Range, and is becoming increasingly important as interest grows in exploration for gas. It also is an important potential future target for oil and gas exploration in the coastal plain of the Arctic National Wildlife Refuge (1002 area). However, relatively little is known about the reservoir characteristics and behavior of the Lisburne and how they change as a result of deformation.

As in many carbonate reservoirs, most of the hydrocarbon production from the Lisburne Group is from naturally occurring fractures. Natural fractures play an essential role in production from the reservoir, but the geologic factors that control the origin, distribution, and character of these fractures are poorly understood. In the Lisburne oil field, less than 10% of the 2 billion barrels in place is recoverable at the present time. A clearer understanding of the nature and origin of these fractures has the potential to aid in the development of secondary and tertiary recovery programs for a reservoir that is large but difficult to produce.

Likely targets for exploration in the Lisburne are along the northern edge of the Brooks Range orogen, where the Lisburne has been modified by fold-and-thrust deformation. Such deformation has long been recognized both to enhance porosity and permeability, largely through the formation of fractures, and to reduce them by compression, as reflected by the formation of cleavage and stylolites. However, the ability to predict patterns of enhancement or reduction in porosity and permeability and how they vary within a particular fold trap remain quite limited. Recent rapid advances in the understanding of the geometry and kinematics of different types of folds that form in fold-and-thrust settings offer great potential to improve the systematic understanding of enhancement or reduction in porosity and permeability in fold traps, but these advances have only begun to be applied.

The Lisburne Group is a structurally competent unit that overlies an incompetent unit. Hence, the Lisburne undergoes a progressive evolution as shortening increases, from its undeformed state, to tightening detachment folds, to detachment folds that either continue to tighten or are truncated by thrust faults, depending on whether they are symmetrical or asymmetrical. How trap geometry and reservoir characteristics vary as this evolution progresses is not systematically understood, particularly with respect to differences in lithology and position within a fold. The basic objective of this study is to document and develop predictive models for structurally induced changes in reservoir geometry and characteristics at different stages in the evolution of detachment folds in the Lisburne Group.

Extensive exposures of the Lisburne Group in the northeastern Brooks Range fold-and-thrust belt

offer the opportunity to develop a clearer understanding of the origin, distribution, and character of structurally induced enhancement and reduction of porosity and permeability in the Lisburne Group. Detachment folds in the Lisburne Group have evolved to different degrees, and thus provide a series of natural experiments in which to observe those structures and to develop models both for their formation and for the resulting patterns of enhancement and reduction of porosity and permeability. The results of these field-based observations and models can then be used to develop quantitative models for characterization of Lisburne reservoirs and the fluid flow within them. Such models can be applied to a spectrum of traps from relatively undeformed to highly folded and thrust faulted.

This study of the Lisburne Group has the following major objectives:

- Establish 'baseline' reservoir characteristics in a relatively undeformed section and develop fracture and fluid flow models and a wellbore placement strategy in such reservoir.
- Document the evolution of trap-scale fold geometry with increasing shortening, with emphasis on changes in thickness across the fold and with respect to mechanical stratigraphy.
- Characterize the differences between folds that continue to shorten by tightening vs. those that are cut by thrust faults as shortening increases.
- Determine patterns in reservoir enhancement and destruction within a fold trap as a function of mechanical stratigraphy and of position within folds at different stages of evolution.
- Use observations of natural folds to constrain predictive models for the evolution of trap-scale fold geometry with increasing shortening and for the resulting modifications of reservoir characteristics.
- Use observations of natural folds and predictive fold models as a basis for fracture models for fluid flow and wellbore placement strategies in fold traps.

The results of this study will apply to current production in relatively undeformed Lisburne and to future exploration in deformed Lisburne. At least as important is the fact that the results will apply generally to carbonate reservoirs and to folded reservoirs, both of which are major producers and exploration targets worldwide.

Scope of this report

This report summarizes preliminary results of this project's third season of field work, which was conducted during the summer of 2001. The report presents field observations and preliminary analysis reflecting progress to January, 2002. Results of data compilation, analysis, and interpretation for all three seasons of field work will be presented in the final report.

Direct participants in this report include two Master's students (J. Brinton, T.D. Bui), a Ph.D. student (M.M. McGee), three University of Alaska faculty (W.K. Wallace, C.L. Hanks, and M.T. Whalen), and one Texas A & M faculty (J.L. Jensen). Some results are also included from four other Master's students that participated in this project (P.K. Atkinson, M.A. Jadamec, A.V. Karpov, and J.R. Shackleton).

The report consists of five chapters that each summarize a different aspect of the study and are written by different authors. These include:

- A. Introduction and geologic setting, by W.K. Wallace
- B. Baseline stratigraphy of the Lisburne Group, by M.M. McGee and M.T. Whalen

•C. Characteristics of detachment folds and thrust-truncated asymmetrical folds in the eastern Brooks Range, by W.K. Wallace

•D. Fracture paragenesis in detachment folded Lisburne Group: Implications for the thermal and structural evolution of the northeastern Brooks Range, Alaska, by C. L. Hanks, T.M. Parris, and W. K. Wallace

•E. Folded Lisburne Group fracture distribution and flow modeling, by T.D. Bui, J. L. Jensen, J. Brinton, and C. L. Hanks

Geologic Setting

The Lisburne Group is the most abundant and widely distributed rock unit in the northern Brooks Range, where it forms the range front in most places and extends a significant distance southward into the range. This rock unit displays two distinct structural styles in different parts of the northern Brooks Range. Imbricately stacked thrust sheets characterize the Lisburne south of the range front in the western and central Brooks Range and south of the projection of that range front into the eastern Brooks Range. These thrust sheets commonly display asymmetrical hangingwall anticlines and footwall synclines, but only rare asymmetrical folds that have not been cut by thrust faults. In contrast, the northeastern Brooks Range is characterized by symmetrical detachment folds that are only rarely cut by thrust faults. The "Continental Divide thrust front" marks the boundary between these two structural styles (Figures 1 and 2) (Wallace and Hanks, 1990; Wallace, 1993).

Folds have formed both north and south of the Continental Divide thrust front in the competent Mississippian to Pennsylvanian Lisburne Limestone above the incompetent Mississippian Kayak Shale. The Lisburne is overlain by another incompetent unit that consists dominantly of shale and sandstone, the Permian to Triassic Sadlerochit Group.

North of the Continental Divide thrust front, in the northeastern Brooks Range, the Kayak forms the roof thrust for a duplex of horses formed in the underlying basement rocks (Wallace and Hanks, 1990; Wallace, 1993). In the western part of the northeastern Brooks Range, thrust spacing is sufficiently greater than displacement so that individual fault-bend anticlines are separated by synclines. These folds are an order of magnitude larger than the upright and symmetrical detachment folds within the cover and are superimposed on the overlying cover to form anticlinoria and synclinoria (Figures 1 and 2). The detachment folds generally reflect the greatest shortening in the synclinoria, although significant shortening has also occurred over some anticlinoria. A general decrease in detachment fold shortening is evident to the north, approaching the range front, but shortening still displays considerable local variation.

By contrast, south-dipping imbricate thrust sheets dominate the structural style south of the Continental Divide thrust front (Figures 1 and 2). Asymmetrical hangingwall anticlines and footwall synclines commonly characterize the leading and trailing edges, respectively, of these thrust sheets. These folds are interpreted to be asymmetrical detachment folds that have been broken through by thrust faults (Wallace, 1993; Wallace et al., 1997; Wallace and Homza, in press). This interpretation is based on an apparent transition from the detachment folds of the northeastern Brooks Range and the local preservation of unbroken detachment folds south of the boundary. The change in structural style across the Continental Divide thrust front coincides with the dramatic southward thickening of a clastic succession beneath the Kayak Shale and the

disappearance of basement-cored anticlinoria as a major influence on the structure of the cover.

A regional structural low in the Porcupine Lake area (Figures 1 and 2) provides a particularly good location to study rocks and structures that span the Continental Divide thrust front. Thrust-truncated asymmetrical folds are especially well exposed along a local range front that bounds the structural low to the south. This local range front likely represents an eastward remnant of the Paleocene range front of the central Brooks Range that was preserved following Eocene and later formation of the northeastern Brooks Range to the north.

References

Imm, T.A., Dillon, J.T., and Bakke, A.A., 1993, Generalized geologic map of the Arctic National Wildlife Refuge, northeastern Brooks Range, Alaska: Alaska Division of Geological and Geophysical Surveys Special Report 42, scale 1:500,000, 1 sheet.

Wallace, W.K., 1993, Detachment folds and a passive-roof duplex: Examples from the northeastern Brooks Range, Alaska, in Solie, D.N., and Tannian, F., eds., Short Notes on Alaskan Geology 1993: Alaska Division of Geological and Geophysical Surveys Geologic Report 113, p. 81-99.

Wallace, W.K., and Hanks, C.L., 1990, Structural provinces of the northeastern Brooks Range, Arctic National Wildlife Refuge, Alaska: American Association of Petroleum Geologists Bulletin, v. 74, no. 7, p. 1100-1118.

Wallace, W.K., and Homza, T.X., in press, Detachment folds, their truncation by thrust faults, and their distinction from fault-propagation folds, in McClay, K.R., editor, Thrust tectonics and petroleum systems: American Association of Petroleum Geologists Memoir.

Wallace, W.K., Moore, T.E., and Plafker, G., 1997, Multistory duplexes with forward dipping roofs, north central Brooks Range, Alaska: Journal of Geophysical Research, v. 102, no. B9, p. 20,773-20,796.

Figure 1. Map of western part of northeastern Brooks Range. Symmetrical detachment folds are formed in Lisburne Limestone above the Kayak Shale north of the Continental Divide thrust front. Asymmetrical folds that have been cut by thrust faults are formed in Lisburne Limestone above the Kayak Shale south of the Continental Divide thrust front. EMA = Endicott Mountains allochthon. Map based on Imm et al., 1993; Wallace, 1993; and Wallace et al., 1997.

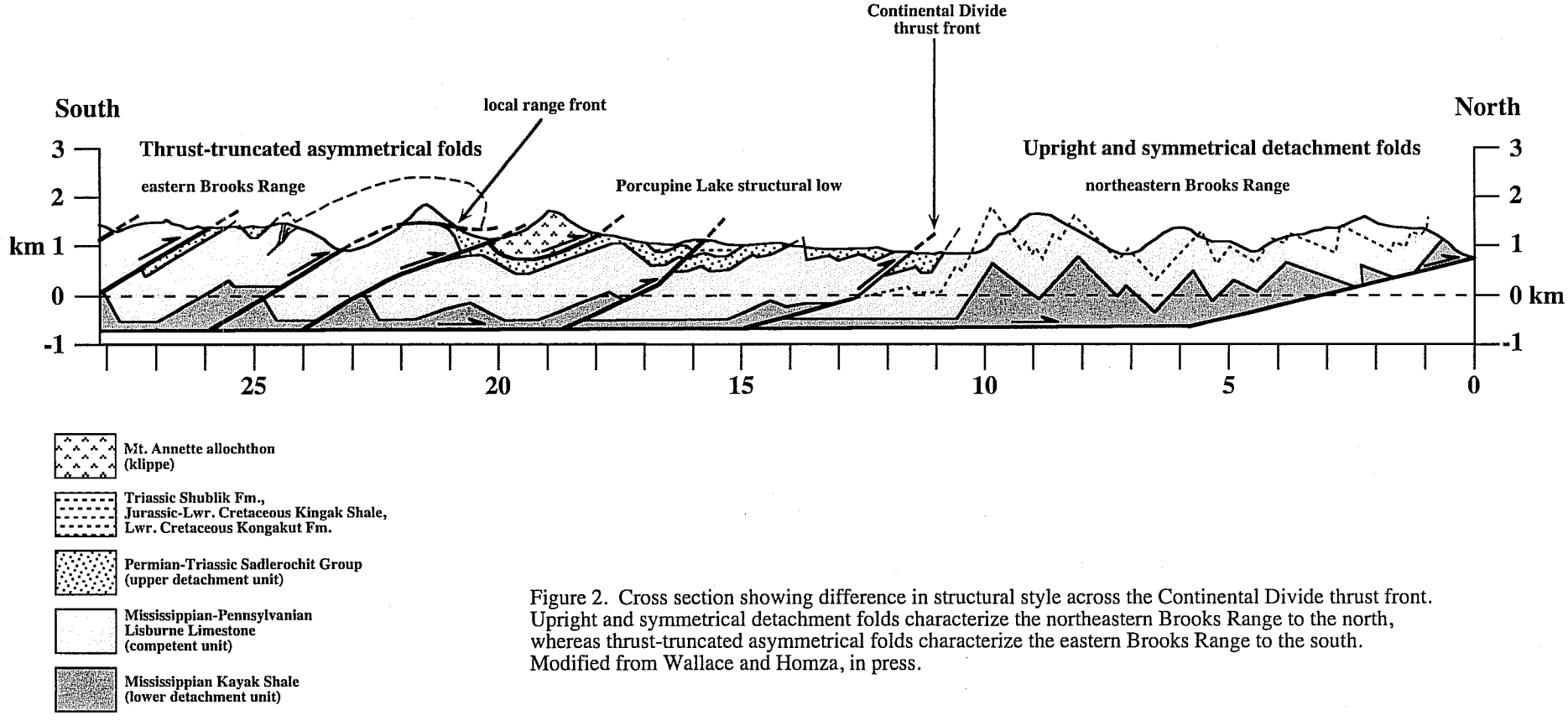

Figure 2. Cross section showing difference in structural style across the Continental Divide thrust front. Upright and symmetrical detachment folds characterize the northeastern Brooks Range to the north, whereas thrust-truncated asymmetrical folds characterize the eastern Brooks Range to the south. Modified from Wallace and Homza, in press.

Baseline stratigraphy of the Lisburne Group

By Michelle M. McGee and Michael T. Whalen, Geophysical Institute and Department of Geology and Geophysics, University of Alaska, Fairbanks, Alaska 99775-5780

ABSTRACT

Further progress has been made on establishing the baseline stratigraphy of the Lisburne Group in the northeastern Brooks Range. This report focuses on the 2001 summer field results from the Porcupine Lake Valley area, Philip Smith Mountains. Five partial stratigraphic sections in the Wachsmuth, Alapah, and Wahoo were described in detail.

The Wachsmuth limestone was previously subdivided into a crinoid limestone member, middle member, and a banded limestone member based on facies and weathering profiles (Bowsher and Dutro, 1957; Brosgé et al., 1962) and we have identified all three informal members in the field area. The Wachsmuth is best exposed in the Marsh Fork area and appears to be gradational with the underlying Kayak Shale and overlying lower Alapah. The lower Alapah is resistant and light colored. The middle Alapah is darkest colored and recessive. The upper Alapah is resistant and lithologically similar to the Wahoo Limestone in the north. Cycles in the Alapah, overall, shallow up from mudstones or wackestones to packstones, grainstones, or rudstones. Based on 2000 and 2001 field results, several parasequences were identified in the upper middle Alapah and upper Alapah. A thin package of Wahoo Limestone overlain by the Sadlerochit Group was identified in the field area. The thin Wahoo Limestone may be due to non-deposition, but is more likely the result of subsequent erosion associated with unconformity development.

OBJECTIVE

The goals of this phase of the research project are to establish a "baseline" for Lisburne reservoir characteristics in relatively undeformed rocks using surface and subsurface data. The goals of this portion of the project are being met through a multi-phase approach to stratigraphic data collection to insure the development of a comprehensive database for establishing the stratigraphic baseline. The multi-phase approach includes collection of high-resolution lithostratigraphic data, petrographic, mineralogic, and X-ray diffraction data, and outcrop spectral gamma ray profiles and comparable subsurface geophysical logs. Progress on the baseline stratigraphic study includes acquisition of outcrop lithologic data from distal portions of the Lisburne Group in the Philip Smith Mountains.

METHODS

During the summer of 2001, high-resolution lithostratigraphic data were collected from five partial stratigraphic sections in the north and south Porcupine Lake area, Philip Smith Mountains (Figure 1) by Michelle McGee with assistance from Mike Whalen, Andrea Krumhardt, Margarete Jadamec, and Jessica Shannahan. Sections include North

Porcupine (NP), West Fork (WF), North Fork (NF), completion of East Fork 2 (EF2 – 2000 field season), and Marsh Fork 3 (MF3). Sections were measured at meter intervals using a Jacob staff. One fist-sized hand sample was collected at meter or smaller intervals. One four to five kilogram conodont sample was collected every ten to twenty meters. Detailed sedimentologic descriptions included: depositional fabrics, identification of dolomitized intervals, sedimentary structures, bed thickness, lithologic contrasts, paleontologic content, chert content, and ichnofabric.

All hand samples collected will be cut and select samples will be thin sectioned and stained for calcite (Alizarin Red S). X-ray diffraction will be completed on samples containing calcite and dolomite to determine percentages of each. Petrographic analysis will be completed to determine reservoir properties, such as primary and secondary porosity. Point counting will quantitatively identify skeletal and other sedimentary grains, matrix, pores, voids, cements, and compaction features. Conodont samples will be crushed, processed in glacial acetic acid, subjected to heavy mineral separation, picked, and identified. Conodonts will be used in biostratigraphy and will aid in the identification of the Mississippian-Pennsylvanian boundary.

Data analysis will include identification of depositional cycles and parasequences, construction of cross-sections, and correlations between Prudhoe Bay cores and outcrop. Depositional cycles and unconformities will be used to classify units that are genetically similar. Cross-sections will be used to identify vertical variations of lithology and changes in reservoir properties. Correlations between subsurface and surface will delineate package geometries, lateral changes of lithology and reservoir characteristics, and paleogeography across the broad carbonate platform.

STRATIGRAPHIC SECTIONS

Five partial stratigraphic sections were measured during the 2001 summer field season. Section descriptions are discussed in order of northern-most to southern-most. Figure 2 is the key to the stratigraphic sections. Table 1 summarizes outcrop data from 2000 and 2001 field season. Table 2 summarizes unit thicknesses for each measured stratigraphic section from 2000 and 2001. Table 3 summarizes unit boundaries for each 2000 and 2001 measured section. 2001 section abbreviations are as follows: NP = North Porcupine, WF = West Fork, NF = North Fork, EF2 = East Fork 2, and MF3 = Marsh Fork 3.

Sections have been measured in three separate field areas. The northern most field area is north of Porcupine Lake and will be identified as the North field area. Section NP is the only section from this area. The Forks field area is southeast of the north field area and includes sections WF, FC, NF, FW, EF, and EF2. Sections MF, MF2, and MF3 are in the Marsh Fork field area, which is approximately 16 km southeast of the Forks area.

SECTION NP

Section NP is in the North field area and is the northern-most section completed (Figure 1). Section NP (Figure 3) was measured on a limb of a syncline. Bedding planes were wavy and the Lisburne Group was almost entirely recrystallized as a result of

tectonic activity. Purple fluorite was observed intermittently between 26 and 32 m. Stylolites with concentrations of red iron oxides were abundant throughout the section. NP is one of four (NF, FW, EF2) measured sections where the Sadlerochit Group is exposed above the Lisburne.

Approximately 44 m of lower Wahoo (?) overlain by 3 m of Sadlerochit Group was measured at section NP. The section appears to be cyclic with cycles approximately 0.25 to 0.5 m thick with shale or wackestone bases coarsening upward into packstones and grainstones. Depositional textures were difficult to determine due to a sugary texture interpreted to have resulted from recrystallization. Petrographic analysis will be needed to determine original depositional fabric.

Between 40 m in the section and the unconformity at 44 m, is a massive crinoid rudstone. The overlying unconformity is wavy and is overlain by a 2.5 cm thick recessive interval, which at one time may have been a thin paleosol.

SECTION WF

Section WF (Figures 4 and 5) is approximately 6.4 km southeast of NP (Figure 1) and contains 402 m of Lisburne carbonates. The section is located on a down-dropped block of a normal fault. The base of the Lisburne is not exposed but the lower contact appears to be in thrust contact with the younger Sadlerochit Group. Section WF is also approximately 10 km south of the edge of the Cretaceous Mt. Annette klippe. Between 0 and approximately 50 m in the section beds are wavy, discontinuous (pinched out) and very fractured. Fracturing decreases upward throughout the section.

The exposed Wachsmuth is 42 m thick and displays dark and light banding similar to that observed in the banded limestone member in the Marsh Fork field area. The dark bands are shale and/or chert and the light bands are limestone. The dark and light banding ends at 42m (Wachsmuth-Lower Alapah contact). Most of the Wachsmuth is made up of massive wackestones with few rare centimeter-thick black shales. Crinoids and bryozoans are the major faunal elements, while syringoporid corals are rare. Bedding appears to have been distorted or destroyed by tectonic activity.

The lower Alapah is 115 m thick, light colored, and resistant. Between 42 and 49 m in the section are cyclic packages measuring 0.5 to 1.0 m thick and have shale bases that coarsen upward into crinoid-bryozoan packstones. Above 49 m to 83 m cycles are 0.25 to 0.5 m thick with wackestone coarsening to crinoid packstone with rare bryozoans, brachiopods, and solitary rugose, syringoporid and tabulate corals. Rare cycles coarsen-up to grainstones or rudstones. Between 83 and 157 m cycles become 5 to 30 m thick. Crinoids and bryozoans are the most abundant fauna. Tabulate corals are a minor faunal component with rare brachiopods and ramose bryozoans. Nodular, lenticular, and "bedded" chert are abundant throughout the lower Alapah.

The middle Alapah is 67 m thick, dark colored, and recessive. Between 157 m and 224 m in the section cycles are 0.25 to 0.5 m thick with shale bases coarsening into crinoid-bryozoan packstone or crinoid-bryozoan grainstone. Brachiopods are a minor faunal component and gastropods were rare. Nodular and lenticular chert increased in abundance near the top of the unit. The 0.25 to 0.5 m cycle interval gave the outcrop a "stair-step" appearance.

The upper Alapah is 180 m thick, light colored, and resistant. Upper Alapah cycles are typically 3 to 15 m thick and coarsen-up from wackestone to packstone, grainstone, or rudstone. Crinoids and fenestrate bryozoans are the most abundant faunal elements throughout the unit. Brachiopods are a minor faunal element while solitary rugose and tabulate corals and gastropods are rare. Between 224 and 226 m, large articulated brachiopods (up to 10 cm across) that appear to have been transported occur in 0.13 m thick beds every 0.5 m. Between 245 and 247 m, 2-3 cm diameter articulated brachiopods grade into intact disarticulated shells, which grade into shell fragments. Nodular to lenticular chert is abundant between 251 and 278 m. Facies become coarser grained above 271 m. A "bed" of nodular and lenticular black chert exists between 377.5 and 378 m. The chert is interbedded with rudstones above and below. The nodular nature of the bed distorts (wavy) the upper and lower contacts. A similar chert interval exists in sections NF and EF2.

SECTION NF

Section NF (Figure 6) is 1.7 km south of section WF (Figure 1), is 140 m thick, and is one of four (NP, FW, and EF2) measured sections where the Sadlerochit Group is exposed above the Lisburne. The section is very similar to WF and will not be described in great detail. NF is also one of three (WF and EF2) sections to contain a 0.5 m thick nodular and lenticular black chert "bed". The lower Wahoo was rubbly and completely covered. The lower Wahoo-Sadlerochit Group contact was identified based on the last appearance of gray limestone and the first appearance of red shale.

SECTION EF2

Section EF2 is 3.4 km to the southeast of NF (Figure 1). The first 320 m of this section were completed during the 2000 field season and were reported in McGee and Whalen, 2001. The remaining 189 m are described below and illustrated in Figure 7. EF2 is one of four (NP, NF, and FW) stratigraphic sections where the Sadlerochit Group is exposed above the Lisburne.

The entire EF2 section (2000 and 2001) is 509 m thick with 32 m of Wachsmuth banded limestone member, 111 m of lower Alapah, 71 m of middle Alapah, 262 m of upper Alapah, and 33 m of lower Wahoo. It is one of three sections (WF and NF) to contain a 0.5 m nodular and lenticular black chert "bed". Only the upper Alapah (above 320 m) and lower Wahoo will be discussed in this report.

The upper Alapah is light colored and resistant. The upper Alapah is a relatively homogeneous fine-grained wackestone between 320 and 374 m and then coarsens upward to grainstone and rudstone above 374 m up to the upper Alapah-lower Wahoo contact at 476 m. The "bed" of nodular and lenticular black chert was identified between 410 and 410.5 m in the section.

The lower Wahoo was rubbly and completely covered. The lower Wahoo-Sadlerochit Group contact was identified based on the last appearance of gray limestone and the first appearance of red shale.

SECTION MF3

Section MF3 (Figure 8) is 15.8 km southeast of Section EF2 (Figure 1). The stratigraphic succession at MF3 is similar to sections MF and MF2 reported in the McGee and Whalen, 2001.

The Wachsmuth is 161 m thick and subdivided into a middle member (0 to 102 m) and a banded member (102 to 161 m; Figure 9). The middle member is cyclic with cycles 0.25 to 6 m thick. They coarsen upward from wackestone or rarely shale to crinoid grainstone or locally rudstone. Crinoids and rare fenestrate bryozoans are major skeletal grains and solitary rugose corals, syringoporid corals, and brachiopods are minor faunal components. Black nodular, lenticular, and "bedded" chert are abundant between 0 and 26.5 m. A channel-shaped feature filled with blocky calcite was observed between 19 and 23 m (Figure 9). A 2 cm thick black shale with minor blocky calcite overlies the blocky calcite.

The banded member is also cyclic, with 0.25 to 0.5 m thick cycles that grade from a shale base into crinoid grainstone. Cycles become thicker and coarser grained upward through the section. Crinoids and fenestrate bryozoans are major components. Brachiopods, solitary rugose corals, and gastropod are minor components. Between 129 and 139 m, fenestrate bryozoans are the major faunal element. Two thick black shales and several thin shales were observed near the top of the banded Wachsmuth. The thick shales occur between 139 and 140.25 m and 148 and 149 m. Chert is abundant between 100 and 107 m, 117 and 123.5 m, and 129 and 140 m. The Wachsmuth above 155 m is darker colored and slightly more recessive. Cycles are 0.25 to 0.5 m thick with shale bases coarsening to crinoid rudstone with a minor solitary rugose coral component. Most coral fragments are found in the rudstones.

OBSERVATIONS AND INTERPRETATIONS

The results of the 2001 summer field season have increased our understanding of the Lisburne Group. Observations and interpretations are based on high-resolution lithostratigraphic data from the 2000 and 2001 field seasons. Brosge, et al. (1962) subdivided the Lisburne Group into the Wachsmuth, Alapah, and Wahoo limestones. Bowsher and Dutro (1957) further subdivided the Wachsmuth into a crinoid limestone member, a middle member, and a banded limestone member. The crinoid limestone member is described as crinoid-rich medium to coarse-grained limestone, fine grained limestone, and shaly to nodular limestone 40 to 78 m thick (Bowsher and Dutro, 1957; Brosgé et al., 1962). The middle member is 126 m thick, dark gray, fine grained, cherty limestone (Bowsher and Dutro, 1957; Brosgé et al., 1962). The banded limestone member has alternating beds of fine and medium grained limestone or laminated chert and is 35 to 52 m thick (Bowsher and Dutro, 1957; Brosgé et al., 1962).

Throughout the field areas, the Lisburne is 820 m thick. We can recognize Bowsher and Dutro's (1957) tripartite subdivision of the Wachsmuth but an entirely complete section of Wachsmuth has not been identified in the field area. We have informally subdivided the Alapah Formation into lower, middle, upper members and we have recognized a thin lower Wahoo Formation based on lithofacies and weathering profiles (Figures 5, 9, and 10). The lowermost Wahoo crops out in the field area as thin

In the Forks area, the banded member is also cyclic but facies are coarser grained, have abundant large colonial rugose corals, and have significantly less chert (especially "bedded" chert). The rock weathers tan-brown to gray and is dark gray on a fresh surface. The cycles described in the lower half of the banded member in the Forks area are 2 to 4 m thick with abundant crinoids and fenestrate bryozoans and minor colonial corals, brachiopods, solitary rugose corals, and rare gastropods. Chert is lenticular to nodular. Cycles in the upper half of the unit are 0.25 to 0.5 m thick with basal shales typically draping colonial corals or coarsening up into crinoid-bryozoan-coral grainstone.

Overall, the faunal components and facies of the Wachsmuth indicate that it represents the initiation of carbonate deposition in a deep ramp environment that was below fair weather wave base. Progressively coarsening upward cycles indicate a progradational facies stacking pattern. In the Marsh Fork area, the Wachsmuth is finer grained and significantly chertier probably indicating a slightly deeper depositional setting.

The lower Alapah overlies the Wachsmuth, is 100 to 115 m thick, and is relatively resistant. The lower Alapah also displays significant lateral variations between the Forks and Marsh Fork field areas. Section WF offers the most complete description in the Forks area. Section EF2 is similar to WF, but has numerous covered intervals.

The lower Alapah contains medium bedded, 0.5 to 1.0 m thick cycles with shale bases coarsening up to packstone. Crinoids and fenestrate bryozoans are common faunal elements with less abundant brachiopods and syringoporid and tabulate corals. Bedding thickness then decreases to 0.25 to 0.5 m with rare meter thick rudstones. In the middle of the unit, bedding becomes thicker than 1.0 m and coarser grained (packstone to grainstone). Crinoids and fenestrate bryozoans are the most abundant faunal components with several intervals of abundant tabulate and lithostrotionoid corals and rare brachiopods and solitary corals. A meter thick interval with ramose bryozoans was observed near the top of the unit.

Only 43 m of the lower Alapah has been described in the Marsh Fork area, even though the entire section has been observed there. The lower Alapah between the Forks and Marsh Fork areas is remarkably similar. The shales at the base in the Marsh Fork area are less numerous, but thicker than those in the Forks area. The lower Alapah represents shallowing from a moderately deep ramp environment below fair weather wave base into a middle ramp near shoal to shoal environment.

The middle Alapah is approximately 69 m thick, darkest colored, and recessive. The middle Alapah was observed, but not described in the Marsh Fork area. Cycles in the Forks area are 0.25 m thick, recessive, and coarsen up from a shale base to crinoid-wackestone, crinoid packstone, and rarely crinoid grainstone or crinoid rudstone. Crinoids and fenestrate bryozoans are the dominant faunal component. Brachiopods were also observed throughout most of the unit with rare gastropods.

To the south in section EF2, middle Alapah cycles are less pronounced, slightly coarser grained, and have a minor solitary rugose coral and colonial rugose coral component. Calcite replaced evaporites were observed at the middle-upper Alapah contact. The replaced evaporites and the cycle stacking patterns are interpreted to indicate shallowing upward to a shallow subtidal environment.

The 262 m thick upper Alapah is relatively resistant, light in color, and coarser grained than the middle Alapah. The upper Alapah was observed in the Marsh Fork area,

but only described in the Forks area. Upper Alapah facies change laterally over short distances in the Forks area. The lower quarter of the unit is coarse grained with cycles thicker than 1.0 m. Cycle thickness decreases and then increases. Above a 0.5 m dolomite interval (EF2 @ 270 m), the cycles are muddier and significantly thinner. The abundance of black lenticular chert also increases. Once again the cycles become thicker than 1.0 m and eventually coarsen from wackestone with rare rudstone to almost entirely crinoid-bryozoan grainstone or rudstone. Near the top of the upper Alapah the rock becomes silicified (?). Stratal stacking patterns and fauna from the Forks area indicate a change from open to restricted lagoonal environments on a shallow ramp.

A 0.5 m thick "bed" of lenticular and nodular black chert has been documented in the upper Alapah in three sections (WF, NF, and EF2). The chert bed may also exist in section FW (upper part of section was not described because of indeterminable fault displacement). The chert bed distorts bed boundaries and is bounded by crinoid rudstone in all three sections. Besides being a useful marker bed, the significance of the chert bed is not known at this time.

The lower Wahoo is recessive and is unconformably overlain by the Sadlerochit Group. The unit is approximately 30 m thick, appears to thin to the north, and has not been described because it is very recessive and rubbly. The recessive nature of the unit makes it easy to identify in the field. The pre-Upper Permian unconformity that separates the Wahoo from the overlying Sadlerochit Group was either the result of simple erosion subsequent to a Permian drop in relative sea level or due to Permian uplift and related erosion (Watts et al., 1995).

CONCLUSIONS

Significant progress has been made on establishing the baseline stratigraphy of the Lisburne Group. Five partial sections were described in detail from the Porcupine Lake Valley, Philip Smith Mountains during the 2001 summer field season. The Lisburne Group records an initiation of deep-water carbonate ramp sedimentation atop the underlying Kayak Shale. In the field areas, the Lisburne Group can be subdivided into the Wachsmuth, Alapah, and Wahoo Formations. The Wachsmuth is further subdivided into a crinoid limestone member, middle member, and a banded limestone member (Bowsher and Dutro, 1957). The Alapah is informally subdivided into lower middle and upper members however the chronostratigraphic relationship with Alapah members to the north (Watts et al., 1995) remains equivocal. The Wachsmuth members are best exposed in the Marsh Fork area and the Alapah and Wahoo limestones were most accessible in the Forks area.

Lithofacies analysis indicates that the Wachsmuth was deposited in a deep ramp environment below fair weather wave base. Facies of the lower Alapah indicate shallowing into shoal environments. Facies stacking patterns in the middle Alapah are interpreted to indicate transgression followed by shallowing upward from deep ramp to shallow subtidal environments as evidenced by calcite replaced evaporites near the middle-upper Alapah boundary. The fauna and stratal stacking pattern in the upper Alapah indicate continued shoaling and deposition in an open marine environment followed by restricted lagoonal environments on a shallow ramp. Lateral facies changes

within the units suggest that the Forks area was depositionally shallower than the Marsh Fork area and indicate a progressive northward onlap of the Lisburne Group.

RESEARCH PLAN FOR PROJECT COMPLETION

The Lisburne Group presents significant challenges to obtaining high-resolution stratigraphic data in outcrop. The lateral extent (along both strike and dip) of the Lisburne ramp necessitates correlation of spatially distant sections. Outcrop gamma ray profiles of well-exposed sections also appear to be a useful correlation tool although nearly continuous exposure is necessary for this tool to be used effectively. Large-scale weathering patterns that define outcrop exposure are related to the overall mechanical stratigraphy. A fruitful approach to determining overall mechanical stratigraphy involves relating sections measured in the field to outcrop photos or photomosaics (Figures 5, 9, 10). Relating the weathering patterns to lithology will permit further evaluation of the lithologic controls on mechanical stratigraphy. Application of these methods to future studies in the Brooks Range and correlation of outcrop exposures with the subsurface will enhance our understanding of the geologic history of Arctic Alaska and improve our ability to predict the reservoir potential of folded and fractured carbonates.

REFERENCES

Armstrong, A. K., and B. L. Mamet, 1975, Carboniferous biostratigraphy, northeastern Brooks Range, Arctic Alaska, U. S. Geological Survey Professional Paper 884, p. 29.

Bowsher, A. L., and J. T. Dutro, Jr., 1957, The Paleozoic section in the Shainin Lake area, central Brooks Range, Alaska, Exploration of Naval Petroleum Reserve No. 4 and Adjacent Areas, Northern Alaska, 1944-53: Part 3, Areal Geology, U. S. Geological Survey Professional Paper 303 A, B, p. 1-39.

Brosgé, W. P., J. T. Dutro, M. D. Mangus, and H. N. Reiser, 1962, Paleozoic sequence in eastern Brooks Range, Alaska: American Association of Petroleum Geologists Bulletin, v. 46, p. 2174-2198.

Gruzlovic, P. D., 1991, Stratigraphic evolution and lateral facies changes across a carbonate ramp and their effect on parasequences of the Carboniferous Lisburne Group: M. S. thesis, University of Alaska, Fairbanks, 201 p.

Hubbard, R. J., S. P. Edrich, and P. R. Rattey, 1987, Geologic evolution and hydrocarbon habitat of the "Arctic Alaska microplate", *in* I. L. Tailleur, and P. Weimer, eds., Alaskan North Slope Geology, Society of Economic Paleontologists and Mineralogists, Pacific Section, and the Alaska Geological Society, Book 50, p. 797-830.

Jameson, J., 1994, Models of porosity formation and their impact on reservoir description, Lisburne field, Prudhoe Bay, Alaska: American Association of Petroleum Geologists Bulletin, v. 78, p. 1651-1678.

McGee, M. M., and M. T. Whalen, 2001, Baseline stratigraphy of the Lisburne Group, *in* Wallace et al., The Influence of Fold and Fracture Development on Reservoir behavior of the Lisburne Group of Northern Alaska: Department of Energy Fossil Energy Second Semi-Annual Report (DE-AC26-98BC15102), May 2000 – Jan.

2001, National Petroleum Technology Office, U.S. Department of Energy, Tulsa, Oklahoma, p. B1-B7.

Watts, K. F., A. G. Harris, R. C. Carlson, M. K. Eckstein, P. D. Gruzlovic, T. A. Imm, A. P. Krumhardt, D. K. Lasota, S. K. Morgan, J. A. Dumoulin, P. Enos, R. H. Goldstein, and B. L. Mamet, 1995, Analysis of reservoir heterogeneties due to shallowing-upward cycles in carbonate rocks of the Pennsylvanian Wahoo Limestone of northeastern Alaska, Final Report for 1989-1992 (DOE/BC/14471-19), Bartlesville Project Office, p. 433.

Table 1. Summary of 2000 and 2001 outcrop data.

Section	Section Measured	Section Location	Measured Thickness	Thickness/ Stratigraphic Interval	# Lithologic Samples
EF	Summer 2000	N68°43.3', W146°34.9'	105 m	91 m Wachsmuth, 14 m L. Alapah	81
EF2	Summer 2000/2001	N68°43.929', W146°38.099'*	509 m	32 m Wachsmuth, 111 m L. Alapah, 71 m M. Alapah, 262 m U. Alapah, 33 m L. Wahoo, Sadlerochit Group	226 (2000) & 72 (2001) = 290 total
FC	Summer 2000	N68°44.356', W146°38.660'*	135 m	22 m L. Alapah, 110 m M. Alapah, 3 m U. Alapah	94
FW	Summer 2000	N68°44.222', W146°38.191'*	178 m	150 m U. Alapah, 28 m L. Wahoo, Sadlerochit Group	108
MF	Summer 2000	N68°43.130', W146°10.607'*	383 m	206 m Wachsmuth, 124 m L. Alapah, 53 m M. Alapah	295
MF2	Summer 2000	N68°43.109', W146°11.175'*	228 m	136 m Wachsmuth, 92 m L. Alapah	164
MF3	Summer 2001	N68°43'55.2", W146°11'49.9"	161 m	161 m Wachsmuth	152
NF	Summer 2001	N68°44'23.4", W146°37'56.6"	140 m	129 m U. Alapah, 11 m L. Wahoo, Sadlerochit Group	117
NP	Summer 2001	N68°48'18.1", W146°39'54.9"	47 m	44 m L. Wahoo (?), Sadlerochit Group	45
WF	Summer 2001	N68°44'45.5", W146°40'6.5"	402 m	42 m Wachsmuth, 115 L. Alapah, 67 m M. Alapah, 180 m U. Alapah	314
TOTALS:			2553 m	17 m Kayak Shale, 850 m Wachsmuth, 544 m L. Alapah, 301 m M. Alapah, 783 m U. Alapah, 116 m L. Wahoo	968 (2000) + 700 (2001) + 113 (2002) = 1781 total

*Latitude and Longitude determined from DeLorme 3-D TopoQuads map software.

Table 2. Summary of 2000 and 2001 unit thickness for each measured section.

Section	Wachsmuth Thick.	L. Alapah Thick.	M. Alapah Thick.	U. Alapah Thick.	L. Wahoo Thick.	Reaches Sadlerochit?	Have _ m chert bed?
EF	91 m*	14 m*				No	No
EF2	32 m*	111 m	71 m	262 m	33 m	**Yes**	**Yes**
FC**		22 m*	110 m	3 m*		No	No
FW				150 m*	28 m	**Yes**	Maybe***
MF	340 m*	43 m*				No	No
MF2	136 m*	92 m*				No	No
MF3	161 m*					No	No
NF				129 m*	11 m	**Yes**	**Yes**
NP					44 m*(?)	**Yes**	No
WF	42 m*	115 m	67 m	180 m*		No	**Yes**

* Complete unit was not measured.

**Section FC unit thicknesses are questionable. A normal fault was inadvertently crossed one or more times.

***Section FW was not described above 120 m because of indeterminate fault displacement. Section was only measured between 120 and 178 m.

Table 3. Summary of unit contacts for each 2000 and 2001 measured section.

Section	Kayak-Wachsmuth	Wachsmuth-L. Alapah	L.-M. Alapah	M.-U. Alapah	U. Alapah-L. Wahoo	L. Wahoo-Sadlerochit Group
EF		91 m				
EF2		32 m	143 m	214 m	476 m	509 m
FC			22 m	132 m		
FW					150 m	178 m
MF		340 m				
MF2						
MF3						
NF					129 m	140 m
NP						44 m
WF		42 m	157 m	224 m		

Figure 1. Location of stratigraphic sections from 2000 and 2001. Cross-section through A-A' is illustrated in Figure 12. Section abbreviations: NP = North Porcupine, WF = West Fork, FC = Forks Canyon, NF = NorthFork, FW = Forks Wahoo, EF = East Fork, EF2 = East Fork 2, MF3 = Marsh Fork 3, MF2 = Marsh Fork 2, MF = Marsh Fork.

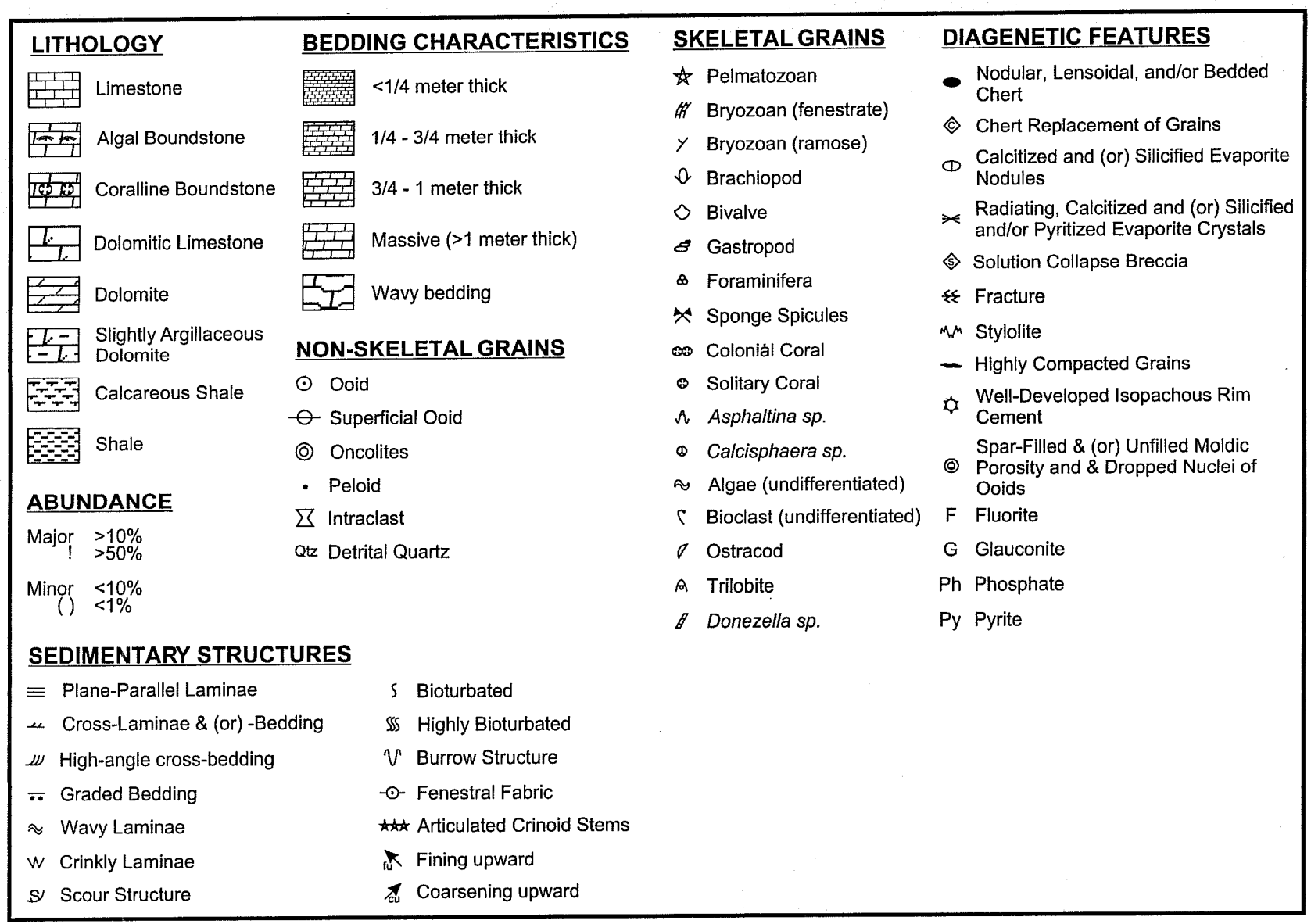

Figure 2. Key to symbols used in measured stratigraphic sections and cores. Modified from Gruzlovic, 1991.

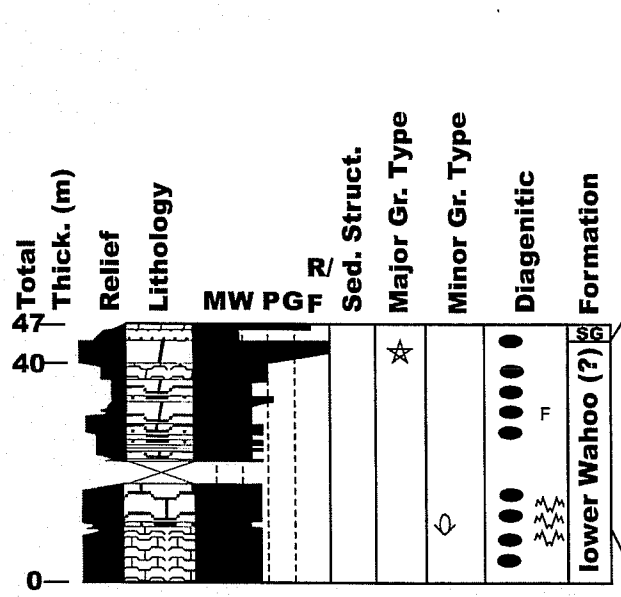

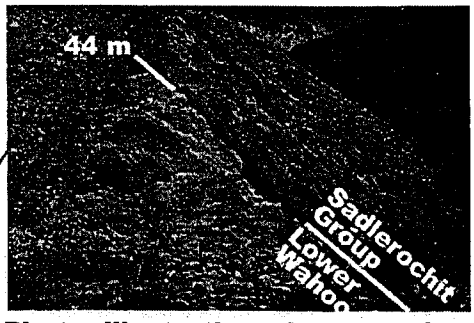

Photo illustrating the top of the section at 47 m. The lower Wahoo (?) is resistant in this section because it has been recrystallized.

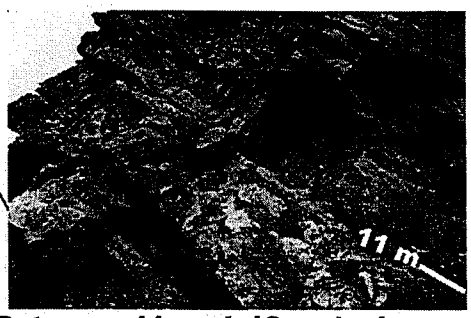

Between 11 and 18 m beds are 0.25 to 0.5 m thick. Cycles have shale bases and coarsen up into packstones with abundant black chert.

Figure 3. Measured stratigraphic section from NP. Section illustrates thickness, relief (weathering profile), lithology, sedimentary and diagenetic features, and faunal elements. Lower Wahoo-Sadlerochit Group contact at 44 m. Section is in the limb on a syncline. Most of the Lisburne has been recrystallized in this section. In the formation column, SG represents Sadlerochit Group.

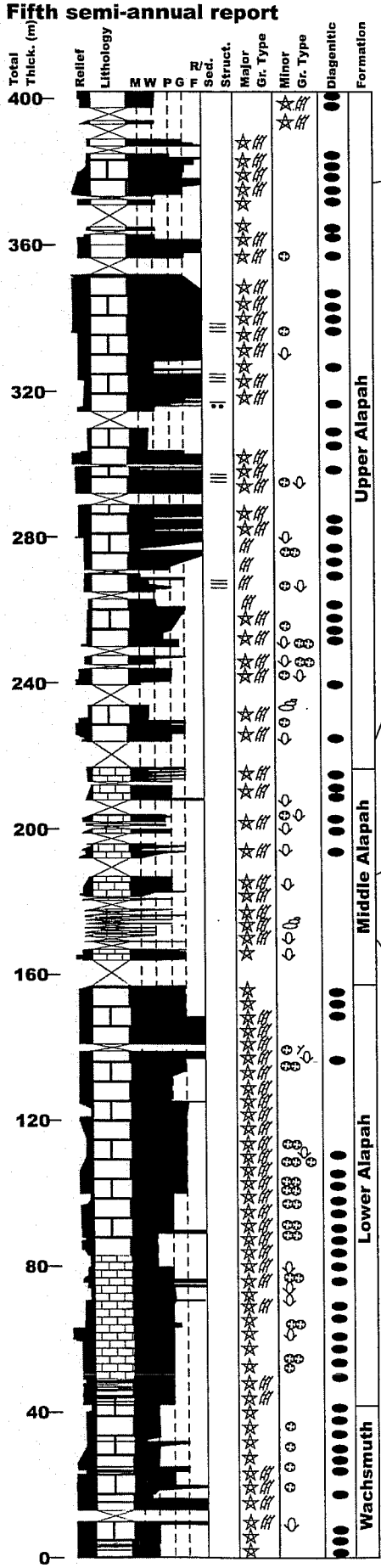

Photo illustrating 0.5 m thick nodular to lenticular black chert "bed". Similar to the chert bed observed in Ef2 and NF.

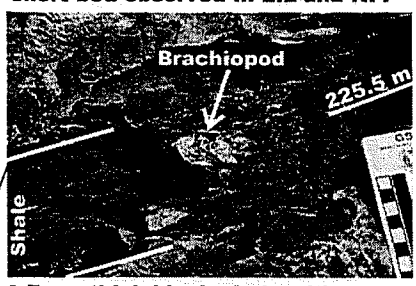

A 7 cm thick black shale with an upside down brachiopod. Grainstone to rudstone is above and below shale.

Middle Alapah cycles have thin black shale bases and coarsen upward to packstones, grainstones, and rudstones. The cycles give the outcrop a "stair-step" appearance.

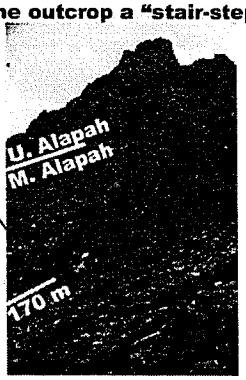

Photo illustrates recessive middle Alapah with "stair-step" appearance and resistant upper Alapah.

Figure 4. Measured stratigraphic section from WF. Section illustrates thickness, relief (weathering profile), lithology, sedimentary and diagenetic features, and faunal elements. Wachsmuth-lower Alapah contact at 42 m. Lower-middle Alapah contact at 157 m. Middle-upper Alapah contact at 224 m. Upper Alapah-lower Wahoo contact at 402 m.

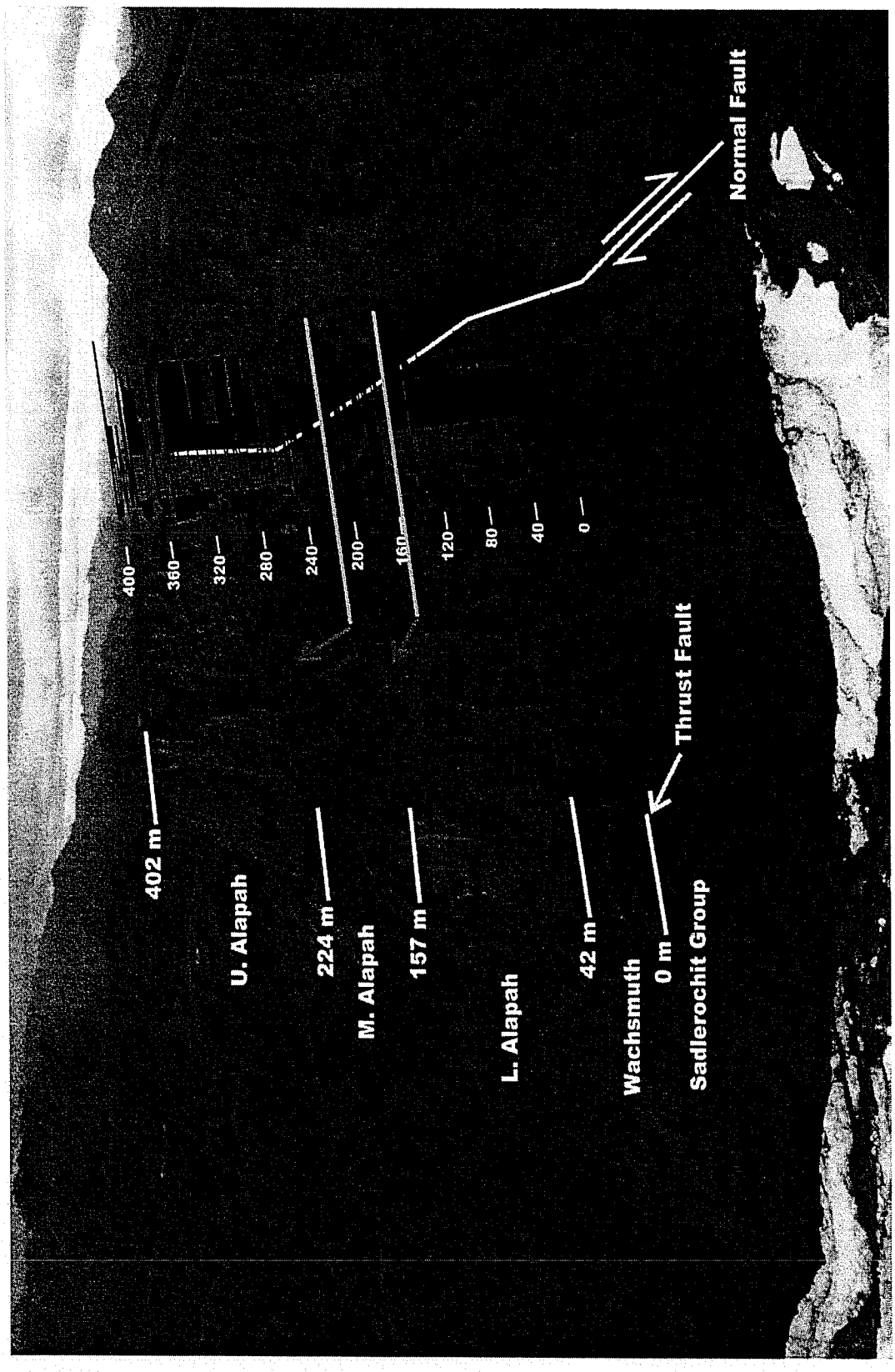

Figure 5. Outcrop photo with measured stratigraphic overlay of section WF. The section was measured along the talus slope on the left (north) side of the photo. The measured section does not fit exactly to the photograph because of the angle the photograph was taken. The left hand column in the stratigraphic section overlay is weathering profile, with resistant to left and recessive to the right. Lithology is in the center of the column and rock type is to the right. In the rock type column rudstone is to the far right and mudstone is closest to the lithology column. Solid white lines correspond to unit boundaries in the measured stratigraphic section.

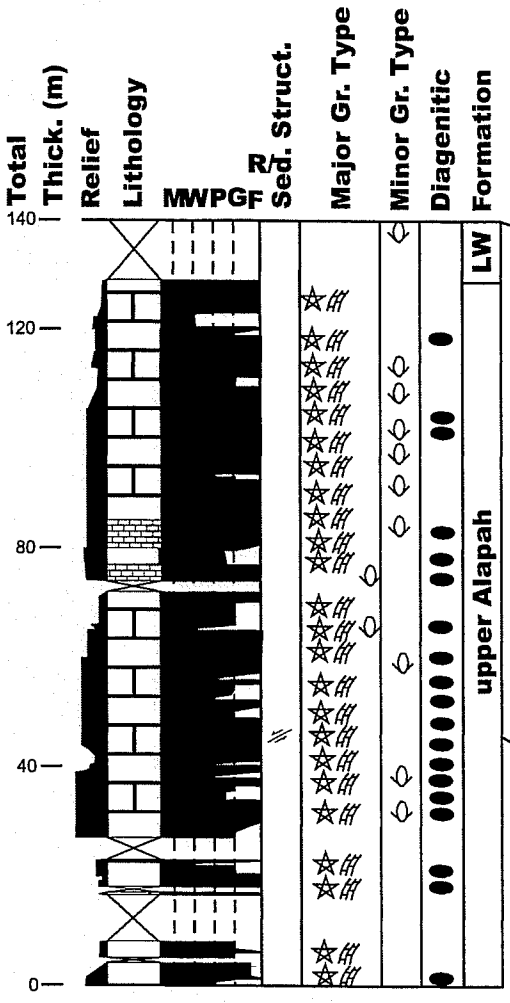

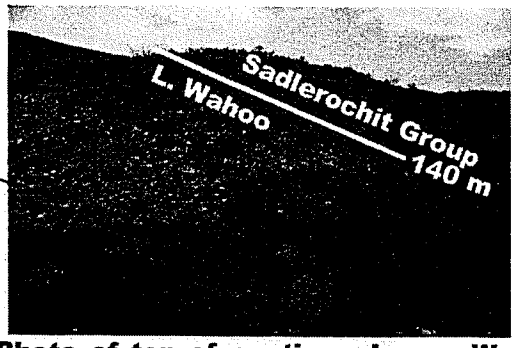

Photo of top of section. Lower Wahoo is rubbly and overlain by the Sadlerochit Group (Kavik Shale member). The contact was determined by the end of the gray limestone and beginning of red shale.

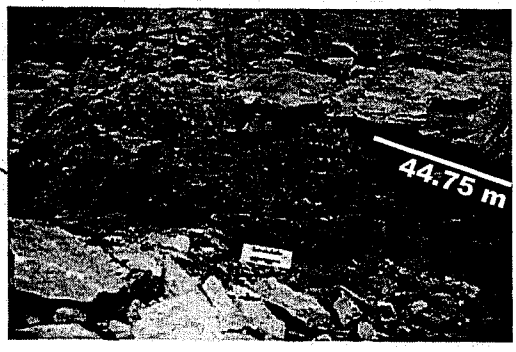

Between 44.25 and 44.75 m is a "bed" composed of lenticular to nodular black chert similar to that found in sections Ef2 and WF.

Figure 6. Measured stratigraphic section from NF. Section illustrates thickness, relief (weathering profile), sedimentary and diagenetic features, and faunal elements. Upper Alapah-lower Wahoo contact is at 129 m. Lower Wahoo-Sadlerochit Group contact at 140 m.

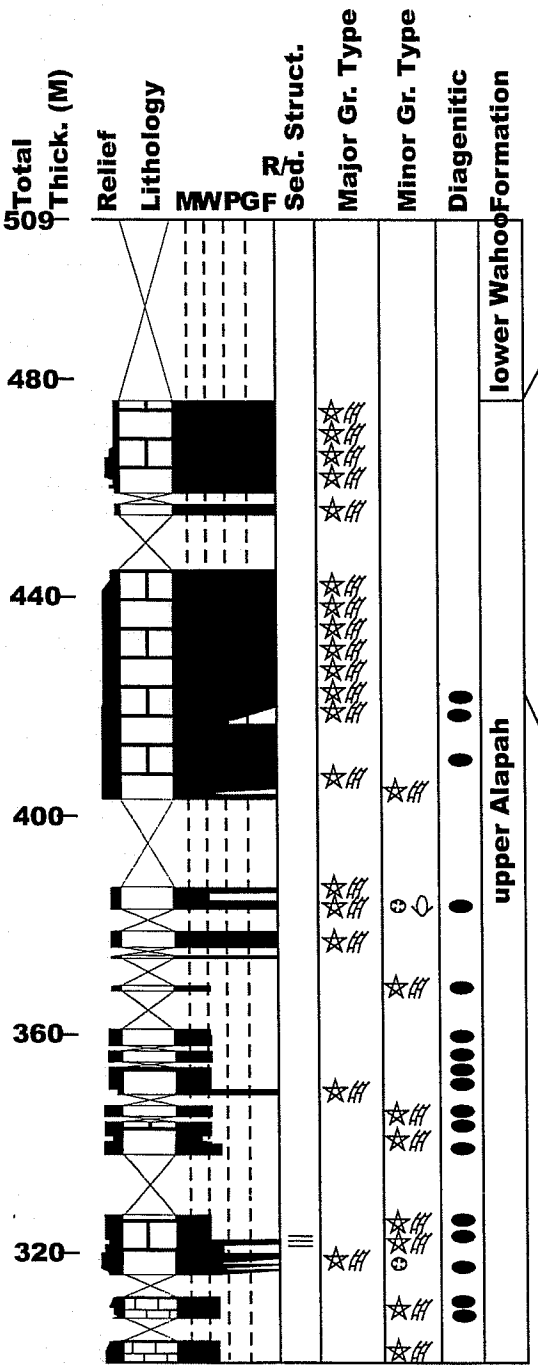

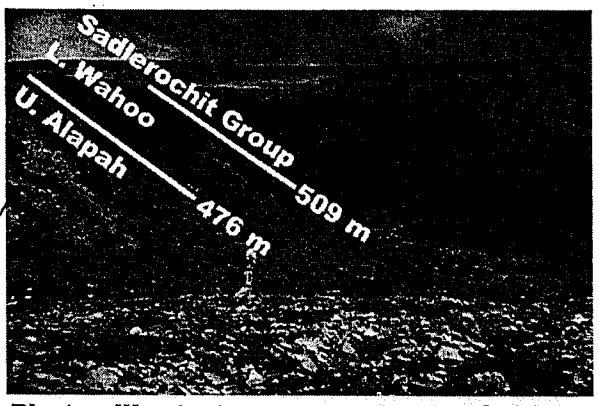

Photo illustrates upper part of Lisburne section. Upper Alapah is very hard, possibly silicified, and is overlain by the covered rubbly lower Wahoo. The Sadlerochit Group is a red silty shale that contains pyrite and septarian concretions mm to half meter in size.

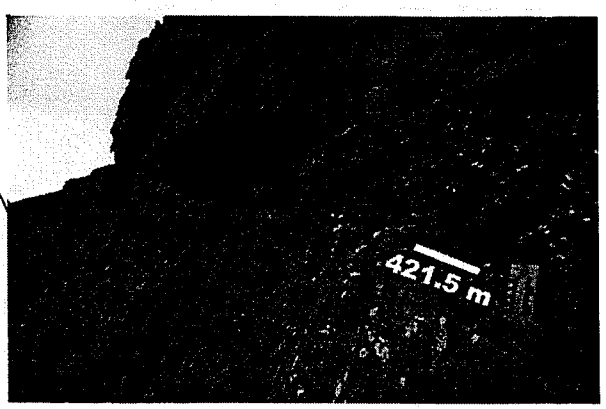

Photo of 0.5 m "bed" of nodular and lenticular black chert. A similar chert "bed" is also occurs in sections NF and WF.

Figure 7. Measured stratigraphic section from EF2. Section illustrates thickness, relief (weathering profile), lithology, sedimentary and diagenetic features, and faunal elements. The upper Alapah-lower Wahoo contact is at 476 m. The lower Wahoo-Sadlerochit Group contact is at 509 m. The lower 320 m of this stratigraphic section was completed during the 2000 summer field season and is recorded in the DOE May 2001 second semi-annual report.

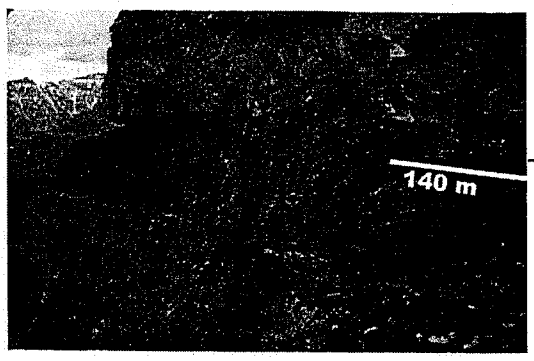

Black shale between 139.25 and 140.25 m. A 10 cm thick blocky calcite vein at the bottom of the shale. A rudstone with planar laminations overlies the shale.

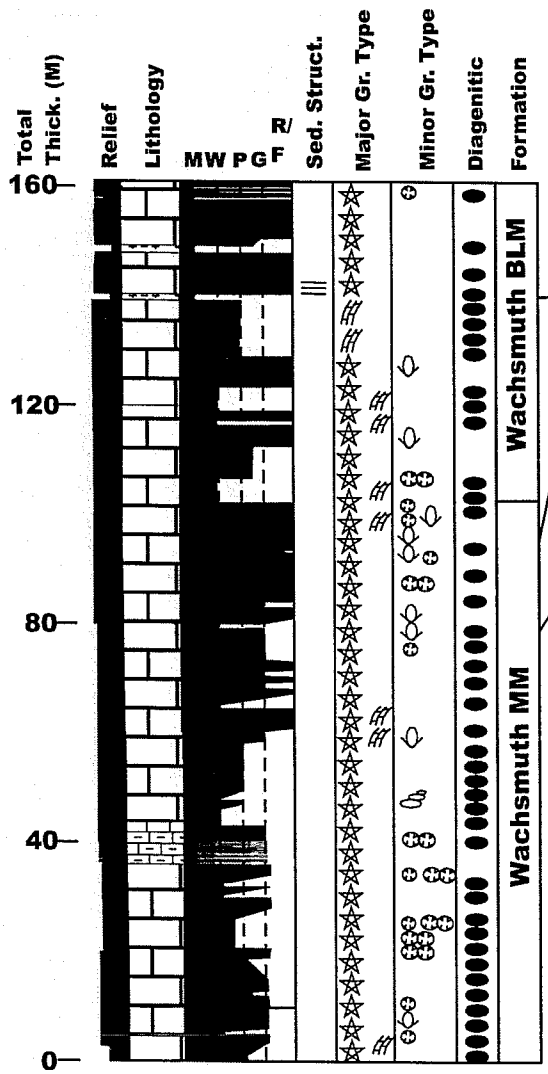

Figure 8. Measured stratigraphic section from MF3. Section illustrates thickness, relief (weathering profile), lithology, sedimentary and diagenetic features, and faunal elements. The Wachsmuth middle member (MM)-banded limestone member (BLM) contact is at 102 m.

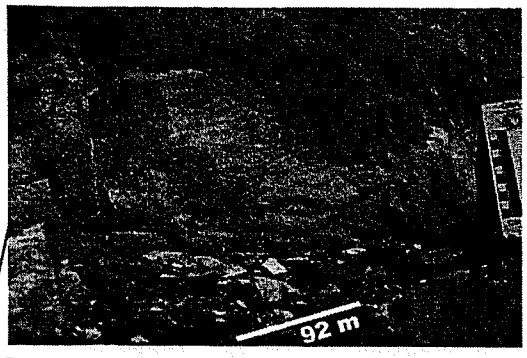

Cross-bedded rudstone with abundant crinoid and brachiopod shell fragments just above 92 m.

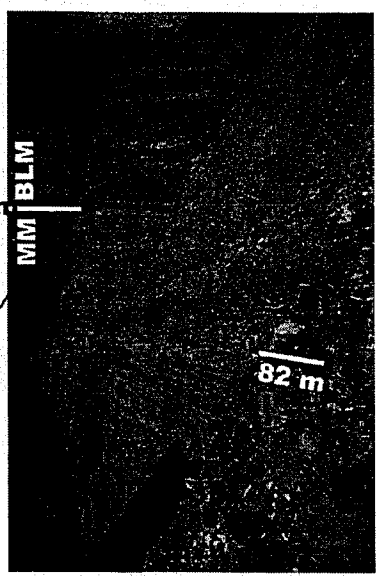

This photo illustrates the Wachsmuth middle member (MM) and banded limestone member (BLM). Above 102 m, are black cherts "interbedded" with wackestone to packstone and deposition of thick black shales with thin grainstone to rudstone units.

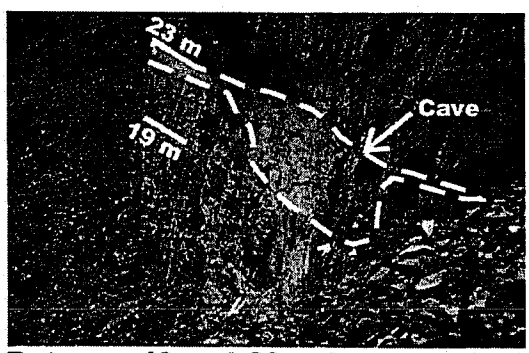

Between 19 and 23 m is a cave (?) filled with coarse blocky calcite. A thin black shale was deposited at the top of the cave.

Figure 9. Measured section MF3 is superimposed over the outcrop photo. The section was measured along the talus slope on the right (east) side of the photograph along the landslide edge (dashed line). The left hand column in the stratigraphic section overlay is weathering profile, with resistant to left and recessive to the right. Lithology is in the center of the column and rock type is to the right, with rudstone to the far right and mudstone closest to the lithology column. The contact between Wachsmuth middle member (MM) and banded limestone member (BLM) is at 102 m.

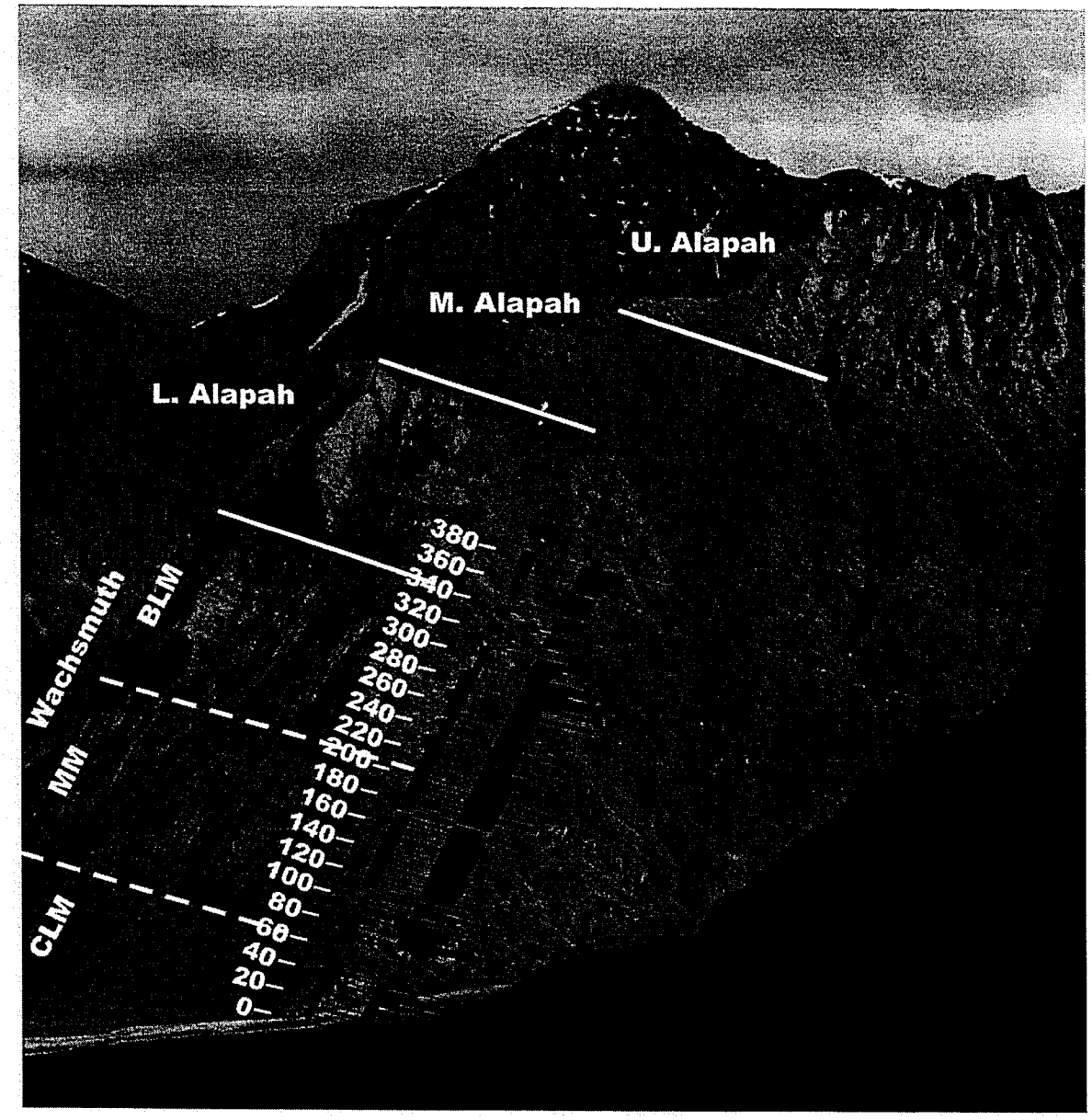

Figure 10. Outcrop photo of section MF with measured section overlay. The Wachsmuth, between 0 and 340 m has three members: a crinoidal limestone member (CLM - 0 to 70 m), a middle member (MM - 70 to 206 m), and a banded limestone member (BLM - 206 to 340 m; Brosge, et. al, 1962). The Wachsmuth-lower Alapah unit boundary is at 340 m. Measured stratigraphic sections are in meters. Weathering profile is in the left column with resistant to the left and recessive to the right. Lithology is in the center and rock type is in the right column. Mudstone is closest to the lithology column and rudstone is farthest away from the lithology. Section MF was measured during the 2000 field season and is recorded in the DOE May 2001 second semi-annual report.

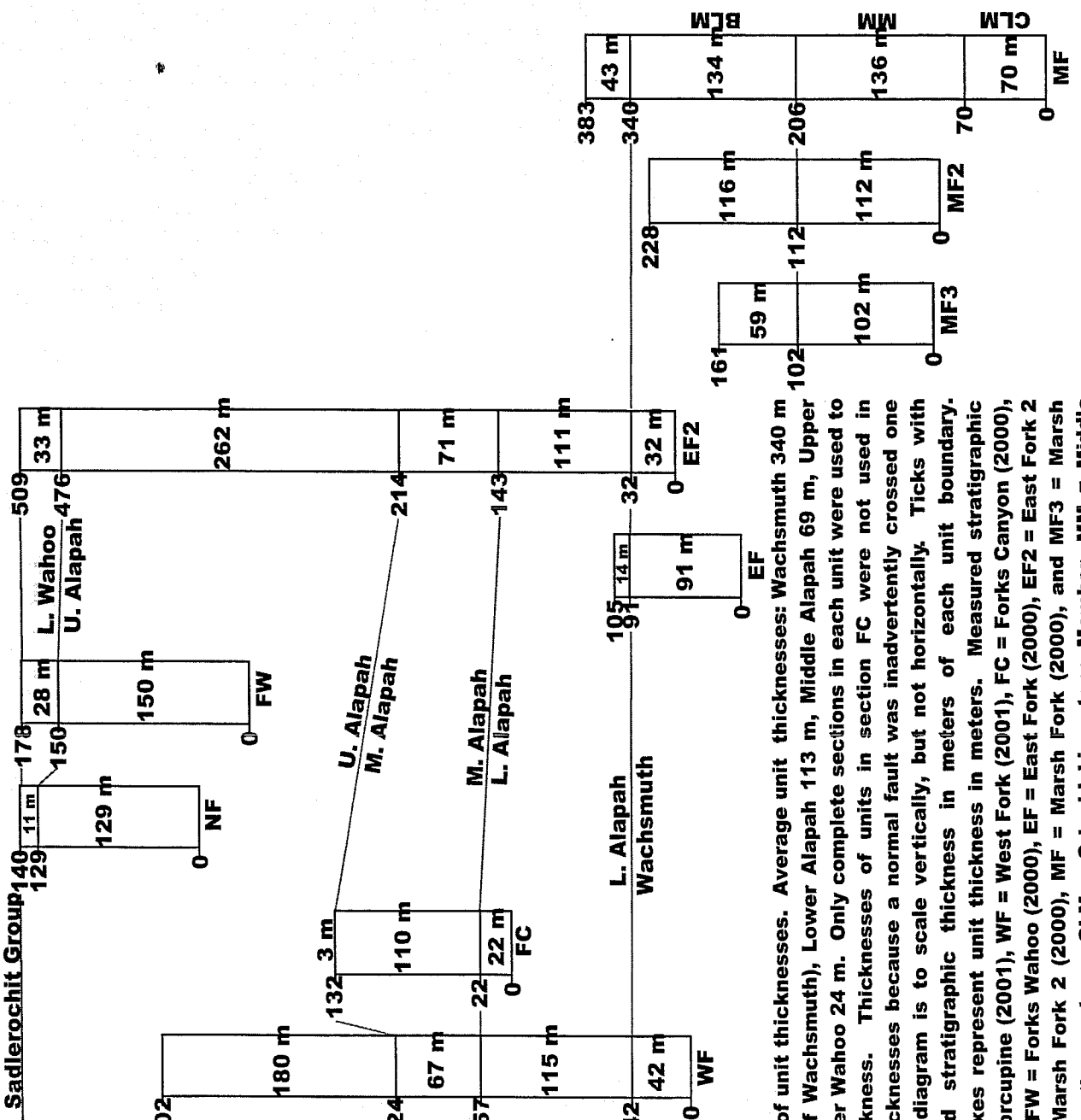

Figure 11. Illustration of unit thicknesses. Average unit thicknesses: Wachsmuth 340 m (no complete section of Wachsmuth), Lower Alapah 113 m, Middle Alapah 69 m, Upper Alapah 262 m, and Lower Wahoo 24 m. Only complete sections in each unit were used to calculate average thickness. Thicknesses of units in section FC were not used in calculating average thicknesses because a normal fault was inadvertently crossed one or more times. This diagram is to scale vertically, but not horizontally. Ticks with numbers are measured stratigraphic thickness in meters of each unit boundary. Numbers inside the boxes represent unit thickness in meters. Measured stratigraphic sections: NP = North Porcupine (2001), WF = West Fork (2001), FC = Forks Canyon (2000), NF = North Fork (2001), FW = Forks Wahoo (2000), EF = East Fork (2000), EF2 = East Fork 2 (2000 & 2001), MF2 = Marsh Fork 2 (2000), MF = Marsh Fork (2000), and MF3 = Marsh Fork 3 (2001). Wachsmuth members: CLM = Crinoid Limestone Member, MM = Middle Member, BLM = Banded Limestone Member.

Characteristics of detachment folds and thrust-truncated asymmetrical folds in the eastern Brooks Range

by Wesley K. Wallace, Geophysical Institute and Department of Geology and Geophysics, University of Alaska, Fairbanks, Alaska, 99775-5780

Abstract

Observations during the summer of 2001 identified several characteristics of the upright and symmetrical detachment folds in Lisburne Group carbonates of the northeastern Brooks Range, north of the Continental Divide thrust front. Where shortening is relatively low, multiple closely spaced folds form local culminations that likely reflect amplification at the preferred wavelength of the entire competent unit. In a transect where shortening is moderate to high, folds typically display an upward decrease in parasitic folding and the amount of shortening apparently accommodated by folding. This likely reflects an overall upward increase in competency and suggests an upward increase in the proportion of shortening that is accommodated by layer-parallel shortening. In one place, a fold that has been truncated and displaced by a thrust fault displays a geometry very similar to that of the thrust-truncated asymmetrical folds south of the Continental Divide thrust front. Typical upright and symmetrical detachment folds that have not been cut by thrust faults exist in the same mechanical stratigraphy nearby.

Observations in the Porcupine Lake area during the summers of 1999 to 2001 identified several characteristics typical of the thrust-truncated asymmetrical folds in Lisburne Group carbonates in the eastern Brooks Range, south of the Continental Divide thrust front. The dominant structures are asymmetrical anticlines that have been cut and displaced over thrust faults. Forelimbs typically are overturned to the north and commonly are thickened by parasitic folding and minor bulk strain. Hinge zones commonly display minor thickening, especially in less competent intervals. Thrust faults follow bedding low within or below the lowermost Lisburne in backlimbs and cut across forelimbs at a high angle. The geometry of thrust-truncated anticlines commonly has been modified by gentle antiformal folding of the underlying thrust faults. Fold asymmetry likely is the critical characteristic that accounts for the folds south of the Continental Divide thrust front being broken through by thrust faults, in contrast with the unbroken upright and symmetrical detachment folds to the north.

Introduction

A major objective of this project has been to characterize the geometry of two different types of folds that formed in carbonates of the Lisburne Group in different parts of the eastern Brooks Range (Figure 1), and to explore how and why these different types of folds formed within the same rock unit. The Lisburne Group of the northeastern Brooks Range displays upright, symmetrical detachment folds that are cut only rarely by thrust faults (Wallace and Hanks, 1990; Wallace, 1993; Homza and Wallace, 1997). By contrast, the Lisburne Group to the south in the eastern Brooks Range displays inclined, asymmetrical anticlines whose forelimbs have broken through and been displaced northward above thrust faults (Wallace, 1993; Wallace et al., 1997). The boundary between these two different structural styles in the Lisburne Group is the Continental Divide thrust front (Figure 1). Previous reports on this project describe the tectonic

setting in which the two types of folds are found, and present earlier observations and interpretations of the two fold types (Atkinson, 2000; Jadamec, 2001; Hanks et al., 2002; Jadamec and Wallace, 2002; Shackleton et al., 2002; Wallace, 2001, 2002).

This report presents observations of both fold types. First, it summarizes new observations of detachment folds made in three areas of the northeastern Brooks Range during the summers of 2000 and 2001. Second, it combines previously reported observations with new observations to develop a synthesis of the characteristics of the thrust-truncated asymmetrical folds studied throughout the Porcupine Lake area.

Detachment folds were studied in three areas of the northeastern Brooks Range (Figure 1) because each area provided different types of information:

- The crest of the Echooka anticlinorium: A well-exposed example of detachment folds at low shortening, early in their evolution.
- The upper Echooka River: A long and well-exposed cross-strike transect across numerous detachment folds at moderate to high shortening.
- East Franklin Creek: Exposure of the entire vertical extent of detachment folds from beneath the detachment surface to the top of the Lisburne Group, as well as an unusual example of a thrust-truncated asymmetrical detachment fold.

The thrust-truncated asymmetrical folds of the Porcupine Lake area were studied during the three summers of field work for this project (1999-2001) in reconnaissance work by Wes Wallace and in detailed Master's thesis projects by Margarete Jadamec and Ryan Shackleton. This report presents a first synthesis of the characteristics of the thrust-truncated asymmetrical folds of the area.

In the final report for this project, the field observations of both detachment folds and thrust-truncated asymmetrical folds will be documented by detailed maps and cross sections that will provide the data for a semi-quantitative assessment of the range of geometric characteristics of both fold types. This, in turn, will serve as the basis for a model of the evolution of each fold type and to explore the possible reasons why each fold type formed where it did.

Crest of Echooka anticlinorium

The lower Lisburne and underlying Kayak Shale display a low magnitude of shortening and gentle regional dip in exposures west of the Echooka River at the crest of the Echooka anticlinorium (Figure 1). A well-exposed train of folds at the ~100 m scale provides the best example of low-shortening folds in the region (Figure 2). These folds are detached from the lowermost Lisburne, but the nature of the contact with the overlying upper Lisburne is less clear because it is mostly eroded. The folds have wavelengths of ~75-300 m, but form culminations with a larger spacing of ~350-450 m. The folds display a kink-style box-fold geometry with angular to rounded hinges (Figure 3). Interlimb angles of anticlines are ~75-135°, generally increasing downward. Common thickening in hinges of anticlines accounts for downward decrease in amplitude and increase in interlimb angle, as in the Epard and Groshong (1995) model for detachment folding.

These folds probably represent an early stage of fold evolution in the lower Lisburne given the low shortening and gentle regional dip in this area. This suggests early nucleation of many folds at short wavelength (second- to third-order detachment folds) in the lower Lisburne. The larger-wavelength culminations (Figure 2) may represent amplification of anticlines at the larger preferred wavelength of the entire composite mechanical stratigraphic unit defined by the Lisburne, including its more competent upper part. This hypothesis could be assessed by tracing the folds up-section into the upper Lisburne where it is exposed to the west as the Echooka anticlinorium plunges gently westward.

Upper Echooka River

The upper part of the Echooka River (Figure 1) provides nearly continuous high-quality exposures of detachment folds typical of an intermediate to high magnitude of shortening in the northeastern Brooks Range. A transect of ~10 km was mapped in detail on both sides of the upper Echooka River. The objective of this work was to document observations of a wide variety of detachment folds to provide data to construct a cross section that will be used to quantify variations in fold geometry, including wavelength and amplitude.

Field observations suggest some preliminary conclusions about fold geometry. Fold geometry is strongly influenced by the difference in competency between the more competent upper Lisburne and the less competent lower Lisburne. Parasitic folds are common in the lower Lisburne, but are larger and less common in the upper Lisburne (Figure 4).

First-order detachment folds with straight to gently curved limbs characterize the upper Lisburne (Figures 4 to 6). Folds are open to close with angular to narrow curved hinges. Gently curved crestal panels are common. Hinge geometry changes between intervals of different competency by hinge thickening and detachment. Parasitic folds are large and uncommon, and are present mostly near the base of the upper Lisburne.

Second- and third-order folds parasitic to the first-order folds in the upper Lisburne characterize the lower Lisburne (Figures 4 and 7). Some of these folds die out upward at the top of the lower Lisburne, whereas others continue upward. These folds are open to tight, angular, and commonly show structural changes in bed thickness. Platy solution cleavage is common in these folds.

More rounded hinges in the upper Lisburne and sharper, more angular hinges in the lower Lisburne commonly characterize the composite fold geometry defined by these two mechanical stratigraphic units (Figure 8). Anticlines commonly display concave-upward limbs. Hinge zones have a gently curved crestal panel upward and cuspate hinges downward. This is transitional between a concentric and flat-crested kink geometry. Synclines typically display straight to concave-upward limbs. Detachment and thickening in the hinge allow hinge zones not to widen downward, toward the outer arc of the syncline. Geometric differences between anticlines and synclines may reflect the upward increase in competency within the Lisburne.

The "first-order" detachment folds described above actually are gently folded or tilted at the scale of the transect. Construction of cross sections is required to define these large structures

better. This will provide some basis to assess whether these structures formed over horses in the basement or are larger, very gentle detachment folds that reflect variations in structural thickness of the underlying Kayak Shale.

East Franklin Creek

The East Franklin Creek area (Figure 1) was selected for study because it exposes the entire detachment-folded section, from the base of the Kayak Shale to the top of the Lisburne Group. The detachment folds represent a moderate amount of shortening in a narrow synclinorium located between the two basement-cored anticlinoria of the Franklin Mountains.

Detachment folds in the area display significantly different behavior in the more competent upper Lisburne and the less competent lower Lisburne (Figure 9). The upper Lisburne displays gentle and rounded first-order and sparse second-order detachment folds, whereas the lower Lisburne displays abundant open to close, angular second- and third-order detachment folds. Folds in the lower Lisburne are largely disharmonic in detail with the larger folds in the upper Lisburne, although they collectively correspond with the relief on the contact between upper and lower Lisburne. Folds in the lower Lisburne display steeper limb dips and greater height than the much more subdued equivalent or comparable folds in the upper Lisburne. The Kayak Shale displays folds comparable in size and geometry to those in the lower Lisburne, but the exposures are too incomplete to determine whether or not they are in harmony with the folds in the lower Lisburne.

Based on fold geometry, the fold shortening in upper Lisburne does not appear to be sufficient to account for the tighter, shorter-wavelength folds below (Figure 9). Greater meso- to microscopic layer-parallel shortening in the competent upper Lisburne could account for this apparent discrepancy. Detachment between upper and lower Lisburne is a less likely possibility. A bottom-to-north shear gradient could also account for the discrepancy, but is very unlikely given the evidence for top-to-north shear described below.

An important but unforeseen discovery in the East Franklin Creek area was a large thrust-truncated asymmetrical detachment fold (Figures 10 and 11). This fold formed over the forelimb of a basement-cored anticlinorium, probably as a result either of slip ahead of a basement horse or of gravity-driven displacement from its top. The structure represents clear truncation through the short limb of an asymmetrical anticline-syncline pair because both the hangingwall anticline and footwall syncline are exposed. The asymmetrical fold clearly originated as a detachment fold because the Kayak Shale is thickened in the core of the anticline above a smooth, non-folded surface defined by the underlying Kekiktuk Conglomerate.

Thrust-truncated folds of very similar geometry are exposed to the south in the Porcupine Lake area (see below) and exemplify the typical fold geometry displayed by the Lisburne throughout the northern part of the main axis of the Brooks Range. Unlike the Porcupine Lake exposures, a footwall syncline is preserved in the east Franklin Creek thrust-truncated fold (Figure 10). This footwall syncline is characterized by multiple hinges that define a box-fold geometry and parasitic folds in some layers. A key point is that the east Franklin Creek thrust-truncated fold is immediately adjacent to upright symmetrical detachment folds typical of those found throughout

the northeastern Brooks Range. This transition provides a strong indication that thrust-truncation of detachment folds is related to fold asymmetry.

Porcupine Lake area

The Porcupine Lake area (Figure 1) provides extensive exposures of thrust-truncated asymmetrical folds that are typical of those displayed by the Lisburne throughout the northern part of the main axis of the Brooks Range (Wallace, 1993, 2002). This report summarizes observations made during 1999, 2000, and 2001 by Wes Wallace and Master's degree students Margarete Jadamec and Ryan Shackleton.

The mechanical stratigraphy of the area is characterized by two uniformly competent intervals (lower Lisburne (~450 m) and upper Lisburne (~300 m)) that are separated by a relatively thin, moderately competent interval (middle Lisburne (~70m)) (Figure 12). The competent intervals consist of beds with a relatively large and uniform thickness, whereas the incompetent interval consists of thinner and finer-grained beds. The surfaces bounding the competent intervals are sharp. The Lisburne is thicker and has a higher ratio of competent to incompetent unit thickness than in the northeastern Brooks Range.

The anticlines of the area typically are asymmetrical, with forelimbs to the north and axial surfaces inclined to the north (Figures 12 and 13). Hinges in the cores of anticlines are sharp and angular (chevron geometry), but hinge zones typically widen and decrease in curvature outward toward fold outer arcs and/or have axial surfaces that branch outward (Figures 13 and 14). The change from a single angular hinge to a wider hinge zone and/or multiple axial surfaces is typically in the less-competent middle Lisburne and may reflect some detachment in this interval. The upward increase in bed length in the angular part of anticlines suggests an upward increase in bed-parallel shear unless the excess bed length happens to be balanced by an unseen upward decrease in bed length in synclines.

Forelimbs have been thickened in a variety of ways in many anticlines of the area. Most commonly, this thickening is accommodated by parasitic anticline-syncline pairs that are second-order to the host anticline, but that still are of map scale (Figure 12 and 13). The geometry of these parasitic folds suggests that they could have originated by folding that occurred preferentially within the north-dipping limbs of originally symmetrical folds. Some anticlines also display thickening by bulk strain, but this thickening is typically restricted to hinges and is most common within the less competent middle Lisburne (Figure 12). A few anticlines display higher-order parasitic folds, either within the middle Lisburne or, more rarely, in the upper Lisburne.

Some anticlines display a change upward in interlimb angle, typically within or between mechanical units. This change in interlimb angle implies a compensatory change in layer thickness, although the required thickness change is typically minor. Interlimb angle most commonly increases upward at the scale of an entire anticline, but may decrease upward across less competent intervals.

The forelimbs of most anticlines in the Porcupine Lake area have been broken through by and displaced above thrust faults (Figures 14 and 15). Footwall cutoffs are only rarely exposed, so the exact location of thrust breakthrough with respect to the originally unbroken forelimb is uncertain. Within the hangingwall, thrust breakthrough is below a simple forelimb or a parasitic anticline-syncline pair. In the forelimbs of a few anticlines, thrusts have broken through both above and below a second-order anticline. A few folds also display up to several small-displacement thrust faults above the main thrust that has truncated the forelimb (Figure 16). In several folds, no thrust faults are visible above the lowest part of the section that is exposed, which varies from near the base of the upper Lisburne down to the upper part of the lower Lisburne. These folds may not have been broken through by thrust faults, although breakthrough below the level of exposure is possible.

Thrust faults generally cut across anticlinal hinges at moderate to small angles (~30-50°) (Figures 14 to 17). Bedding is cut off at very high angles in anticline forelimbs (~110-130°) and, in most folds, the forelimb is overturned with respect to the underlying thrust fault (Figures 14 to 17). In several folds, bedding within a panel immediately above and parallel to the thrust fault is strongly overturned and highly strained, reflecting shear strain localized above the thrust (Figures 15 to 17). In the backlimb, the thrust follows a flat that typically is located near the base of the Lisburne (Figure 17) but is in the Kayak in a few folds.

Thrust faults commonly display a gentle convex-upward curvature (Figures 15 and 17). These thrust faults probably are folded because they follow folded bedding in the footwall. The folds overlying these folded thrusts display a distinctive profile, resembling a fault-bend fold with an overturned forelimb. These folds typically have an anticlinal hinge that is curved, with an upward increase in inclination that results in forward tilt of the backlimb as it approaches the anticlinal hinge. This curvature requires extension of the backlimb, which may be accommodated by the fractures, normal faults, and/or thinning that are observed in some folds.

An upward increase in bed-parallel shear within folds is supported by a consistent top-to-north sense of shear indicated by fractures, strain, and parasitic folds. Such a shear gradient could help account for the asymmetry and thrust breakthrough of the folds, but its cause remains uncertain.

In summary, the observations define a number of significant structural characteristics of the folds of the area (Figures 13 and 15):

- The basic structural style is characterized by asymmetrical anticlines that are cut and displaced over thrust faults.
- The forelimbs of these anticlines commonly are thickened by parasitic fold pairs and/or bulk strain.
- Hinges commonly branch towards the outer arc of folds within the competent unit rather than at its bounding contacts, implying strain and/or bed-parallel shear.
- The folds display thickness changes that reflect minor departures from parallel geometry, but to a lesser extent than in the northeastern Brooks Range.
- The forelimbs of some folds are cut by subsidiary thrusts that may represent incipient break-through thrusts.
- Zones of shear strain are observed or inferred to be adjacent to some thrusts.
- Some folds are not cut by thrusts in those parts of the Lisburne that are exposed.

Comparison of fold geometry across the Continental Divide thrust front

Folds display significantly different characteristics across a boundary near the Continental Divide thrust front (Wallace and Hanks, 1990; Wallace, 1993, 2001, 2002). To the north, folds are upright, symmetrical, and only rarely cut by thrust faults. These folds vary considerably in their geometry, from angular to rounded and commonly with significant internal thickness change accommodated by bulk strain or parasitic folds. Typically, hinges are thickened and limbs are thinned, which may reflect flattening of folds to accommodate increasing shortening.

To the south, folds are inclined, asymmetrical, and typically cut and displaced by thrust faults in their forelimbs. These folds generally are angular and display significantly less internal thickness change than the folds to the north. Thrust breakthrough may have resulted to accommodate increasing shortening in these folds. Fold geometry and minor structures suggest a top-to-north gradient in bed-parallel shear that may have favored fold asymmetry and thrust breakthrough.

Increasing shortening was accommodated to the north by a regional-scale approximation of pure shear in the form of symmetrical folds that evolved by a combination of flexural slip and flattening. To the south, increasing shortening was accommodated by a regional-scale approximation of simple shear in the form of asymmetrical folds that formed by flexural slip but eventually broke through by thrust faults.

Differences in mechanical stratigraphy may in part account for the differences in fold geometry and evolution. Competency increases gradually upward within the Lisburne to the north, whereas two uniformly competent intervals are separated by a relatively thin less competent interval within the Lisburne to the south. The Lisburne is thicker to the south and the ratio of competent (Lisburne) to incompetent (Kayak) unit thickness is greater to the south than to the north. The final report on this project will address these and other differences between the north and the south, and explore how they might have influenced the differences observed in fold geometry and evolution.

References

Atkinson, P.K., 2001, A geometric analysis of detachment folds in the northeastern Brooks Range, Arctic National Wildlife Refuge, Alaska, and a model for their kinematic evolution, in Wallace, W.K., Hanks, C.L., Whalen, M.T., Jensen, J., Lorenz, J., Atkinson, P.K., Brinton, J.S., and Karpov, A.V., The influence of fold and fracture development on reservoir behavior of the Lisburne Group of northern Alaska: Department of Energy, Fossil Energy, National Petroleum Technology Office, Tulsa, Oklahoma, Annual report for work performed under contract no. DE-AC26-98BC15102, May, 1999 - May, 2000, p. D-1-31.

Epard, J.-L., and Groshong, R.H., Jr., 1995. Kinematic model of detachment folding including limb rotation, fixed hinges and layer-parallel strain: Tectonophysics, v. 247, p. 85-103.

Hanks, C.L., Wallace, W.K., Lorenz, J., Atkinson, P.K., Brinton, J.S., Shackleton, J.R., 2002, Timing and character of mesoscopic structures in detachment folds and implications for fold development, in Wallace, W.K., Hanks, C.L., Jensen, J., Whalen, M.T., Atkinson, P.K.,

Brinton, J.S., Bui, T., Jadamec, M.A., Karpov, A.V., Krumhardt, A.P., Lorenz, J., McGee, M.M., Shackleton, J.R., The influence of fold and fracture development on reservoir behavior of the Lisburne Group of northern Alaska: Department of Energy, Fossil Energy, National Petroleum Technology Office, Tulsa, Oklahoma, Semi-annual report for work performed under contract no. DE-AC26-98BC15102, January to June, 2001, p, E-1-24.

Homza, T.X., and Wallace, W.K., 1997, Detachment folds with fixed hinges and variable detachment depth, northeastern Brooks Range, Alaska: Journal of Structural Geology, v. 19, p. 337-354.

Imm, T.A., Dillon, J.T., and Bakke, A.A., 1993, Generalized geologic map of the Arctic National Wildlife Refuge, northeastern Brooks Range, Alaska: Alaska Division of Geological and Geophysical Surveys Special Report 42, scale 1:500,000, 1 sheet.

Jadamec, M.A., 2001, Kinematic evolution of thrust-truncated folds, in Wallace, W.K., Hanks, C.L., Whalen, M.T., Jensen, J., Shackleton, J.R., Jadamec, M.A., McGee, M.M., and Karpov, A.V., The influence of fold and fracture development on reservoir behavior of the Lisburne Group of northern Alaska: Department of Energy, Fossil Energy, National Petroleum Technology Office, Tulsa, Oklahoma, Semi-annual report for work performed under contract no. DE-AC26-98BC15102, May, 2000 to January, 2001, p. C-1-16.

Jadamec M.A., and Wallace, W.K., 2002, Geometry and evolution of thrust-truncated detachment folds in the upper Marsh Fork area of the eastern Brooks Range fold-and-thrust belt, Alaska, in Wallace, W.K., Hanks, C.L., Jensen, J., Whalen, M.T., Atkinson, P.K., Brinton, J.S., Bui, T., Jadamec, M.A., Karpov, A.V., Krumhardt, A.P., Lorenz, J., McGee, M.M., Shackleton, J.R., The influence of fold and fracture development on reservoir behavior of the Lisburne Group of northern Alaska: Department of Energy, Fossil Energy, National Petroleum Technology Office, Tulsa, Oklahoma, Semi-annual report for work performed under contract no. DE-AC26-98BC15102, January to June, 2001, p, C-1-27.

Shackleton, J.R., Hanks, C.L., and Wallace, W.K., 2002, The relationship between fracturing, asymmetric folding, and normal faulting in Lisburne Group carbonates: West Porcupine Lake valley, northeastern Brooks Range, Alaska, in Wallace, W.K., Hanks, C.L., Jensen, J., Whalen, M.T., Atkinson, P.K., Brinton, J.S., Bui, T., Jadamec, M.A., Karpov, A.V., Krumhardt, A.P., Lorenz, J., McGee, M.M., Shackleton, J.R., 2002, The influence of fold and fracture development on reservoir behavior of the Lisburne Group of northern Alaska: Department of Energy, Fossil Energy, National Petroleum Technology Office, Tulsa, Oklahoma, Semi-annual report for work performed under contract no. DE-AC26-98BC15102, January to June, 2001, p. D-1-32.

Wallace, W.K., 1993, Detachment folds and a passive-roof duplex: Examples from the northeastern Brooks Range, Alaska, in Solie, D.N., and Tannian, F., eds., Short Notes on Alaskan Geology 1993: Alaska Division of Geological and Geophysical Surveys Geologic Report 113, p. 81-99.

Wallace, W.K., 2001, Detachment folds and their truncation by thrust faults, in Wallace, W.K., Hanks, C.L., Whalen, M.T., Jensen, J., Lorenz, J., Atkinson, P.K., Brinton, J.S., and Karpov, A.V., The influence of fold and fracture development on reservoir behavior of the Lisburne Group of northern Alaska: Department of Energy, Fossil Energy, National Petroleum Technology Office, Tulsa, Oklahoma, Annual report for work performed under contract no. DE-AC26-98BC15102, May, 1999 - May, 2000, p. C-1-28.

Wallace, W.K., 2002, Introduction and geologic setting, in Wallace, W.K., Hanks, C.L., Jensen, J., Whalen, M.T., Atkinson, P.K., Brinton, J.S., Bui, T., Jadamec, M.A., Karpov, A.V.,

Krumhardt, A.P., Lorenz, J., McGee, M.M., Shackleton, J.R., The influence of fold and fracture development on reservoir behavior of the Lisburne Group of northern Alaska: Department of Energy, Fossil Energy, National Petroleum Technology Office, Tulsa, Oklahoma, Semi-annual report for work performed under contract no. DE-AC26-98BC15102, January to June, 2001, p. A-1-10.

Wallace, W.K., and Hanks, C.L., 1990, Structural provinces of the northeastern Brooks Range, Arctic National Wildlife Refuge, Alaska: American Association of Petroleum Geologists Bulletin, v. 74, no. 7, p. 1100-1118.

Wallace, W.K., Moore, T.E., and Plafker, G., 1997, Multistory duplexes with forward dipping roofs, north central Brooks Range, Alaska: Journal of Geophysical Research, v. 102, no. B9, p. 20,773-20,796.

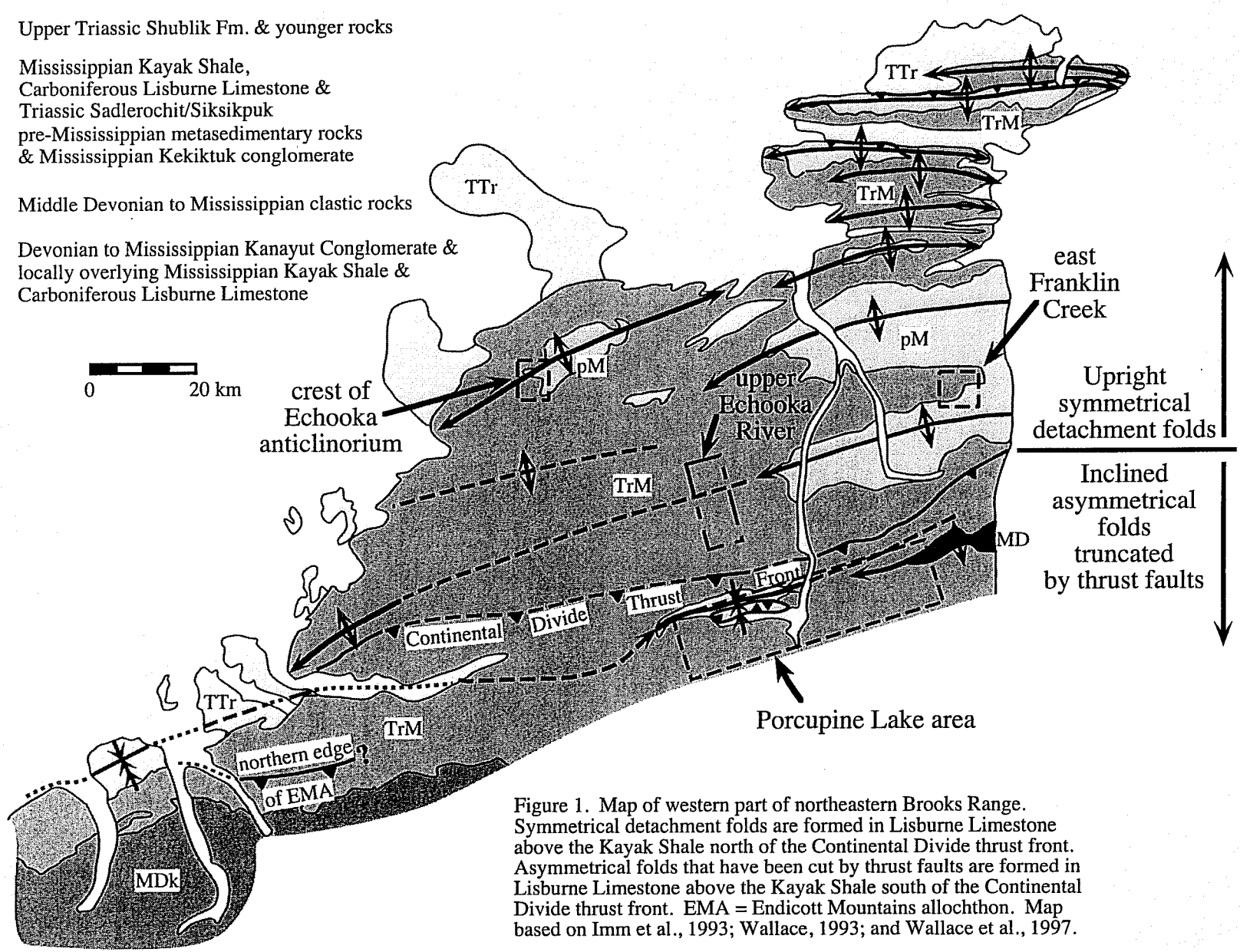

Figure 1. Map of western part of northeastern Brooks Range. Symmetrical detachment folds are formed in Lisburne Limestone above the Kayak Shale north of the Continental Divide thrust front. Asymmetrical folds that have been cut by thrust faults are formed in Lisburne Limestone above the Kayak Shale south of the Continental Divide thrust front. EMA = Endicott Mountains allochthon. Map based on Imm et al., 1993; Wallace, 1993; and Wallace et al., 1997.

DE-AC26-98BC15102

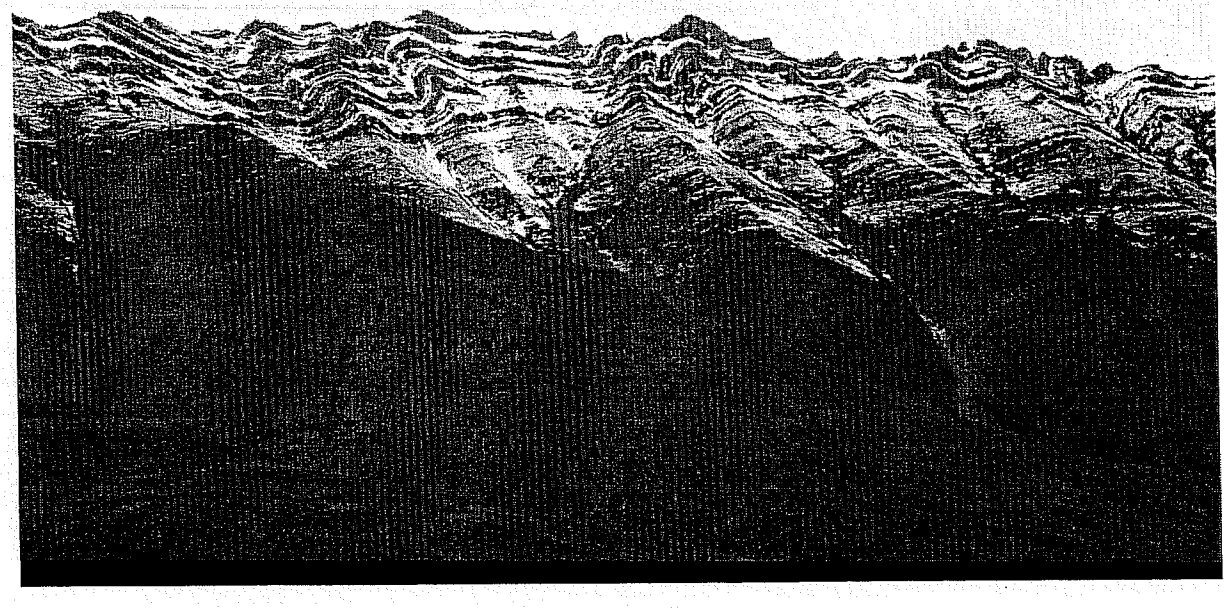

Figure 2. Detachment folds within lower Lisburne in the crest of the Echooka anticlinorium. Folds are detached above a horizon within lowermost Lisburne. Highest peaks are near the lower-upper Lisburne contact, but upper Lisburne is mostly eroded. Culminations defined by multiple small folds may represent the cores of larger anticlines within upper Lisburne.

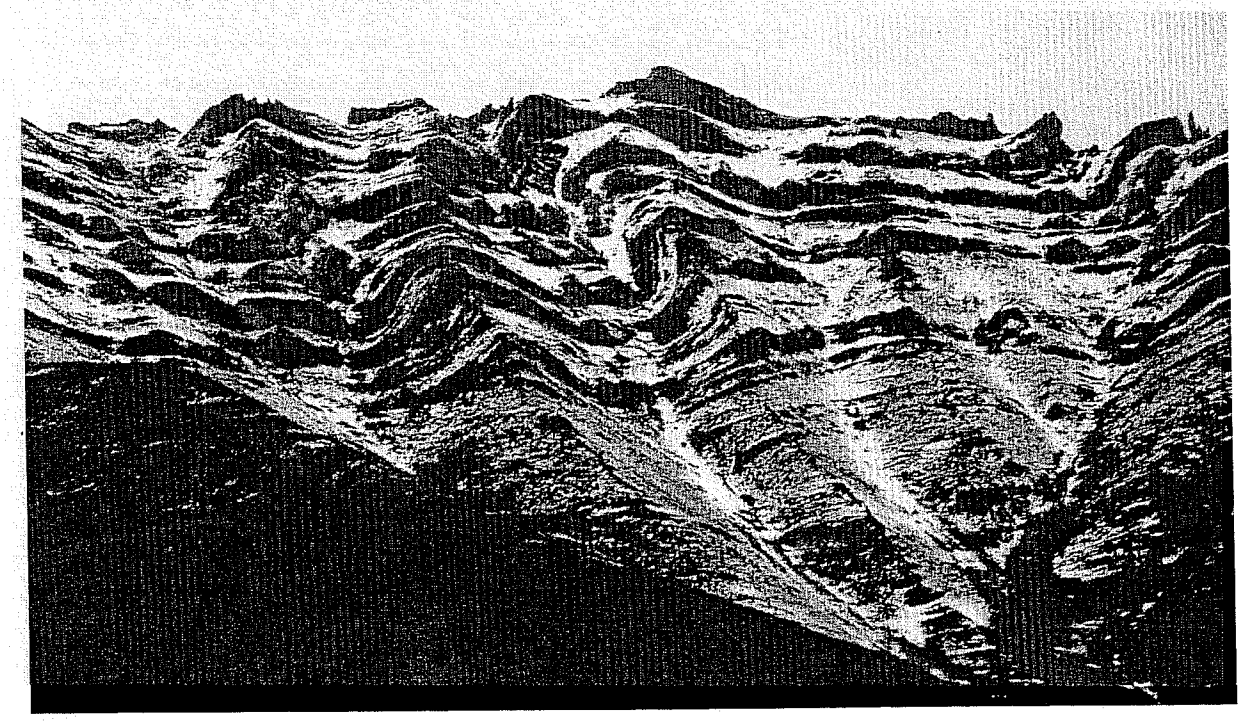

Figure 3. Detailed view of culmination to left in figure 2. Hinge zones widen outward within folds, upward within anticlines and downward within synclines. Angular hinges grade outward to curved or box-like hinge zones.

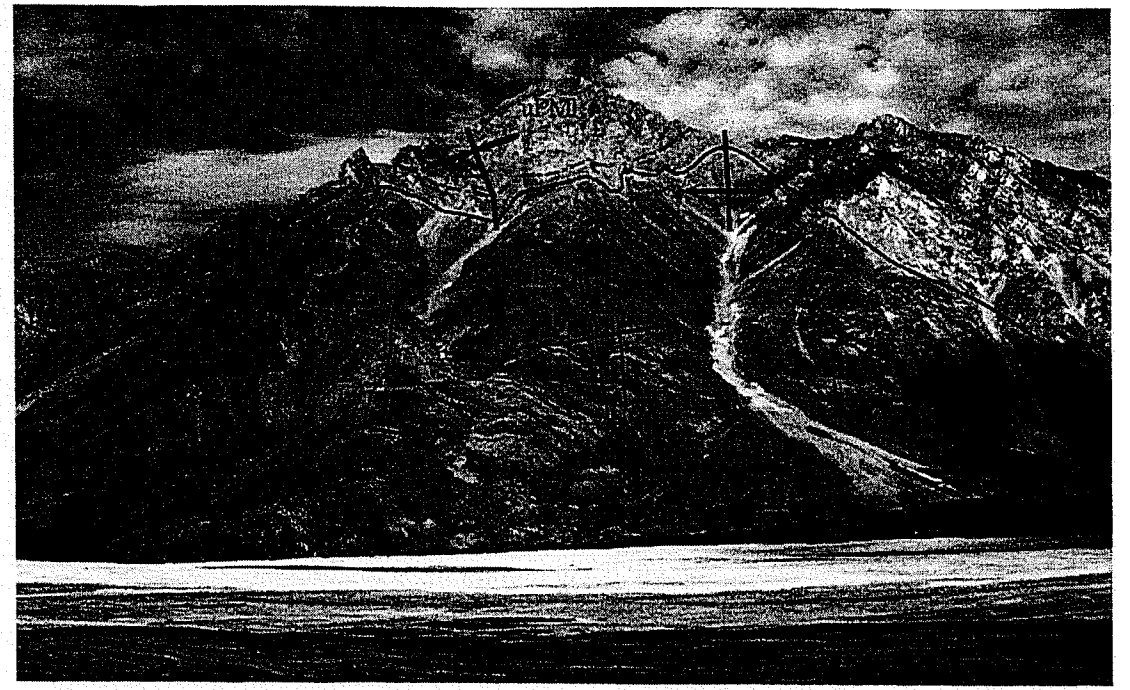

Figure 4. Typical first-order open anticline with straight limbs. Parasitic folds are abundant in the lower Lisburne, but die out upward in the upper Lisburne. East side of upper Echooka River valley.

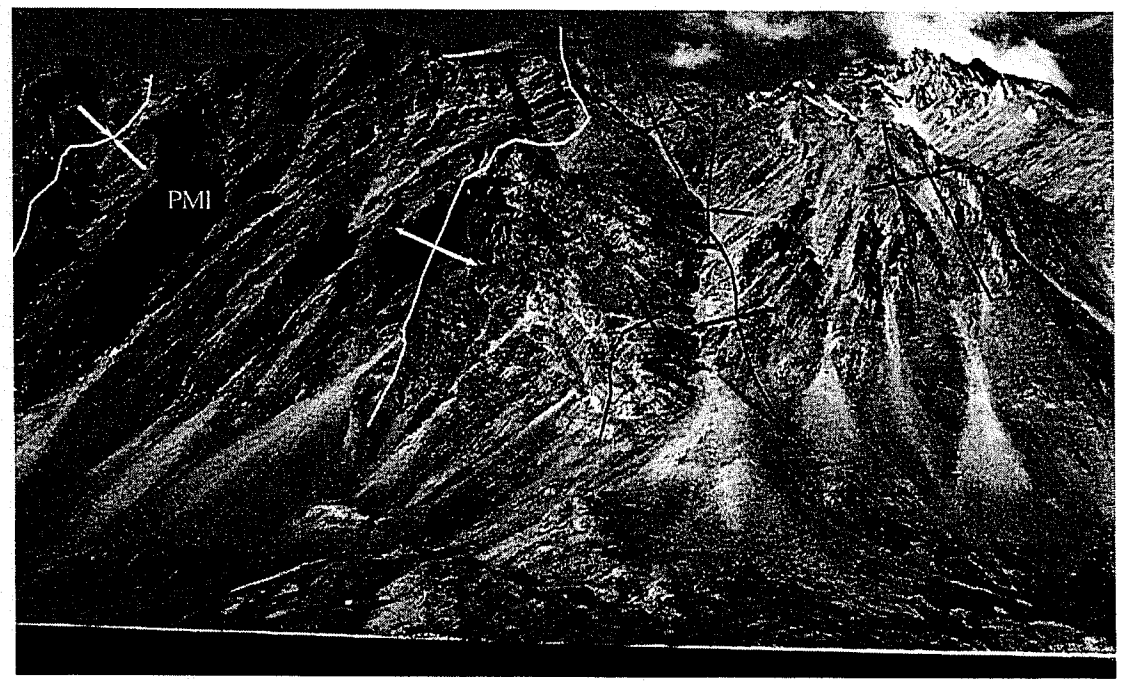

Figure 5. An anticline-syncline pair that is tighter than in figure 4, with hinges and limbs that are more curved. Mostly within upper Lisburne, but approaching the contact with the lower Lisburne toward the lower right. Local parasitic folding in fold cores. West side of upper Echooka River valley.

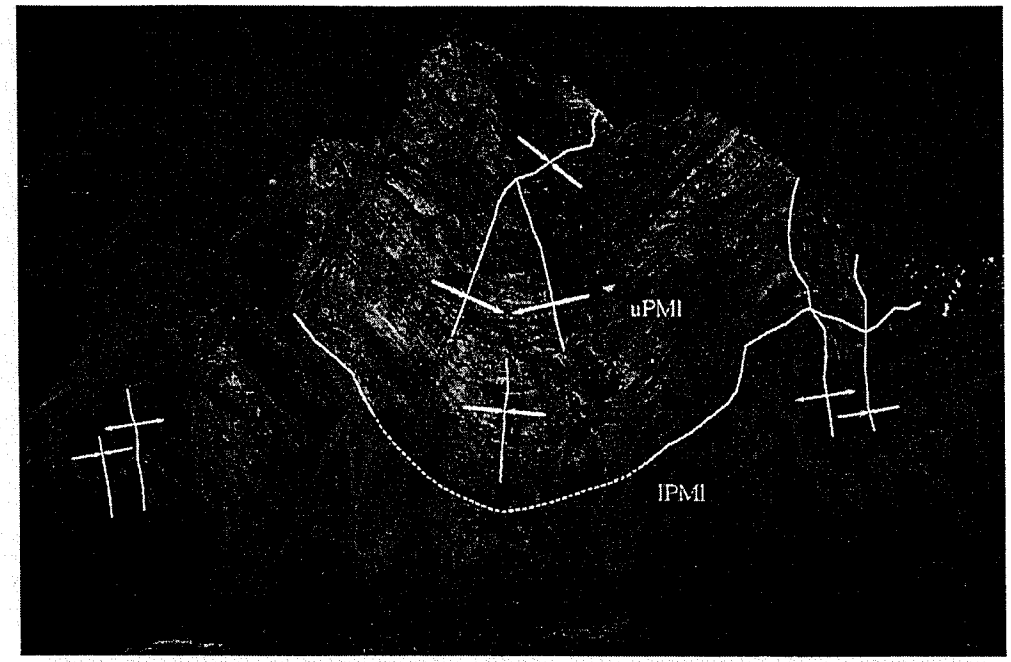

Figure 6. Well exposed syncline within upper Lisburne that displays upward internal changes in hinge zone width, curvature, and interlimb angle. Parasitic folds are best developed within lower Lisburne. West side of upper Echooka River valley.

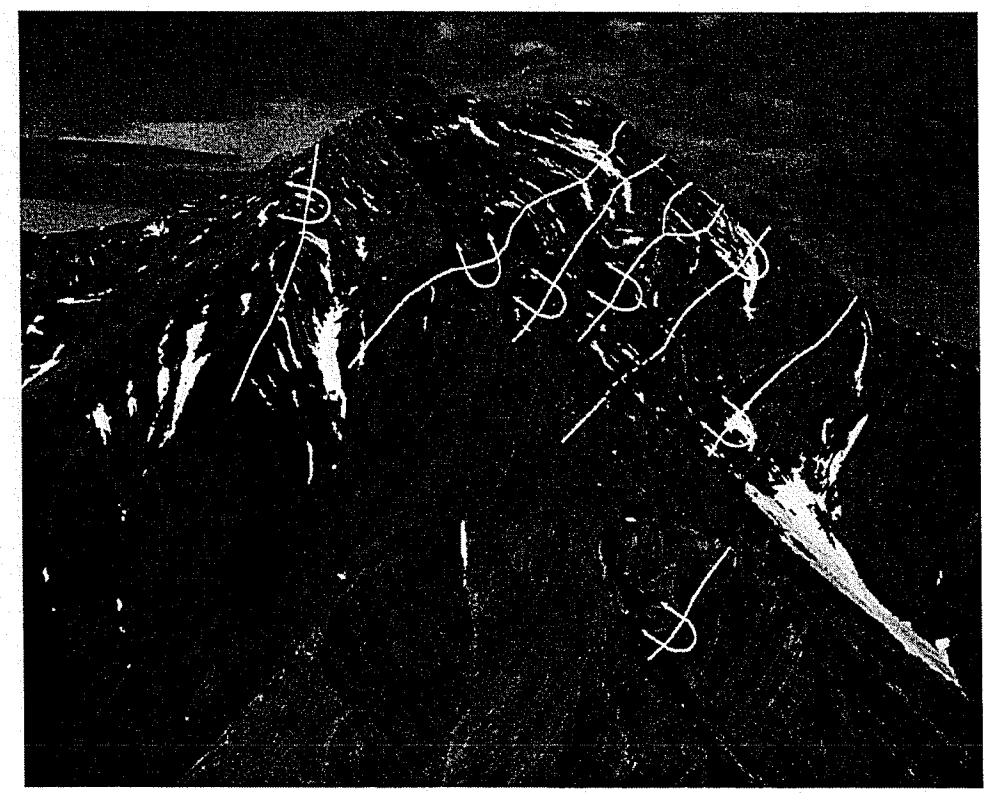

Figure 7. Parasitic folds within lower Lisburne in core of tight anticline. West side of upper Echooka River valley.

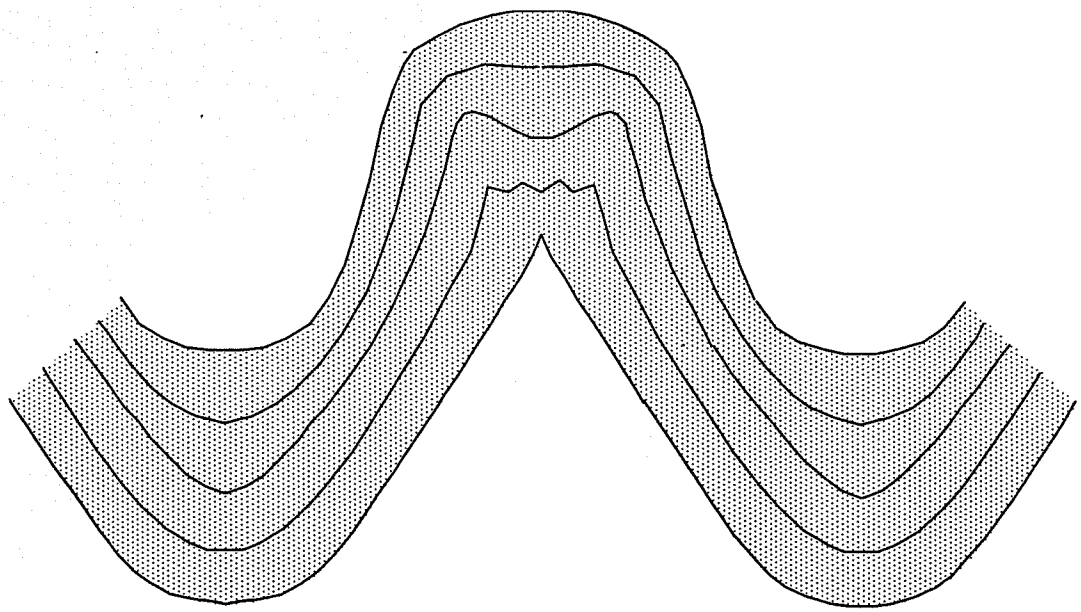

Figure 8. Idealized geometry of detachment folds as observed along upper Echooka River transect. In anticlines, limbs are straight to gently curved and hinge zones widen upward. Parasitic folding decreases upward to gently rounded anticlinal crests. Synclines tend to display less widening of the hinge zone downward, into the outer arc of the fold. This is accommodated by differing amounts of hinge thickening in different parts of the stratigraphy.

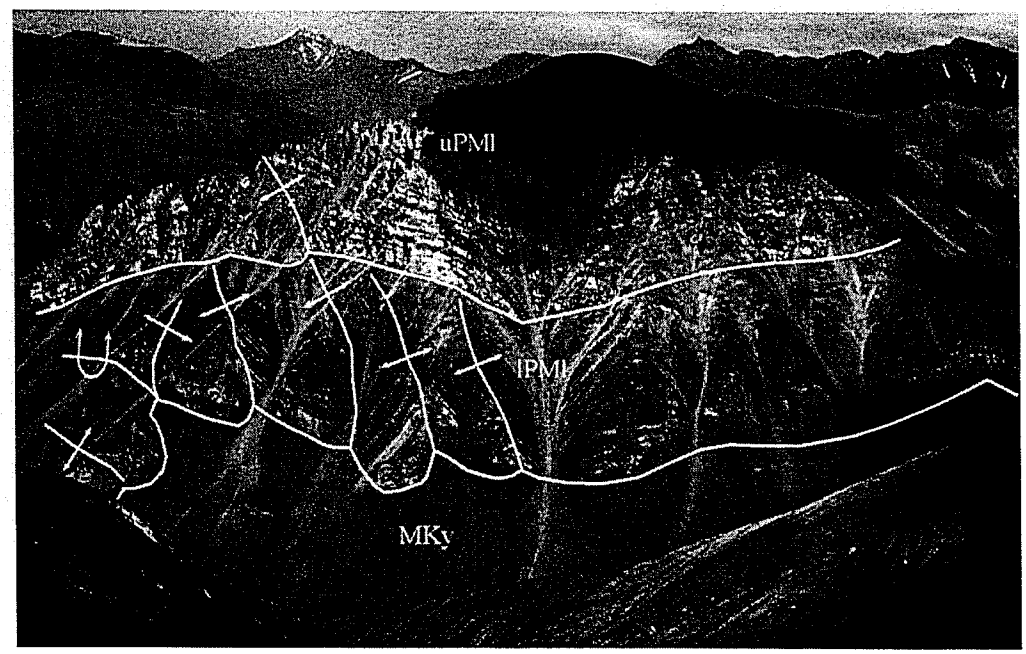

Figure 9. Anticline-syncline pair exposed from the Kayak to the upper Lisburne. Parasitic folds are tighter and more abundant within the Kayak and lower Lisburne and die out upward near the contact between lower and upper Lisburne. Fewer, gentler, and larger folds in upper Lisburne appears to reflect less fold shortening upward. South of eastern Franklin Creek, view to northeast.

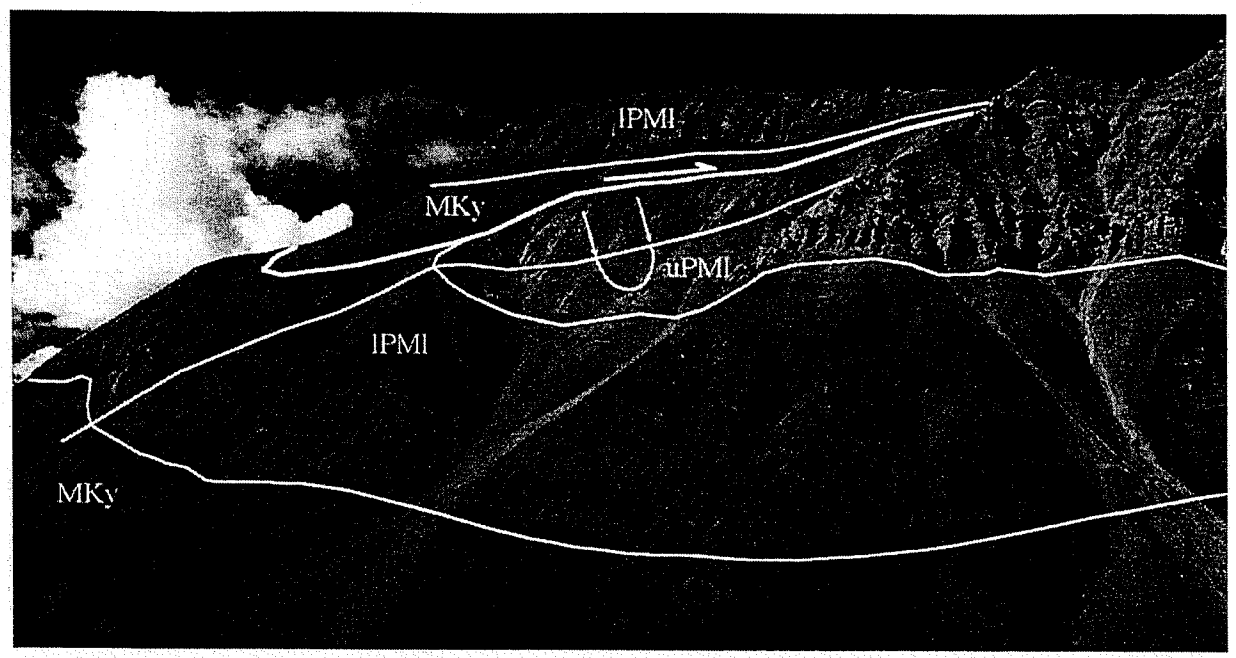

Figure 10. Footwall syncline of thrust-truncated asymmetrical anticline-syncline pair. Disharmonic parasitic folds are present in the core of the syncline in both the lower and upper Lisburne. South of eastern Franklin Creek, view to northwest.

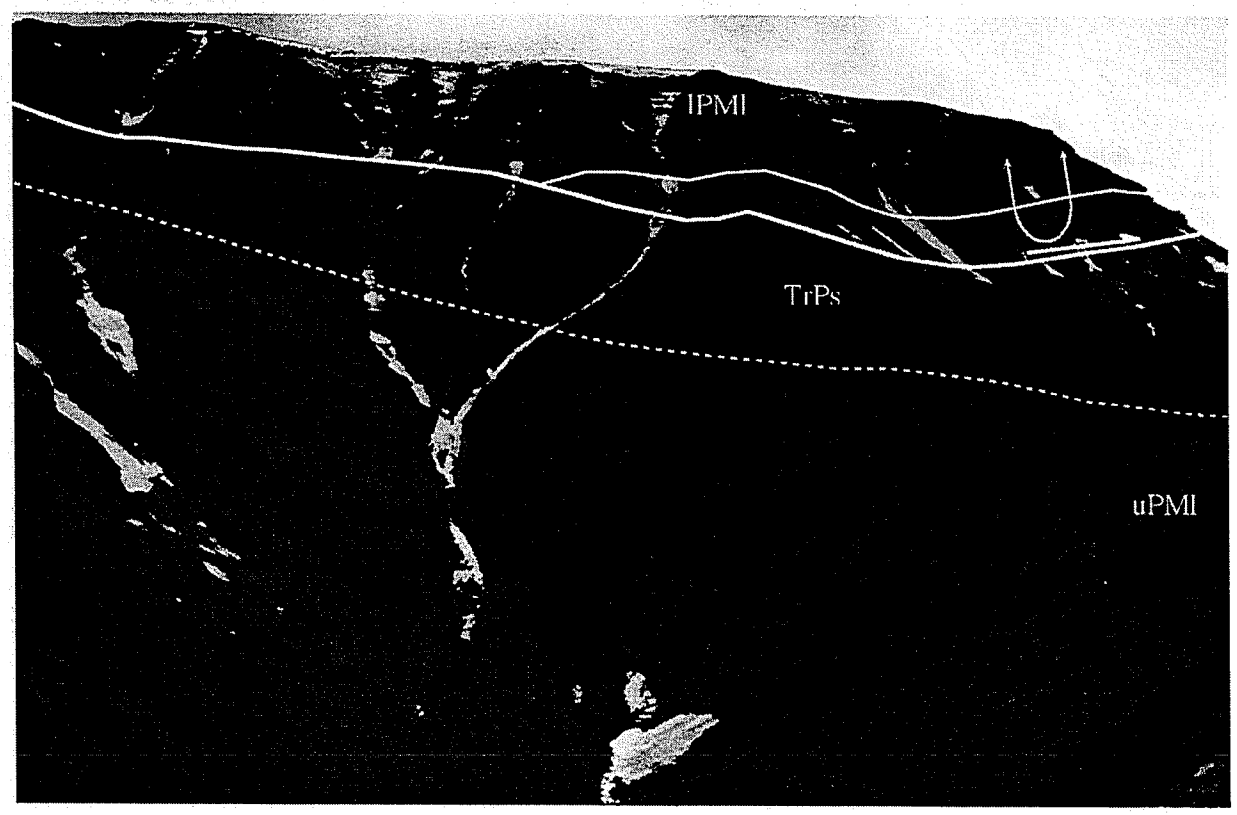

Figure 11. Tight, angular hangingwall anticline of thrust-truncated asymmetrical anticline-syncline pair. South of eastern Franklin Creek, view to southeast.

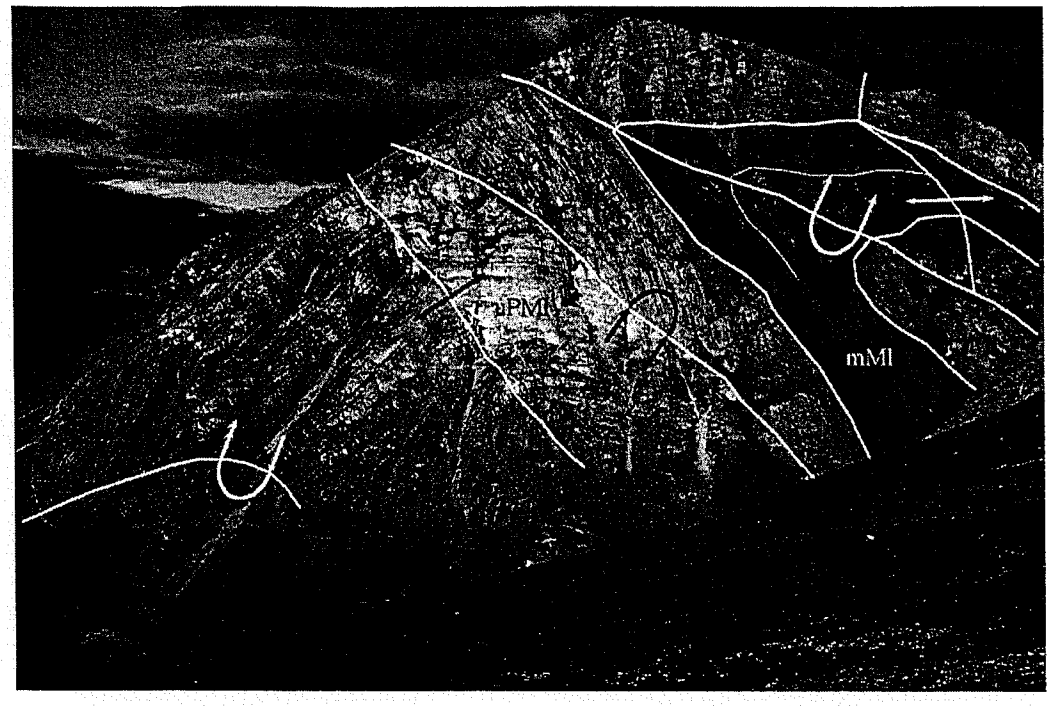

Figure 12. View to east of folded forelimb of large asymmetrical anticline. Thickening in middle Lisburne in hinge zone of main anticline (to right) accommodates different fold geometries in the more competent lower and upper Lisburne. North-dipping forelimb displays parasitic anticline-syncline pair (to left). Forelimb may be truncated by a covered thrust fault below the overturned panel (lower left) at the base of the forelimb. South of Porcupine Lake.

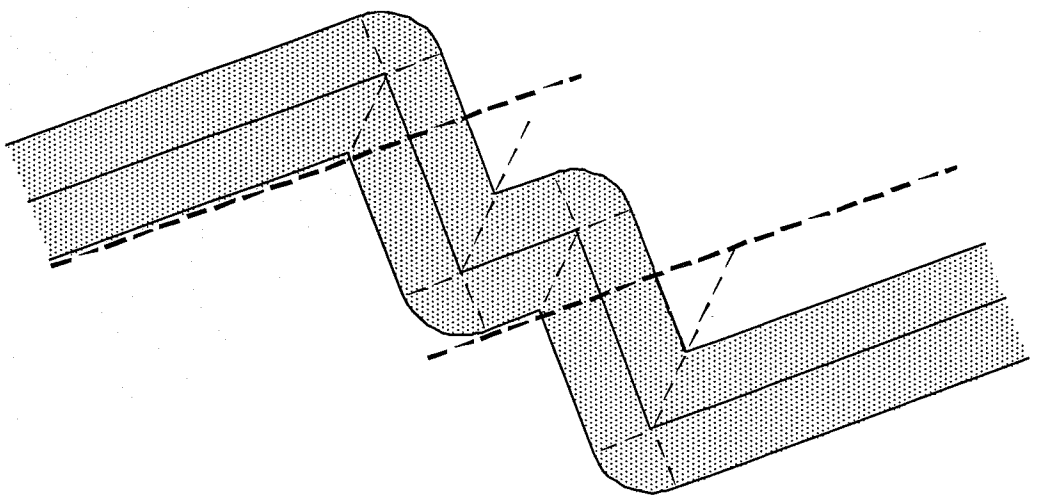

Figure 13. Idealized asymmetrical fold geometry as observed in the Porcupine Lake area. Backlimbs of anticlines (to south) are long and straight, whereas forelimbs (to north) are commonly thickened by parasitic folds, typically a single syncline-anticline pair. Angular hinge zones widen outward into the outer arcs of folds between diverging axial surfaces with branch points typically located in the middle Lisburne. Bold dashed lines mark the typical location of thrust faults that break through the forelimbs.

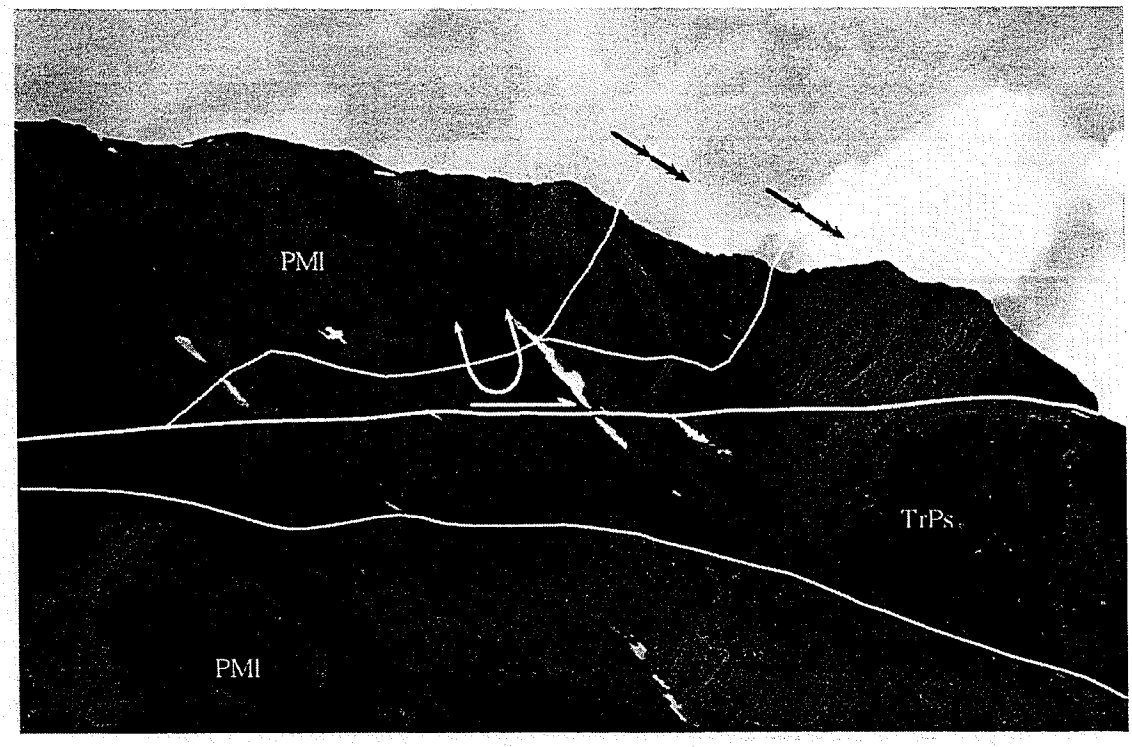

Figure 14. View to west of truncated and displaced asymmetrical anticline. Thrust cuts across inclined anticline hinge at low angle and overturned bedding in the forelimb at a high angle. Anticline hinge branches upward to define box-fold geometry. Thrust follows a flat in the Sadlerochit Group in the footwall. Near south fork of Canning River.

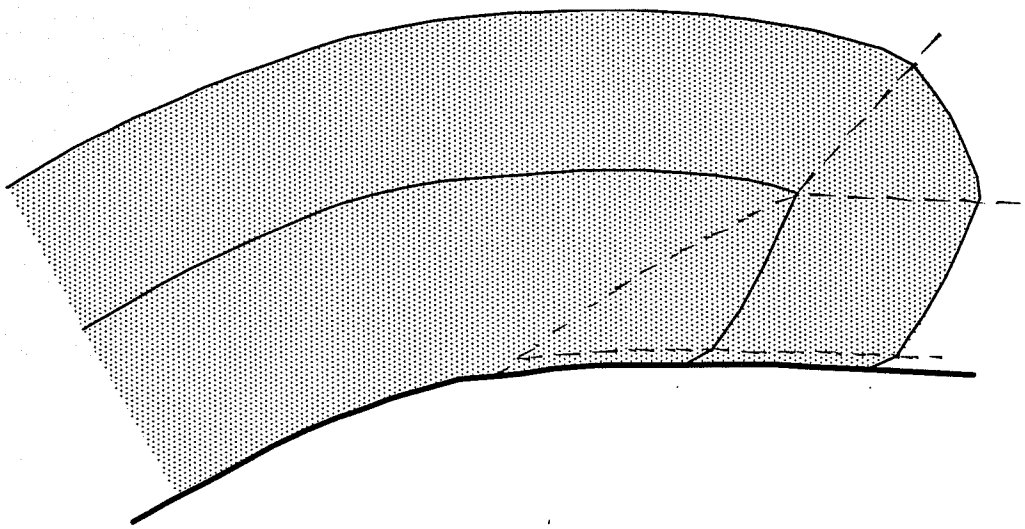

Figure 15. Idealized geometry of thrust-truncated asymmetrical fold as observed in the Porcupine Lake area. Anticline geometry as illustrated in Figure 12 is modified by displacement on a thrust fault that follows a flat in the backlimb and cuts across the forelimb at a high angle. Bedding in the forelimb is typically rotated in the sense of thrust displacement in a panel immediately above the thrust. The thrust and overlying anticline are commonly gently curved above an anticline in the footwall.

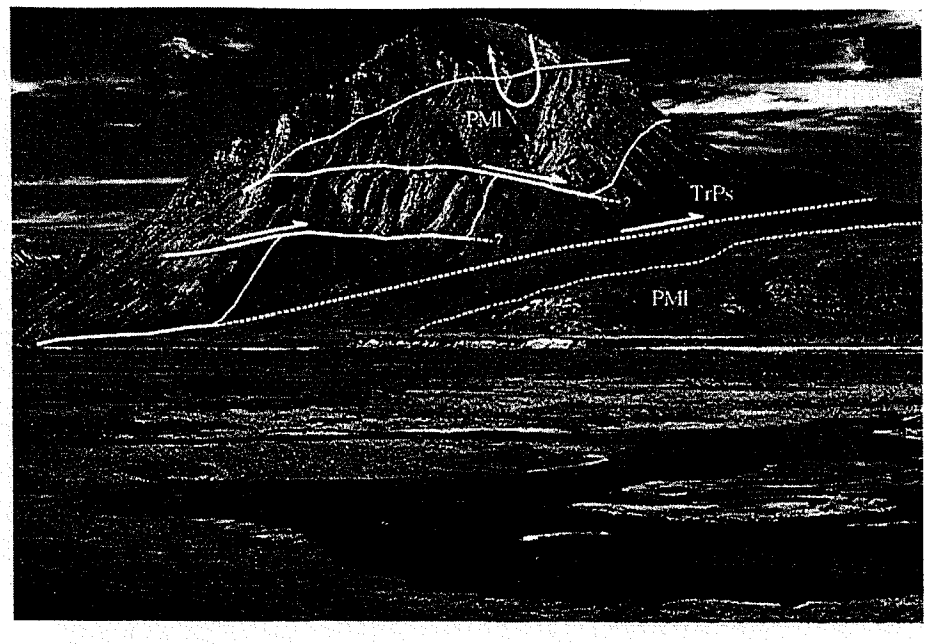

Figure 16. View to west of truncated and displaced asymmetrical anticline with angular hinge. Forelimb below inclined anticline hinge is cut at high angle by two thrust faults that are subsidiary to the main thrust fault at the base of the anticline. Bedding in a narrow zone above and below each fault is deflected in a sense consistent with fault displacement. West of Marsh Fork of Canning River.

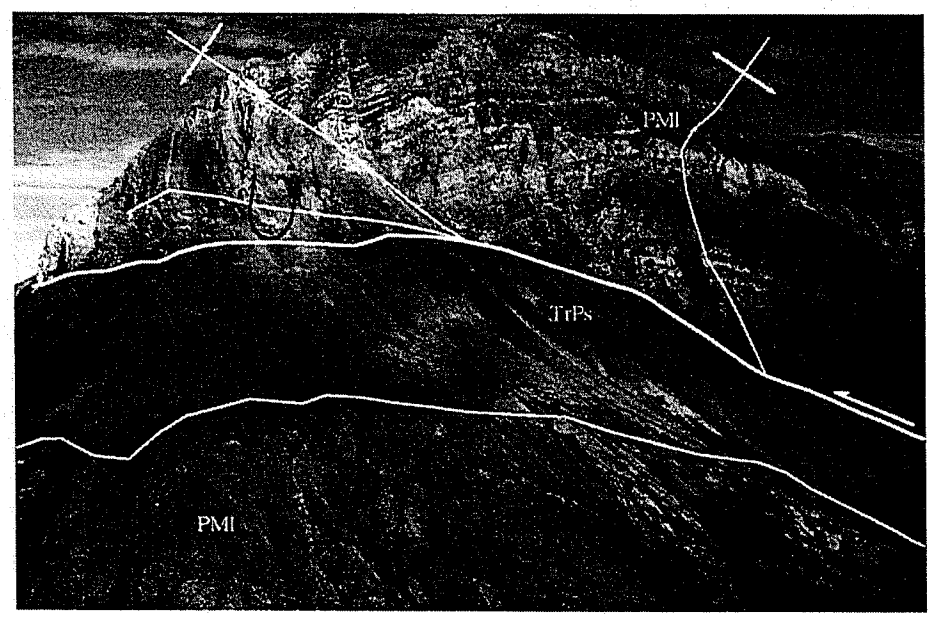

Figure 17. View to east of truncated and displaced asymmetrical anticline. Steeply dipping panel of forelimb is bounded between two inclined hinges that branch upward. Bedding in a narrow zone above the thrust fault is deflected in a sense consistent with fault displacement. Thrust follows a flat in the lowermost Lisburne in the backlimb of the anticline in the hangingwall. Thrust follows a flat in the Sadlerochit Group in the footwall. East of Marsh Fork of Canning River.

Fracture paragenesis in detachment folded Lisburne Group: implications for the thermal and structural evolution of the northeastern Brooks Range, Alaska

by C. L. Hanks, Geophysical Institute, University of Alaska, Fairbanks, Alaska, 99775, T.M. Parris, U.S. Geological Survey, Denver, Colorado, and W. K. Wallace, Geophysical Institute and Department of Geology and Geophysics , University of Alaska, Fairbanks, Alaska, 99775

Abstract

The distribution, character and relative age of fractures in detachment folded Mississippian-Pennsylvanian Lisburne Group carbonates and overlying Permo-Triassic clastic rocks in the northeastern Brooks Range of northern Alaska provide important clues as to the thermal and deformational sequence that these rocks have experienced. While paleo-thermal indices in the host rock limit the conditions of folding to temperatures equal to or less than 280 deg. Celsius, field and petrographic relationships suggest that different fracture sets formed at different times during the deformational history of the rocks, providing a record of changing temperature-pressure conditions. These rocks probably initially entered the oil generation window (100-150°C) during early Cretaceous formation of the Colville basin via thrust loading by the Brooks Range to the south. Regional fractures formed during this time as a result of high pore pressures and low in situ differential stresses. These rocks began to experience shortening related to the advancing northeastern Brooks Range fold-and-thrust belt at ~80 Mybp. Early phases of detachment folding were via flexural slip, with associated fracturing. With continued shortening and growth of detachment folds, structural thickening resulted in deeper burial of the bottom portion of the deforming wedge. Early fold-related fractures were subsequently overprinted by penetrative strain during peak folding at temperatures $\leq$280°C. Continued shortening resulted in uplift. Late fold-related fractures formed at ~150°C. Subsequent uplift of the thickened wedge through 60°C occurred after 25 Mybp. Late pervasive extension fractures related to unroofing and/or regional stresses formed at relatively shallow depths and low temperatures, overprinting all the earlier fractures and penetrative structures.

Introduction

Accumulation of oil and gas in stratigraphic or structural traps is strongly dependent on where and when the traps form relative to generation and migration. Fractures play an important role in both providing a potential migration pathway from source rocks to reservoir, and in providing permeability within that reservoir. However, fractures can form at various times and under various conditions in the evolution of a fold-and-thrust belt. Integrating the timing of fracture development with the timing of oil and gas generation and migration could provide valuable information on the both thermal evolution of the basin, and the timing of structures in the basin. Such information would be valuable in understanding evolving petroleum systems in the basin.

The North Slope of northern Alaska is a well-established petroleum province, with cumulative production of over 9.9 billion barrels of oil and condensate, and identified reserves of 6.1 BBO and 26.5 TCFG (State of Alaska, 1994). However, the producing and most intensely explored area on the North Slope is limited to the northern margin of a large foreland basin, the Colville basin. Initial exploration in the central and southern Colville basin during the 1960's and 70's

established that significant gas and light oil accumulations could exist in this part of the basin, but further exploration for these potential resources has been slow, in large part because of a lack of understanding of the controls on the distribution and trapping of the oil and gas.

In this part of our study, the age, distribution and character of fractures associated with detachment-folded Lisburne Group in the northeastern Brooks Range is integrated with new fluid inclusion microthermometric and existing geochronologic data. The integrated data are used to construct a burial history for the Lisburne Group at the sampled location that illustrates key deformation events, and variation in pressure and temperature through time. This burial history suggests that a significant regional fracture network was probably in place during hydrocarbon generation, providing hydrocarbon migration pathways to other parts of the basin. However, hydrocarbon generation and migration most likely occurred prior to the development of major. Several generations of fractures associated with and postdating folding could have enhanced reservoirs within the Lisburne during Tertiary generation and migration.

Background

Geologic setting

The Brooks Range is the northernmost part of the Rocky Mountain fold-and-thrust belt (figure 1). The majority of shortening in the fold-and-thrust belt occurred in Late Jurassic to Early Cretaceous time when a wide, south-facing late Paleozoic to early Mesozoic passive continental margin collapsed in response to the collision of an intraoceanic arc (Mayfield and others, 1988; Moore and others, 1994). Structural loading of the old passive continental margin by northward advancing thrust sheets resulted in the initiation of a foreland basin, the Colville basin. Shortly after the main phase of compressional collapse of the continental margin, rifting led to formation of the oceanic Canada basin to the north (present geographic coordinates) in Early Cretaceous time (Grantz and May, 1983; Moore and others, 1994). Post-collisional contraction has occurred episodically throughout the Cenozoic to the present, and has resulted in northward advancement of fold-and-thrust deformation in the northeastern Brooks Range and locally across the Cretaceous rifted margin (Grantz and others, 1990; Hanks and others, 1994).

The stratigraphy of the northeastern Brooks Range can be divided into three depositional sequences (figure 2; Reiser, 1970; Mull, 1982). Slightly metamorphosed, deformed Proterozoic to Devonian sedimentary and volcanic rocks are depositional basement for northerly derived Mississippian to Lower Cretaceous passive margin sedimentary rocks of the Ellesmerian sequence (Reiser, 1970; Reiser and others, 1980; Lane, 1991; Moore and others, 1994). These Ellesmerian sequence rocks are overlain by Lower Cretaceous to Recent clastic rocks of the Brookian sequence, which were derived from the Brooks Range fold-and-thrust belt to the south and deposited in the Colville basin.

The regional and local structural style of the northeastern Brooks Range is strongly influenced by mechanical stratigraphy of this lithostratigraphy (figure 3; Wallace and Hanks, 1990; Wallace, 1993). The largest structures are regional anticlinoria cored by pre-Mississippian metasedimentary and metavolcanic rocks. These regional anticlinoria are interpreted to reflect horses in a regional duplex between a floor thrust at depth and a roof thrust in the Mississippian

Kayak Shale (figure 4). The overlying Ellesmerian and Brookian sequences are decoupled from the basement and deform as the roof of a passive-roof duplex. The Carboniferous Lisburne Group (figure 2) is the most rigid member of this roof sequence and deforms predominantly into kilometer-scale symmetrical detachment folds that are only rarely cut by thrust faults. These detachment folds are second-order folds above the basement anticlinoria. Overlying Permian and Triassic clastic rocks are slightly decoupled from the Lisburne Group, resulting in third-order folds.

The regional thermal history of the northeastern Brooks Range is constrained by a variety of thermal data. All of the Paleozoic rocks exposed in this part of the Brooks Range are thermally overmature (Johnsson and others, 1993). Conodont samples from Lisburne Group carbonates in the northeastern Brooks Range have CAI values generally >4, indicating exposure to temperatures in excess of 150°C (Watts and others, 1995, Rejebian, and others, 1987; Atkinson, 2001). Thermal and structural modeling based on both outcrop data and data from nearby wells (Cole and others, 1999) suggests that Lisburne Group rocks reached temperatures in excess of 200°C in some parts of the range.

40Ar/39Ar and fission track data constrain the age of uplift and unroofing in the northeastern Brooks Range. Published 40Ar/39Ar ages suggest thrusting at ~60 Mybp (e.g., refs) and apatite fission track analysis indicates periods of uplift and unroofing at 60, ~43 and ~28 Mybp (Peapples and others, 1997; O'Sullivan and others, 1995).

The origin of multiple generations of fractures in folded rocks

It has long been assumed by many authors that the fractures observed associated with folded rocks in a fold-and-thrust belt are directly related to the formation of those folds (e.g., Stearns and Friedman, 1972; Cosgrove, 2000). The orientation of shear and extension fractures is interpreted as related to the orientation of stresses during folding. (e.g., Stearns and Friedman, 1972; Cosgrove, 2000). Fracture characteristics, such as height and spacing, are interpreted to be related to structural position and the amount of bed curvature (e.g. Jamison, 1997).

However, pervasive fracturing is not limited to deformed rocks. Regional extension fractures are also observed in flat-lying rocks. These extension fractures are interpreted as forming either at depth under low differential stresses and high pore fluid pressure (e.g. Lorenz and others, 1991) or at near surface conditions as a result of uplift and erosion and subsequent removal of lithostatic load (e.g. Hancock and Engelder, 1989).

Rocks that have been incorporated into a foreland fold-and-thrust belt and are now exposed at the surface have undergone a complex history of changing pressure, temperature and stress conditions that would provide several different opportunities for fracturing to occur (figure 5). Early extension fracturing could occur in the foreland basin, while the rocks were flat-lying and experiencing low differential stresses and high pore pressures due to dewatering. These fractures would be regional in scale and oriented parallel to the maximum stress direction, perpendicular to the active thrust front. Incorporation of these rocks into the advancing fold-and-thrust belt would result in extension and shear fractures related to folding and faulting. This deformation would also result in overall structural thickening of the thrust belt. Structural

thickening or continued foreland development of the thrust wedge would result in uplift and unroofing of the deformed rocks. If fluid pressures are high, fractures could form under the low differential stresses present in the thrust wedge. Alternatively, fractures could form as a result of unroofing and reduction in lithostatic pressure.

Previous results of this study suggest that such a progression in fracturing is observed in detachment-folded Lisburne Group of the northeastern Brooks Range fold-and-thrust belt (Hanks and others, 2002). Fractures predate folding, are apparently related to folding, and postdate peak folding. Key to establishing the relative timing of these fractures is the penetrative strain associated with peak shortening in the tightest folds. The penetrative strain provides an important marker in establishing which fractures predate and which post-date folding.

New constraints on the conditions of deformation provided by this study

Up to this point, field observations and analysis of detachment folds and the mesoscopic structures associated with them have provided a relative sequence of deformational events. However, this relative sequence of events does not establish when the folds and fractures formed with respect to hydrocarbon generation and migration. This can be achieved by combining the qualitative structural information with quantitative constraints on the thermal and uplift history of the rocks.

Structural Constraints

There are four generations of fractures associated with detachment-folded Lisburne carbonates in the northeastern Brooks Range (Table 1). These fractures sets are identified as pre-, early, late and post-folding based on cross cutting and/or abutting relationships, and relationship to penetrative strain that developed at peak folding.

The first fracture set (set 1, table 1) has been interpreted to be a regional, pre-folding set of extension fractures that formed in the undeformed foreland basin in front of the advancing thrust belt (Hanks and others, 1997). In this interpretation the fractures formed at depth and at high pore pressures, parallel to maximum in situ horizontal stress. Fractures in this set are best preserved in relatively undeformed sections of Lisburne and are rarely identified in folded sections.

Extension fractures in the second set (set 2, table 1) are oriented parallel and perpendicular to the fold axes and are usually filled with calcite. Rare bed parallel fractures and shear fractures oblique to the fold axes are included in this set (figure 6). The fractures in this set are interpreted to have formed during the early phases of detachment folding, probably as a consequence of flexural slip folding and/or outer arc extension in the hinge region. The fractures predate ductile structures that facilitated thickening in the hinges and thinning in the limbs during peak folding.

Penetrative strain post-dates fracture sets 1 and 2 and predates fracture sets 3 and 4 (Table 1, figure 7). Evidence for strain includes stretched and elongated chert nodules, deformed crinoids and peloids, and sheared stylolites. Penetrative strain occurs primarily in the fold hinges, where

it accommodates thickening. In the tightest detachment folds, penetrative strain also is evident in the fold limbs where beds are thinned.

The third fracture set consists of extension fractures that strike parallel to the fold axes and extensional shear fractures that are oblique to the fold axes. Both fracture types dip perpendicular to bedding and cut ductile structures that formed during peak folding (set 3, table 1; figure 8). These fractures are occasionally filled with calcite. Statistical analysis of fracture spacing in set 3 suggests that these fractures are not closely related to folding (Bui and others, in review). This fracture set is interpreted to have formed during late folding or after folding, possibly as a result of the decrease in overburden due to uplift and erosion and subsequent release of stored elastic strain.

Fracture set 4 consists of pervasive open, unfilled extension fractures that strike NNW perpendicular to fold axes (set 4, table 1; figure 9). These fractures are vertically extensive and cut across bedding. Statistical analysis suggests that this fracture set does not have a close relationship to folding (Bui and others, in review). While superficially similar to fracture set 1, fracture set 4 is undeformed and not filled with calcite. Fracture set 4 can be interpreted as similar in origin to fracture set 1 (i.e, related to in situ horizontal stresses in the subsurface) or, alternatively, related to overburden removal during uplift and erosion.

Thermal constraints

Thermometric analysis of fluid inclusions in fracture cements can provide information about the temperature, pressure, and fluid composition conditions of cement formation (e.g. Kisch and Van Den Kerkhof, 1991; Evans and Battles, 1999). Thermometric measurements made in this study include: (1) homogenization temperature of aqueous two-phase inclusions, which is a measure of the temperature of cement formation; (2) final ice melting temperature of aqueous two-phase inclusions, which is a measure of bulk salinity; and (3) homogenization temperature of single-phase gas-rich inclusions, which can be used qualitatively assess gas composition. Measurements were made on inclusions trapped during (i.e. primary and pseudosecondary) and after crystal growth (i.e. secondary). For more details of the systematics of inclusion measurements and their interpretation the reader is referred to Roedder (1984) and Goldstein and Reynolds (1994). In addition, all samples were analyzed for oil inclusions using ultraviolet light as outlined by Burruss (1991). No oil inclusions were found.

Fluid inclusion data generated to date are from fracture sets 2 and 3, and are summarized below and in Table 2. Fracture set 1 was also cemented, but was often overprinted and/or reactivated by set 4 and thus difficult to identify reliably in the field.

STRK01-5A (Upper Lisburne Group)

This sample was collected from the south limb of an isoclinal anticline, and contains examples of fracture sets 2 and 3. Fracture set 2 contains heavily twinned calcite, which is replaced by quartz. Fracture set 3 is cemented with less deformed calcite, which is also replaced by quartz, but to a lesser degree. To date, no measurements have been made in the twinned calcite of set 2 or in the less deformed calcite of fracture set 3. The quartz cement in fracture set 2, however, is

notable because it contains "bent" fibers and possible crack-seal fluid inclusion trails, suggestive of syntectonic crystal growth (figure 10A). Initial measurements of primary aqueous two-phase inclusions in the quartz cement suggest that crystal growth occurred from a dilute fluid (Tm_{ice}= -2.2°±0.2°C) at ~195°C (Th= 194°±7°C; figure 10B). Younger secondary aqueous inclusions along a healed microcrack have a mean homogenization temperature of 226°±7°C and similar final ice melting temperatures (Tm_{ice}= -2.2°±0.1°C). Homogenization temperatures in both inclusion populations represent minimum trapping temperatures.

STRK01-5E (Upper Lisburne Group)

This sample was collected on the south limb of the same isoclinal anticline as STRK01-5A, and contains calcite-cemented fractures assigned to sets 2 and 3. The set 2 fracture-fill is heavily twinned and contains shear bands (figure 7B). Thermometric analysis of questionable primary inclusions in set 2 yields a homogenization temperature of 273°±4.4°C. We view these results with caution because of deformation of cement in fracture set 2.

Fracture set 3 contains undeformed calcite spar. An attempt to do freezing analysis of aqueous single- and two-phase inclusions in the spar resulted in stretching and leakage of the inclusions. The presence of aqueous single-phase inclusions and their behavior during freezing suggests that set 3 fracture cement formed at low temperature, possibly less than 80°C (Goldstein and Reynolds, 1994).

STRK01-4D (Upper Lisburne Group)

This sample was collected from the south limb of a tight anticline at some distance from the hinge region. The sample contains one relatively undeformed calcite cemented fracture that is interpreted to belong to either fracture set 1 or 2. An initial analysis of inclusion populations in close proximity to each other reveals a wide range of composition and thermometric characteristics. The oldest population consists of possible coeval aqueous two-phase and single-phase gas-rich inclusions of possible primary origin. The aqueous inclusions have a mean homogenization temperature of 223°±4°C, which in this case, is close to true trapping temperature. On cooling to -170°C, the single-phase gas-rich inclusions produce a vapor bubble that homogenizes from -100° to -90°C. This behavior suggests the presence of a CH_4-rich gas mixture.

The coeval assemblage of inclusions is cut by younger secondary inclusions trapped along a healed microcrack. This younger assemblage consists only of single-phase inclusions, which are also CH_4-rich gas mixtures. Because of the lack of aqueous two-phase inclusions, it is not possible to get thermal data from this assemblage.

The youngest population of inclusions consists of secondary aqueous two-phase inclusions trapped along a different healed microcrack. The inclusions have a mean homogenization temperature of 147°±5.5°C. Final melting temperatures greater than 0°C (Tm_{clath}= 0.2° to 1.2°C) indicate the presence of clathrate, which is due to dissolved gas in the inclusions.

STRK01-1D (Echooka Formation)

This sample is from clastic rocks preserved in a synclinal hinge. The sample is included because the Echooka Formation immediately overlies and shares the same structural style as the Carboniferous Lisburne Group. Fractures in sandstone and siltstone of the Echooka Formation tend to be cemented with quartz, and inclusions trapped in the quartz are less prone to post-entrapment leakage as compared to inclusions in carbonate.

At least two generations of quartz cemented fractures are recognized. The oldest is parallel to bedding and is interpreted to be part of fracture set 2. Quartz cement in this fracture set is highly sheared. The younger fracture-fill, interpreted to belong to set 3, is orthogonal to bedding and the older fracture-fill, and has vague fracture walls. Quartz cement in the younger fracture-fill is relatively undeformed, and inclusion-free and clearer as compared to quartz in the older fracture-fill (figure 6B). Similar inclusion-free quartz cement also fills possible former pore spaces.

Initial thermometric analysis of possible primary aqueous two-phase inclusions in the quartz cement of the older fracture yields a mean homogenization temperature of 153°±11°C. Mean final ice melting temperature equals -3.9°±0.6°C, which is equivalent to a bulk salinity of 6.3 wt. % NaCl equivalent (Bodnar, 1992). Even though this inclusion population appears to be from quartz cement of the set 2 fractures, the quartz crystal containing the inclusions is undeformed and relatively inclusion free compared to the surrounding quartz cement. Hence the quartz cement and inclusions contained in it may belong to quartz of the younger fracture set 3

Summary of fluid inclusion analysis

The oldest inclusions analyzed thus far occur in cements of fracture set 2. Set 2 fractures and their cements are often, but not always, extensively deformed. This deformation calls into question the accuracy of the high homogenization temperatures found in some samples (e.g., STRK01-5E). The temperature conditions during cementation of set 2 fractures are probably best represented by the homogenization temperatures from STRK01-4D. In this sample, homogenization temperatures of ~223°C from coeval aqueous and gas-rich inclusions are likely representative of true trapping temperatures. Therefore, it appears that set 2 fractures were cemented at temperatures on the order of 200° to 225°C.

In STRK01-5A homogenization temperatures of ~195°C came from fluid inclusions in quartz cement that replaced calcite cement in set 2 fractures. Syntectonic growth textures in the quartz suggest that quartz replacement of calcite occurred contemporaneous with deformation of the fracture and older calcite cement. These homogenization temperatures, however, represent minimum trapping temperatures.

If homogenization temperatures (mean Th= 153°±11°C) in STRK01-1D are indeed from quartz belonging to set 3 fractures, then this suggests that cementation of set 3 fractures occurred at lower temperatures as compared to set 2 fractures. Additional evidence of low temperature deformation and cementation that postdates set 2 fractures includes: (1) aqueous secondary inclusions in STRK01-4D (Th~153°C°) that cross-cut set 2 calcite fracture cement; and (2) stretching and leaking of aqueous single- and two-phase inclusions during freezing in set 3 fracture cement in STRK01-5E.

Interpretation: pressure-temperature-time-deformation path

The relative age of the four different fracture sets, temperature information from fluid inclusions in the fracture-fills and existing regional uplift ages are used to construct a burial-deformation history for the Lisburne Group in the Fourth Range area (figure 11).

Pre-60 Mybp

Burial of the Lisburne Group during the late Paleozoic and early Mesozoic was predominantly related to subsidence along a south facing (present coordinates) passive continental margin. Approximately 1300 meters of Late Paleozoic, Triassic and Jurassic sediments were deposited on top of the Lisburne Group during this time. Initiation and growth of the main axis of the Brooks Range south of this location during late Jurassic/Early Cretaceous time resulted in approximately 4000 meters of southerly-derived Cretaceous clastic sediments being deposited in the foreland basin in the future location of the northeastern Brooks Range (Bird, 1999).

Burial of the Lisburne Group and overlying sediments in the foreland basin was accompanied by heating, compaction and dewatering. Structural and thermal modeling by Cole et al. (1999) suggests that the Lisburne Group and overlying source rocks in the Shublik Formation were probably at 4-6 km depth at this time and well within the oil generation window (assuming a 25°C paleogeothermal gradient). The earliest fractures probably formed at this time (figure 11), in response to low differential stresses and high fluid pressures in the growing foreland basin. These fractures formed perpendicular to the thrust front to the south and would have been open at considerable depths, possibly forming good migration pathways for the hydrocarbons being generated.

60 Ma regional deformational event

Regional apatite and zircon fission track data, and $^{40}Ar/^{39}Ar$ data suggest that a major uplift event occurred in the northeastern Brooks Range at ~60 mybp (O'Sullivan and others, 1995; Peapples and others, 1997). This uplift can be interpreted to reflect development of the regional pre-Mississippian cored anticlinoria in the northeastern Brooks Range. It is not clear how much deformation of the passive roof of this regional duplex (Lisburne Group and younger rocks) occurred at this time. It is likely that some detachment folding of the cover rocks began during this initial deformational episode, probably accompanied by fracturing related to flexural slip folding (figure 11). Fluid inclusion data from set 2 fracture cements suggest that this folding and associated fracturing occurred at fairly high temperatures (200°-225°C).

However, deformation of the Lisburne Group at this time was probably not accompanied by local uplift. Conodont alteration indices indicate that these rocks experienced temperatures as high as ~280°C, probably accompanied by penetrative deformation in fold cores. This increase in paleotemperature reflects continued burial of the rocks and/or an increase in the geothermal gradient. Progressive burial was probably facilitated by the combination of continued deposition of Brookian clastic rocks and deformational thickening of the foreland basin, with structural depression of the lower parts of the deformational wedge. With an assumed geothermal gradient

of 25°C/km, Ellesmerian sequence rocks would have been heated to temperatures exceeding those for oil generation (~100°-150°C) and would have reached temperatures for dry gas generation (Bird et al., 1999).

Early Tertiary deformation and uplift

Contractional deformational in the northeastern Brooks Range continued episodically into the Tertiary, with three different regional events recorded by apatite fission track analysis (45, 35 & 25 mybp; e.g., O'Sullivan and others, 1995). This deformation tightened individual folds and thickened the overall tectonic wedge. In the Fourth Range, the Lisburne Group initially experienced an increase in temperature, probably reflecting an increase in structural burial as deformation intensified (path A, figure 11). Peak folding occurred under temperature and pressure conditions that facilitated penetrative strain---~280°C as suggested by the conodont alteration indices (Johnsson et al., 1992).

Subsequent tightening of the folds and uplift resulted in late-folding to post-folding fractures of set 3. Cements in these fractures suggest that the fractures formed and filled at temperatures significantly lower that those experienced during peak folding (~153°C vs 280°C; figure 11, path A).

However, these deformational events may not have affected all areas or all parts of the stratigraphic column equally. Different burial and uplift paths are possible depending upon the regional structural setting and/or the stratigraphic position of the sample (paths A, B & C, figure 11). Rocks low in the stratigraphic section and/or located in a major synclinorium (such as the Lisburne Group in the Fourth Range) could see continual burial and temperature increase during these Cenozoic events (path A, figure 11). Higher parts of the stratigraphic section in the same location may have experienced a flatter burial curve and never experienced the highest temperatures (path B, figure 11). Rocks located on the crests of anticlinoria may have only experienced uplift and an overall reduction of temperatures during these deformation episodes (path C, figure 11).

At this point there are no constraints on the depth and temperature of formation of the north-south striking, post-fold fractures (set 4, table 2). These fractures are unfilled and appear quite young. They could have formed at 3-5 km depth in response to the low differential stresses in the upper part of the deformational wedge, if pore fluid pressures were sufficiently high. Alternatively, they could have formed very near to the surface due to uplift and removal of overburden. The first hypothesis is preferred, as bore hole breakouts in wells near the thrust front suggest that in situ stresses become highly variable near the surface (Hanks and others, 2000)

Implications

In order to accumulate hydrocarbons, trap formation must precede or coincide with oil generation and migration. This is a complex process in fold-and-thrust belts, where burial and generation of hydrocarbons in any one location generally precedes deformation. Effective

migration pathways out of the 'hydrocarbon kitchen' are necessary to fill distant traps and reservoirs.

The sequence of fracturing and fracture cementation with respect to folding at this one location in the northeastern Brooks Range provides important constraints on the relative timing of deformation versus burial and heating. Fracturing occurred prior to folding, during folding and after folding.

The earliest fracture set may have formed in early Mesozoic time, coincident with early hydrocarbon generation and migration. While it is unlikely that there were any structural traps at this time. hydrocarbons might have accumulated in stratigraphic traps.

In detachment folded Lisburne Group, fracturing occurred during early folding, probably in latest Cretaceous-Early Tertiary time, at temperatures exceeding those for oil generation (~100°-150°C). Thus traps in these types of structures would have post-dated local hydrocarbon generation and migration. This does not preclude hydrocarbons generated elsewhere in the basin migrating into these traps. However, the temperatures at which fractures formed were probably too high for significant hydrocarbons to be preserved. Peak folding and penetrative strain occurred at very high temperatures, probably destroying much existing porosity and permeability, including much of the fracture network.

Late fold and post-fold fractures occurred at significantly lower temperatures, but by this time the local hydrocarbon generation potential was probably exhausted. However, these deformed and fractured rocks were thrust over significantly younger rocks in the foredeep to the north, which could possibly provide a source mechanism.

Conclusions

The distribution, character and relative age of fractures in detachment folded Mississippian-Pennsylvanian Lisburne Group carbonates and overlying Permo-Triassic clastic rocks in the Fourth Range, and thermal information from fluid inclusions in fracture cements can be integrated to constrain the thermal and deformational sequence of these rocks. The Lisburne Group in the Fourth Range probably entered the oil generation window (100°-150°C) during early Cretaceous formation of the Colville basin due to thrust loading by the growing Brooks Range to the south. Regional fractures formed during this time as a result of high pore pressures and low in situ differential stresses possibly served as a migration pathway for hydrocarbons. These rocks did not experience significant shortening until ~60 Mybp, with the first phases of formation of the northeastern Brooks Range. Early detachment folding was characterized by flexural slip and fracturing. With continued shortening during the early Tertiary, structural thickening resulted in continued burial and/or increasing temperatures. Early fold-related fractures were subsequently overprinted by penetrative strain during peak folding at temperatures ~280°C.

Late fold-related fractures formed during at ~150°C during subsequent uplift of the thickened wedge. Late pervasive post-folding extension fractures formed at relatively shallow depths and

low temperatures, and are related to unroofing and/or regional stresses within the orogenic wedge.

While these results indicate that hydrocarbon generation predated trap formation at this location, it does not necessarily constrain the regional evolution of the petroleum system through time. Thus, hydrocarbons generated elsewhere could migrate into these rocks. Juxtaposition of these deformed rocks with less mature sediments capable of generating oil and/or gas could occur via thrusting. Alternatively, traps could be filled by lateral migration of gas from the Colville basin from the west. Collecting and integrating structural, thermal and geochronologic data from various locations throughout the North Slope, the Brooks Range and the northeastern Brooks Range fold-and-thrust belt would provide additional important clues as to the evolution of this particular petroleum system.

References

Atkinson, P.K., 2001, A geometric analysis of detachment folds in the northeastern Brooks Range, Alaska, and a conceptual model for their kinematic evolution: Master of Science thesis, University of Alaska, Fairbanks, Alaska, 209 p.

Bird, K., 1999, Geographic and Geologic setting: in The Oil and Gas Resource Potential of the Arctic National Wildlife Refuge 1002 area, Alaska: USGS Open File Report 98-34, pp GG-1-GG-51.

Bird, K.J., Burruss, R.C., and M.J. Pawlewicz, 1999, Thermal maturity, in The Oil and Gas Potential of the 1002 Area, Arctic National Wildlife Refuge, Alaska: U.S. Geological Survey Open file Report 98-34.

Bodnar, R.J., 1992, Revised equation and table for freezing point depressions of H_2O-salt fluid inclusions (abstract): PACROFI IV, Fourth Biennial Pan-American Conference on Research on Fluid Inclusions, Program and Abstracts, Lake Arrowhead, CA, v. 14, p. 15.

Burruss, R.C., 1991, Practical aspects of fluorescence microscopy of petroleum fluid inclusions, in, Barker, C.E., and Kopp, O.C., eds., Luminescence Microscopy and Spectroscopy: SEPM Short Course 25, 195 p.

Bui, T., Brinton, J., Karpov, A.V., Hanks, C.L., and Jensen,J. L., in review, Evidence and Implications for Significant Late and Post-Fold Fracturing on Detachment Folds in the Lisburne Group of the Northeastern Brooks Range: SPE publication 76754.

Cole, F., Bird, K.J., Mull, C.G., Wallace, W.K., Sassi, W., Murphy, J.M., and Lee, M., 1999, A balanced cross section and kinematic and thermal model across the northeastern Brooks Range mountain front, Arctic National Wildlife Refuge, Alaska: in The Oil and Gas Potential of the 1002 Area, Arctic National Wildlife Refuge, Alaska: U.S. Geological Survey Open file Report 98-34.

Cosgrove, J.W., 2000, Forced folds and fractures: An introduction: in Cosgrove, J.W. and Ameen, M.S., Forced Folds and Fractures, Geological Society Special Publication no. 169, pp. 1-6.

Evans, M.A., and Battles, D.A., 1999, Fluid inclusion and stable isotope analyses of veins from the central Appalachian Valley and Ridge province: Implications for regional synorogenic hydrologic structure and fluid migration: Geological Society of America Bulletin, v. 111, p. 1841-1860.

Goldstein, R.H., and Reynolds, T.J., 1994, Systematics of fluid inclusions in diagenetic minerals: SEPM Short Course 31, 199 p.

Grantz, A., and May, S.D., 1983, Rifting history and structural development of the continental margin north of Alaska, in Watkins, J.S., and Drake, C.L., eds., Studies in continental margin geology: AAPG Memoir 34, p. 77-100.

Grantz, A., May, S.D., and Hart, P.E., 1990, Geology of the Arctic continental margin of Alaska, in Grantz, A., Johnson, L., and Sweeney, J.F., eds, The Arctic Ocean region: Boulder, Colorado, GSA, The Geology of North America, v. L., p. 257-288.

Hancock, P.J., and Engelder, T., 1989, Neotectonic joints: Geological Society of America Bulletin, v. 101, p. 197-1208.

Hanks, C.L., Parker, M., and Jameson, E., 2000, Regional stress patterns of the northeastern North Slope, Alaska: Alaska Division of Geological and Geophysical Surveys' Short Notes on Alaskan Geology, 1999, p. 33-44.

Hanks, C.L., Wallace, W.K., and O'Sullivan, P., 1994, The Cenozoic structural evolution of the northeastern Brooks Range, Alaska, in Thurston, D., and Fujita, K., eds., 1992 Proceedings International Conference on Arctic Margins, U.S. Minerals Management Service Outer Continental Shelf Study 94-0040, p. 263-268.

Hanks, C.L., Lorenz, J., Teufel, L., and Krumhardt, A.P. 1997, Lithologic and structural controls on natural fracture distribution within the Lisburne Group, northeastern Brooks Range and North Slope subsurface, Alaska: American Association of Petroleum Geologists Bulletin, vol. 81, no. 10, p. 1700-1720.

Hanks, C.L., Wallace, W.K., Lorenz, J., Atkinson, P.K., Brinton, J., and Shackleton, J.R., 2002, Timing and character of mesoscopic structures in detachment folds and implications for fold development--an example from the northeastern Brooks Range, Alaska: in Wallace, W.K., and others, 2002, The influence of fold and fracture development on reservoir behavior of the Lisburne Group of northern Alaska: fourth semiannual report. Department of Energy, award DE-AC26-98BC15102. E1-E24

Jamison, W.R., 1997, Quantitative evaluation of fractures on Monkshood anticline, a detachment fold in the foothills of western Canada; American Association of Petroleum Geologists Bulletin, v. 81, no. 7, p. 1110-1132.

Johnsson, M. J., Howell, D. G., and Bird, K. J., 1993, Thermal maturity patterns in Alaska; implications for tectonic evolution and hydrocarbon potential: American Association of Petroleum Geologists Bulletin 77, no. 11, p. 1874-1903.

Johnsson, M.J., Pawlewicz, M., Harris, A.G., and Valin, Z.C., 1992, Vitrinite reflectance and conodont color alteration index from Alaska: U.S. Geological Survey Open-File Report 92-409, 3 computer disks, 1 sheet.

Kisch, H.J., and Van Den Kerkhof, A.M., 1991, CH_4-rich inclusions from quartz veins in the Valley and Ridge province and anthracite fields of the Pennsylvanian Appalachians: American Mineralogist, v. 76, p. 230-240.

Lane, L.S., 1991, The pre-Mississippian "Neruokpuk Formation," northeastern Alaska and northwestern Yukon: review and new regional correlation: Canadian Journal of Earth Sciences, v. 28, pp. 1521-1533

Lorenz, J. C., Teufel, L. W., and Warpinski, N. R., 1991, Regional fractures 1: A mechanism for the formation of regional fractures at depth in flat-lying reservoirs: American Association of Petroleum Geologists Bulletin, v. 75, no. 11, p. 1714-1737, 16 figs.

Mayfield, C.F., Tailleur, I.L., and Ellersieck, I., 1988, Stratigraphy, structure, and palinspastic synthesis of the western Brooks Range, northwestern Alaska: in Gryc, G. ed., Geology and Exploration of the National Petroleum Reserve in Alaska, 1974 to 1982: U.S. Geological Survey Professional Paper 1399, p. 143-186.

Moore, T.E., Wallace, W.K., Bird, K.J., Karl, S.M., Mull, C.G., and Dillon, J.T., 1994, Chapter 3: Geology of northern Alaska, in Plafker, G., and Berg, H.C., eds., The geology of Alaska: The Geology of North America, Geological Society of America, Boulder, Colorado, v. G1, p. 49-140.

Mull, C.G., 1982, Tectonic evolution and structural style of the Brooks Range, Alaska: An illustrated summary, in Powers, R.B., Ed., Geologic studies of the Cordilleran thrust belt: Rocky Mountain Association of Geologists, Denver, Co., v.1, p.1-45.

O'Sullivan, P.B., Hanks, C.L., Wallace, W.K., and Green, P.F., 1995, Multiple episodes of Cenozoic denudation in the northeastern Brooks Range: Fission track data from the Okpilak batholith, Alaska: Canadian Journal of Earth Sciences, v. 32, no. 8, p. 1106-1118.

Peapples, P.R., Wallace, W.K., Hanks, C.L., O'Sullivan, P.B., and Layer, P.W., 1997, Style, controls, and timing of fold-and-thrust deformation of the Jago stock, northeastern Brooks Range, Alaska: Canadian Journal of Earth Sciences, vol. 34, p. 992-1007.

Reiser, H.N., 1970, Northeastern Brooks Range--a surface expression of the Prudhoe Bay section, in W.L. Adkison and M.M. Brosgé, eds., Proceedings of the geological seminar on the North Slope of Alaska: AAPG Pacific Section, p. K1-K13.

Reiser, H.N., Brosgé, W.P., Dutro, J.T., Jr., and Detterman, R.L., 1980, Geologic map of the Demarcation Point quadrangle, Alaska: U. S. Geological Survey Miscellaneous Investigations Series Map I-1133, scale 1:250,000, 1 sheet.

Rejebian, V.A., Harris, A.G., and Huebner, J.S., 1987, Conodont color and textural alteration: an index to regional metamorphism, contact metamoprhism, and hydrothermal alteration: Geological Society of America Bulletin vo. 99, p. 471-479

Roedder, E., 1984, Fluid inclusions: Mineralogical Society of America, Reviews in Mineralogy, v. 12, 646 p.

Stearns, D.W., and Friedman, M., 1972, Reservoirs in fractured rock: in American Association of Petroleum Geologists Memoir 16, p. 82-100.

Wallace, W.K., 1993, Detachment folds and a passive-roof duplex: Examples from the northeastern Brooks Range, Alaska, in Solie, D.N., and Tannian, F., eds., Short Notes on Alaskan Geology 1993: Alaska Division of Geological and Geophysical Surveys Geologic Report 113, p. 81-99.

Wallace, W.K., and Hanks, C.L., 1990, Structural provinces of the northeastern Brooks Range, Arctic National Wildlife Refuge, Alaska: American Association of Petroleum Geologists Bulletin, v. 74, no. 7, p. 1100-1118.

Wallace, W.K., Moore, T.E., and Plafker, G., 1997, Multistory duplexes with forward dipping roofs, north central Brooks Range, Alaska: Journal of Geophysical Research, v. 102, no. B9 (special section on the USGS Trans-Alaska Crustal Transect), p. 20,773-20,796.

Watts, K.F., Harris, A.G., Carlson, R.C., Eckstein, M.K., Gruzlovic, P.D., Imm, T.A., Krumhardt, A.P., Lasota, D.K., Morgan, S.K., Enos, P., Goldstein, R.H., Dumoulin, J.A., and Mamet, B.L., 1995, Analysis of reservoir heterogeneities due to shallowing-upward cycles in carbonate rocks of the Pennsylvanian Wahoo Limestone of northeastern Alaska: United States Department of Energy, Final Report for 1989-1992, Bartlesville Project Office.

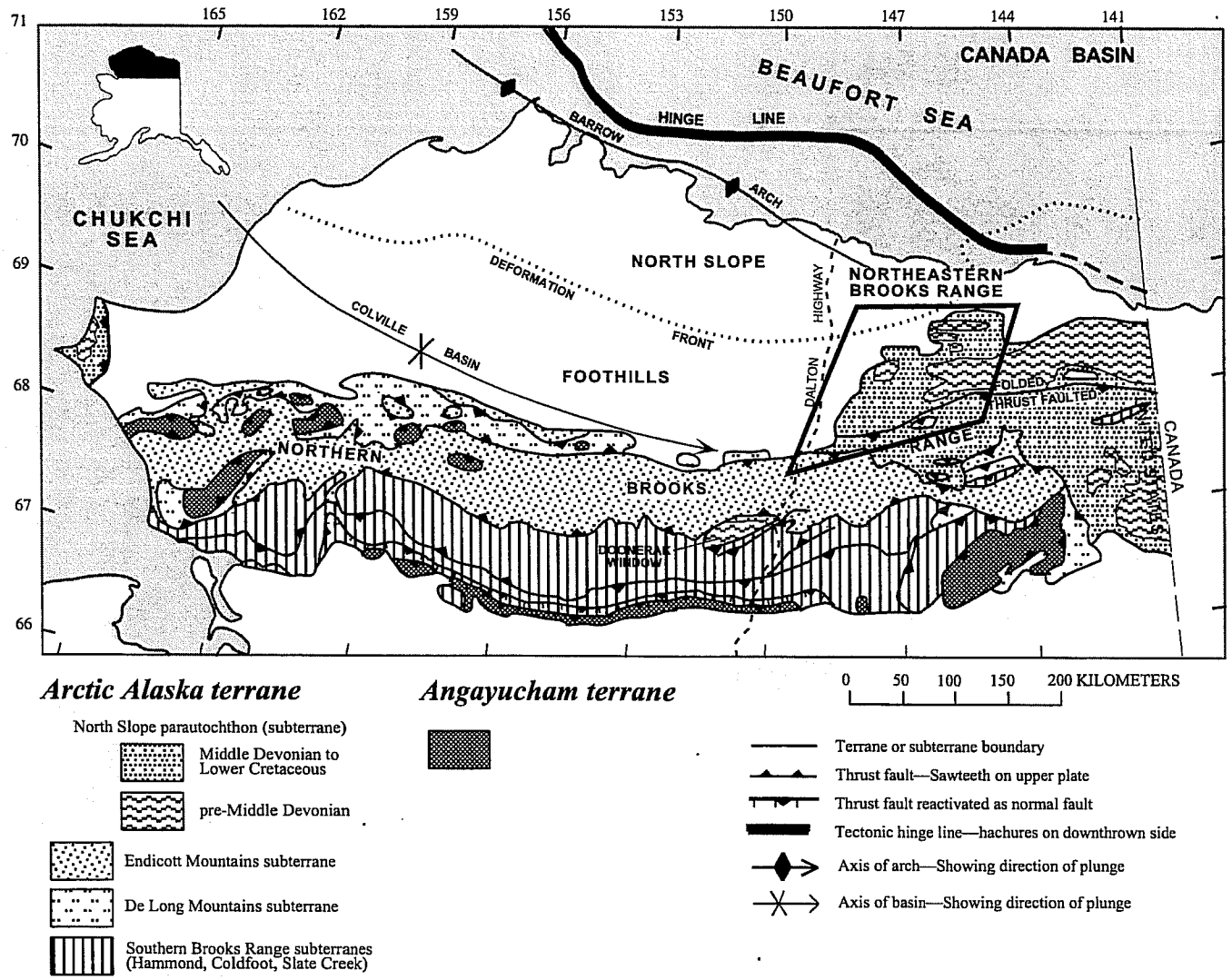

Figure 1. Tectonic map of northern Alaska, showing distribution of major structural features. Outlined area shown in figure 2. Modified from Wallace and others, 1997.

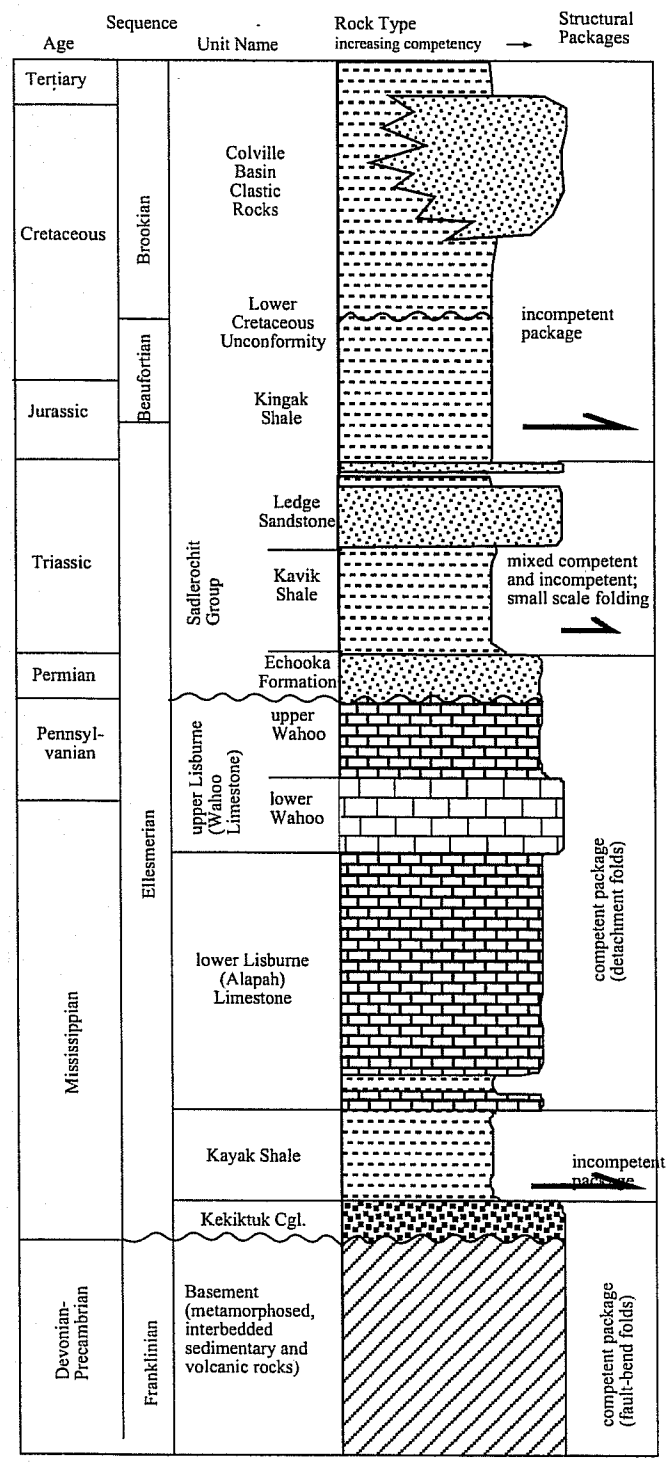

Figure 2. Generalized stratigraphy of the northeastern Brooks Range, emphasizing the mechanical stratigraphy of structural packages. Only the Triassic and older rocks are exposed in the Straight Creek area.

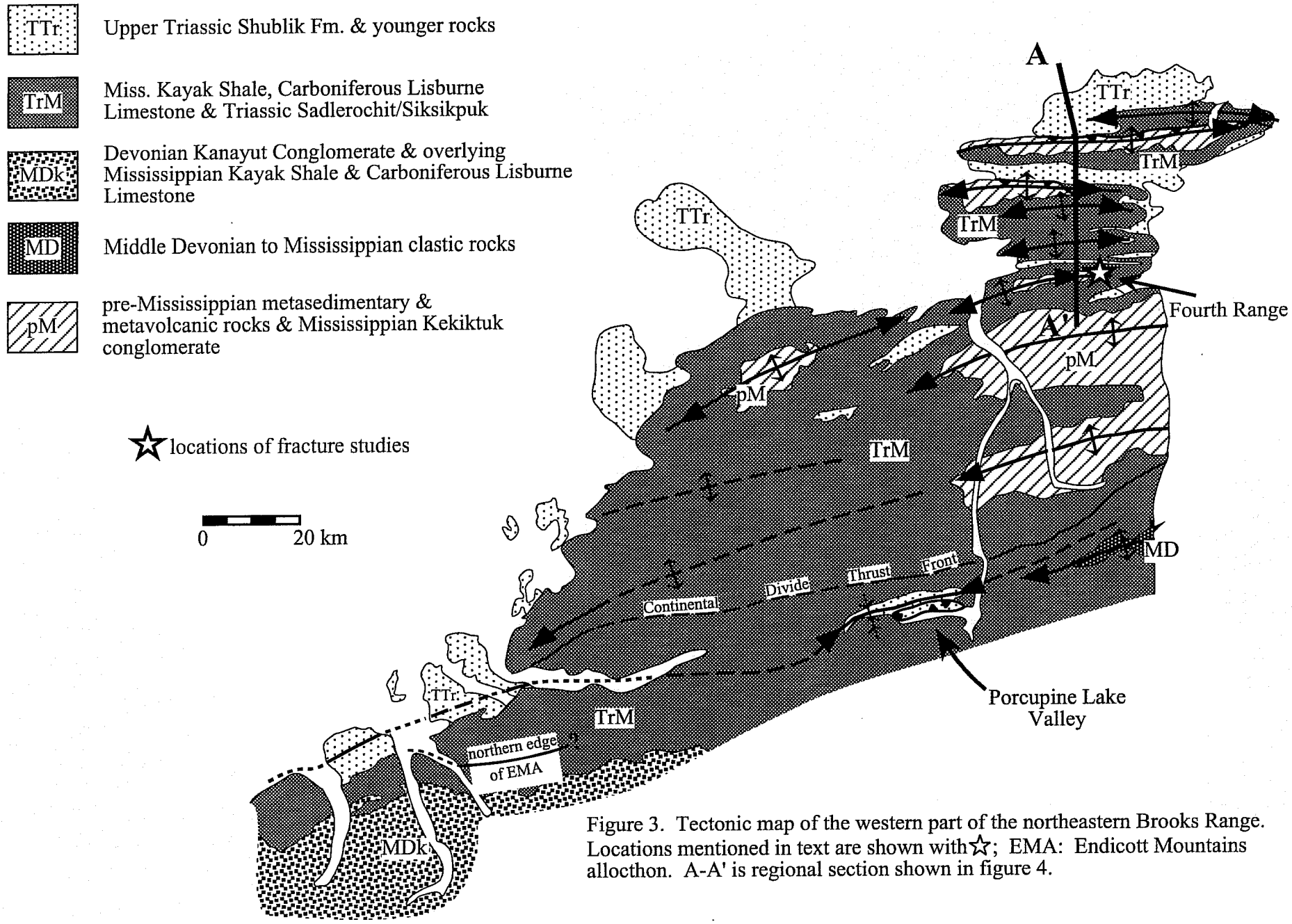

Figure 3. Tectonic map of the western part of the northeastern Brooks Range. Locations mentioned in text are shown with☆; EMA: Endicott Mountains allocthon. A-A' is regional section shown in figure 4.

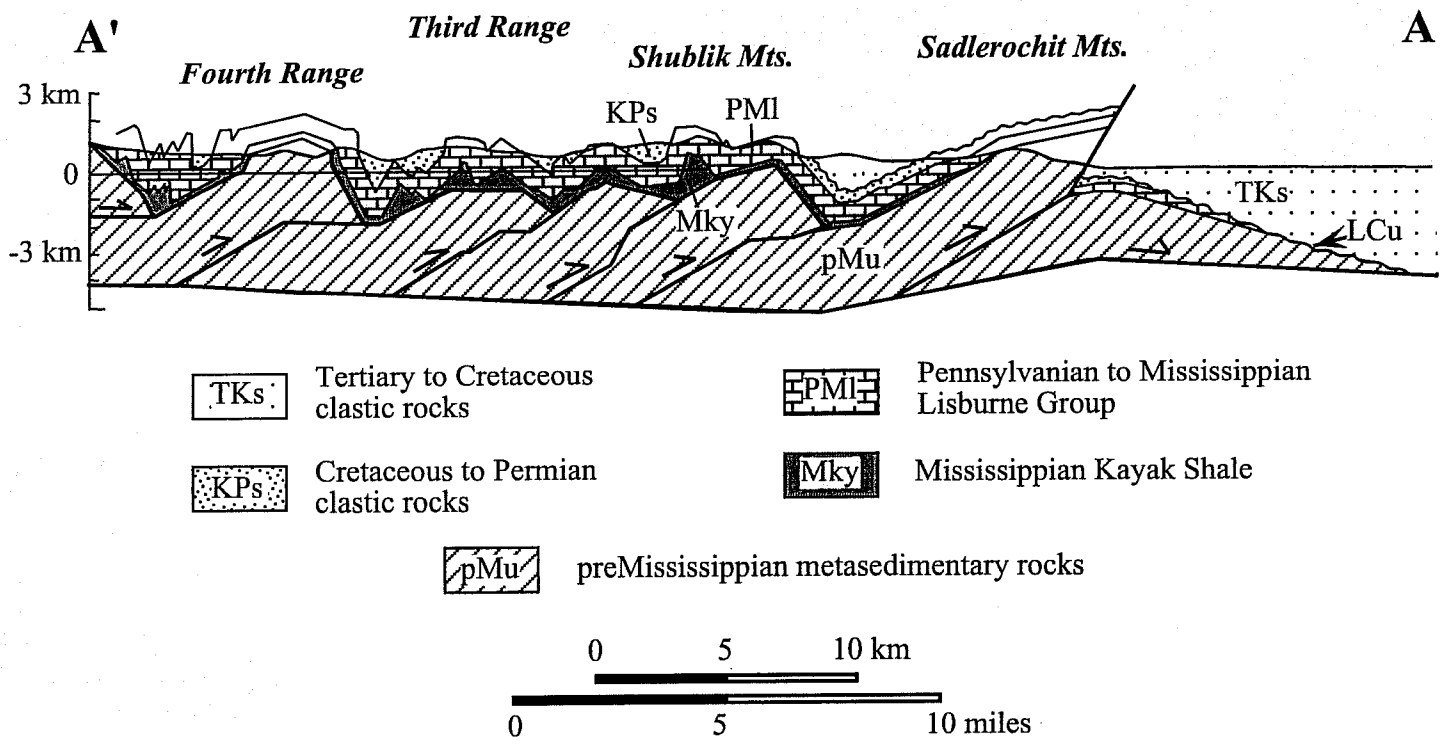

Figure 4. Regional balanced cross section across the northwestern part of the northeastern Brooks Range. Location of section line shown on figure 3. Modified from Wallace, 1993.

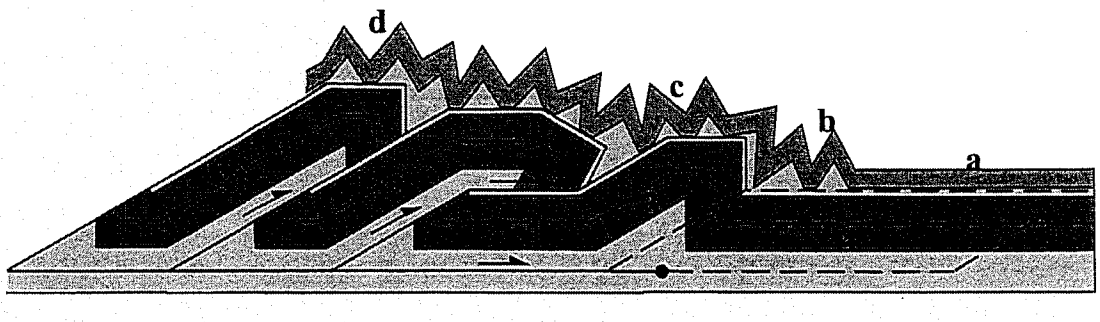

Figure 5. A fold-and-thrust belt is a dynamic structural environment where fractures can form at various times under various conditions. In the standard passive roof duplex model, the thrust belt grows at its leading edge, with the cover rocks deforming over roof thrust. Thrust sheet 1 is the oldest sheet; thrust sheet 4 is the future thrust sheet. Fractures that formed in the foreland of the fold-and-thrust belt in sheet 4 would thus be overprinted by fractures and other mesoscopic structures formed during folding and thrusting. Undeformed cover rocks (a) are initially folded above a roof thrust (b), and subsequently uplifted as during progressive growth of the underlying duplex (c and d). In this model, folds at **d** are the oldest, **b** are the youngest, and rocks at **a** are undeformed.

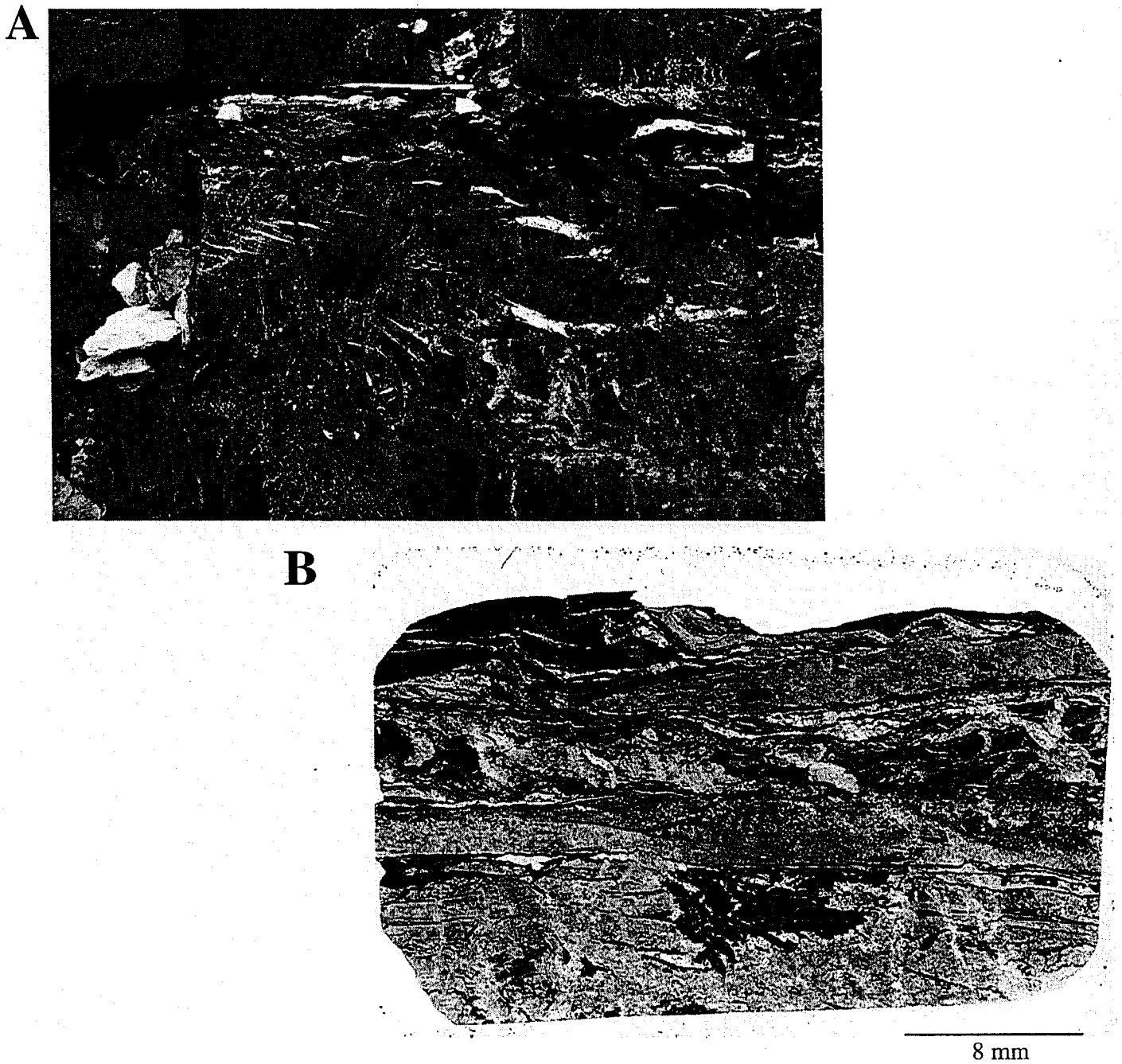

Figure 6. Outcrop photo and photomicrograph of fractures related to early folding (set 2) on the northern limb of a syncline in sandstones of the lowermost PermoTriassic Echooka Formation. A. Three different orientations of fractures appear to be related to folding--2 sets of en echelon extension fractures and a set of bed parallel fractures. B. Bedding parallel fractures of set 2 are highly deformed by subsequent deformation.

A

B

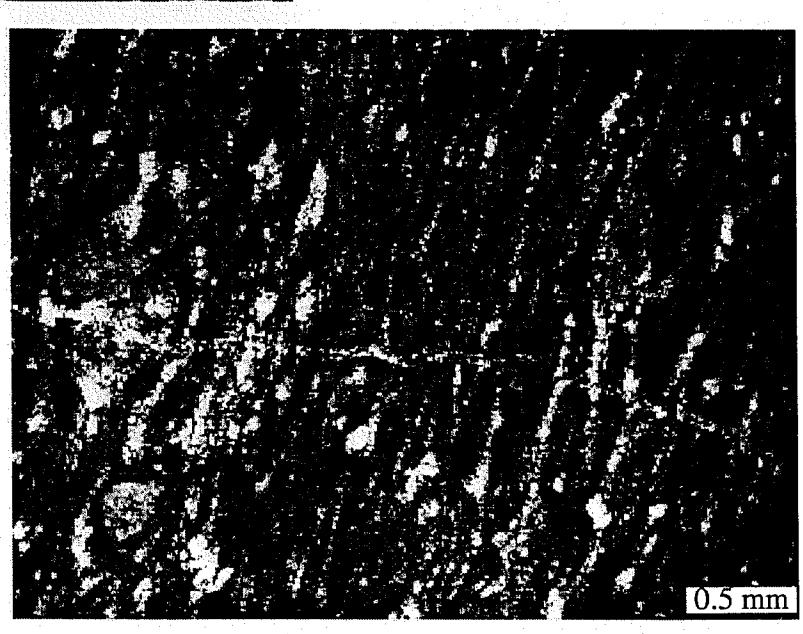

Figure 7. Outcrop photo and photomicrograph illustrating penetrative strain in the hinges of tight detachment folds and its relationship to fracturing. A. Penetrative deformation and distortion of chert lenses in hinge of isoclinal detachment fold. B. Pelloidal grainstone shows evidence of bulk flattening, with post-flattening fractures (set 3)

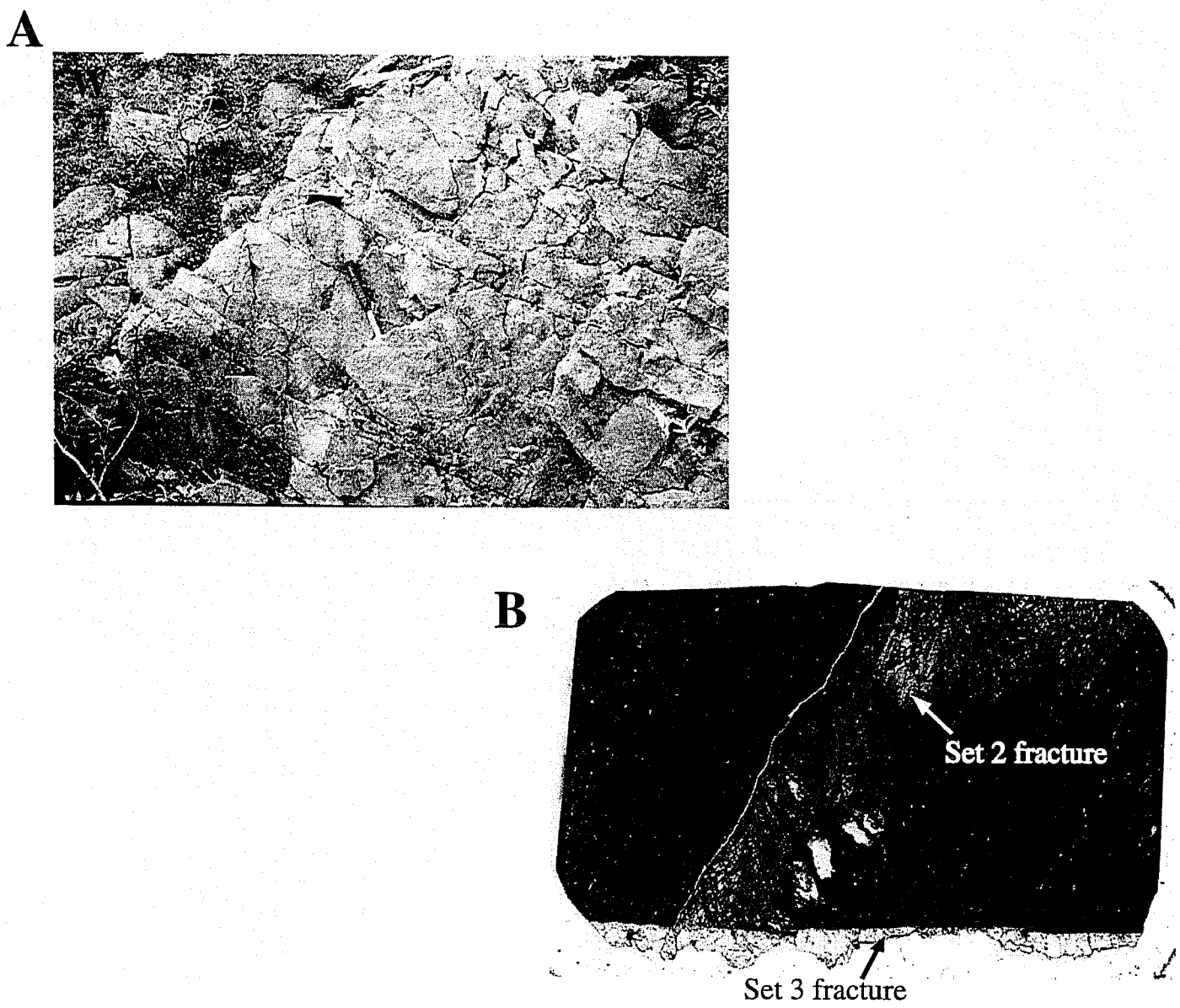

Figure 8. Outcrop and photomicrograph of late to post-fold EW striking fractures. A. Outcrop photo of bedding surface in upper Lisburne Group on southern limb of isoclinal detachment fold showing prominent E-W striking fractures. B. Photomicrograph of STRK01-5E showing two sets of fractures preserved at this location. Highly sheared and deformed early fractures (Set 2) are cross cut by undeformed fractures of set 3. Note the highly flattened host rock.

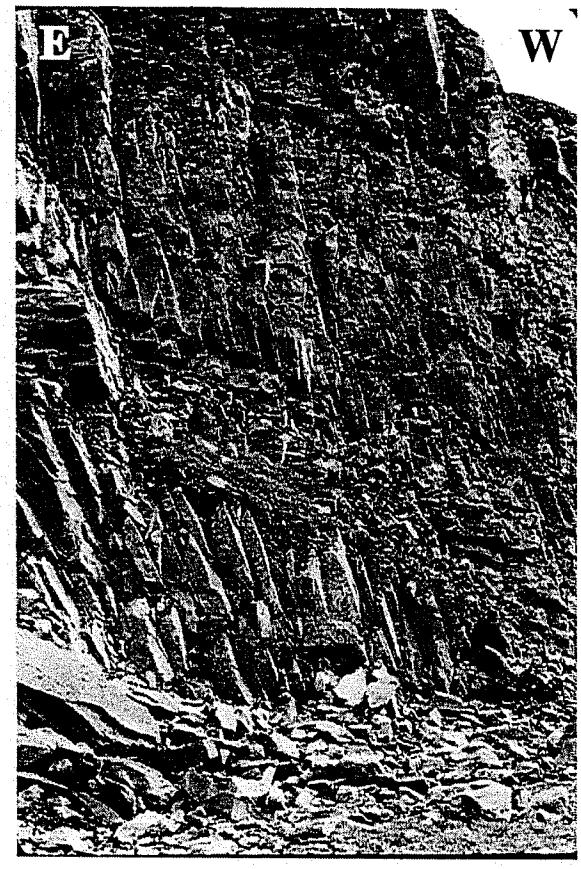

Figure 9. Fractures of set 4 usually strike north-south, are vertically dipping and cross bedding planes. View looking south at upper Lisburne Group carbonates exposed on the south limb of a detachment fold.

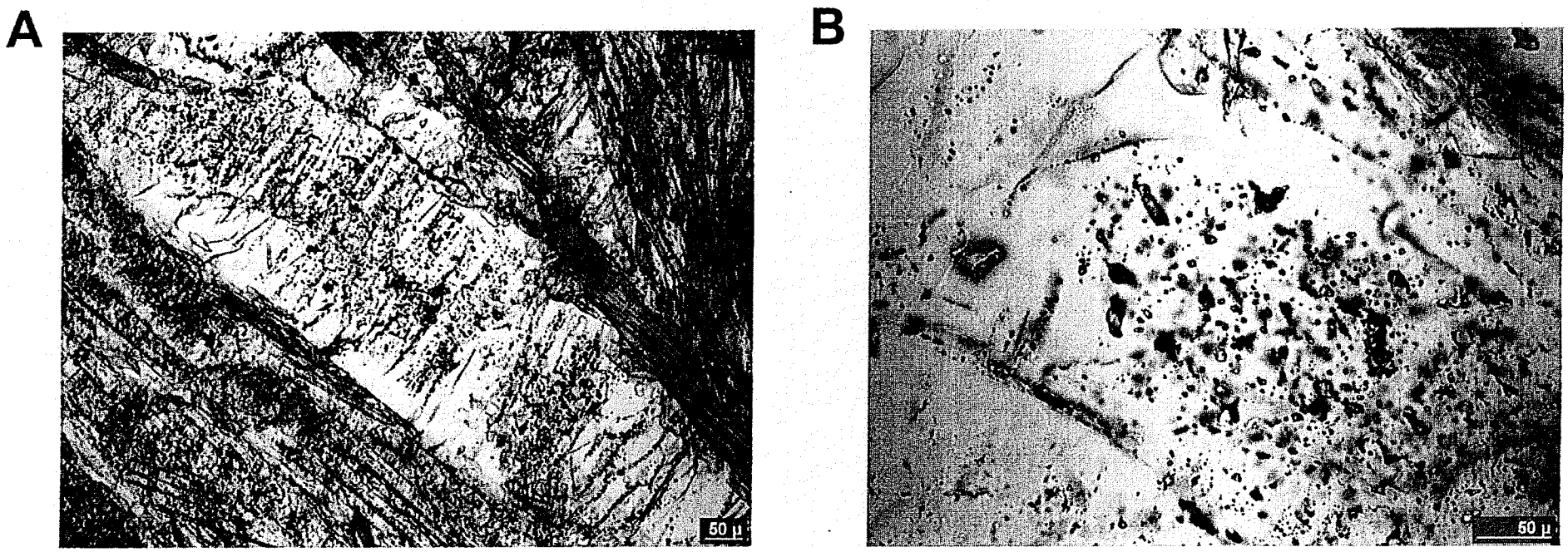

Figure 10. Photomicrographs from STRK01-5A and quartz cement that postdates deformed calcite of fracture set 2. A. Quartz fiber trending from upper left to lower right, and surrounded by twinned calcite, contains many fluid inclusion trails oriented at a high angle with respect to the fiber long axis. The fluid inclusion trails are interpreted to be crack-seal textures resulting from repeated opening and cementing episodes. Following crack opening, precipitation of quartz resulted in trapping of inclusions along the former crack. Healing of the crack produced an incremental addition of cement to the quartz fiber length. This interpretation requires that growth of the fiber be syntectonic. B. Higher magnification view of aqueous two-phase inclusions trapped along crack-seal trails. Quartz fiber axis trends from the upper left to the lower right and crack-seal trails are oriented orthogonal to the fiber axis. Inclusions trapped along the crack-seal trails are considered to be pseudosecondary, and therefore, thermometric analysis of these inclusions provides an indication of conditions during deformation and quartz fiber growth. In contrast, inclusions along trails in the upper center and upper right of the image and trending parallel to the fiber length are interpreted to be secondary. These inclusions, which are younger than the quartz fiber, can provide information about conditions postdating fiber growth. See text for initial results of the inclusion analysis.

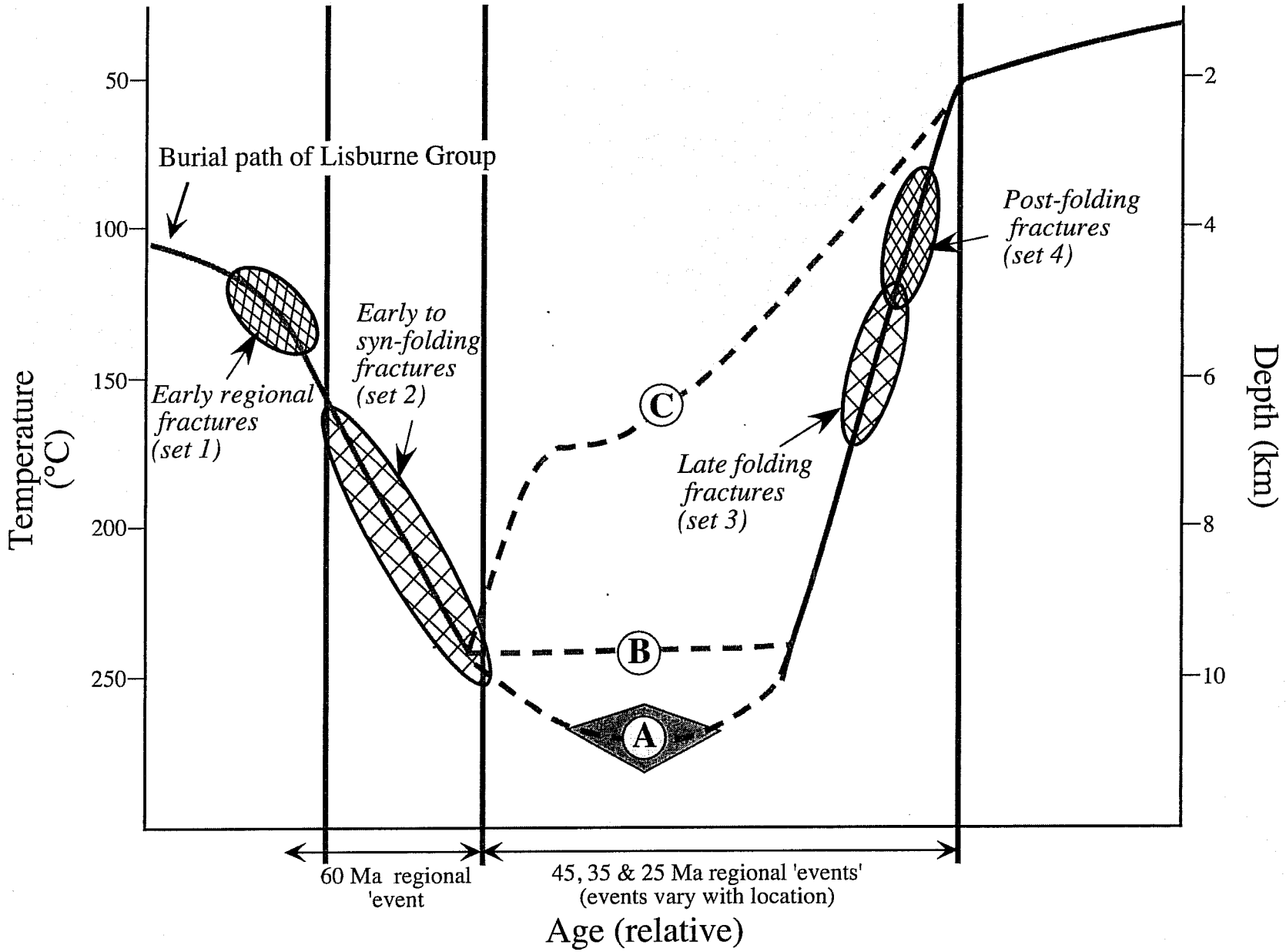

Figure 11. Depth/Temperature/Time graph showing the possible burial and uplift path of the Lisburne Group and lower PermoTriassic Echooka Formation in the Fourth Range. Curves A, B and C discussed in text. Temperature constraints are provided by fluid inclusion measurements from fracture fill (this report), conodont alteration indices (Watts and others, 1995, Rejebian, and others, 1987; Atkinson, 2001), and vitrinite reflectance data (Bird, 1999; Cole and others, 1999). Temperature is converted to depth using a constant geothermal gradient of 25°C/km. Age of deformational events as plotted on the horizontal axis is relative, and based on regional apatite fission track data from various localities in the northeastern Brooks Range (Peapples and others, 1997, O'Sullivan and others, 1995).

Fracture Set	Fracture Orientation	Fracture characteristics	Relative Age: Pre Folding	Early folding	Peak Folding	Late folding	Post Folding
1	NNW-striking	extension fractures; calcite-filled vertically extensive, crossing multiple bedding planes; wide apertures, evenly distributed & pervasive	—		Homogeneous Flattening and Penetrative Strain		
2	parallel and subparallel to fold axis; some parallel to bedding	Both extension and shear fractures; calcite filled; en echelon geometries widely spaced, not evenly distributed & not pervasive		—			
3	parallel and subparallel to fold axis, perpendicular to bedding	filled and unfilled extension fractures; evenly spaced across fold hinges; truncate at bedding surfaces				- - - —	
4	NNW-striking; perpendicular to fold axis	unfilled extension fractures with plumose surface ornamentation; vertically extensive, crossing multiple bedding planes; evenly distributed & pervasive					- —

Table 1. Characteristics, orientation and relative age of fracture sets observed in the Fourth Range.

Sample (unit, lithology)	Fracture sets	Characteristics of fracture and fracture fill	Fluid Inclusion results Inclusion type	mean Th (n)	mean Tmice (n)
STRK01 1D (TrPe, silty shale)	2 and 3	2 generations of fractures: **A.** early quartz-filled fractures (set 2?). Parallel to bedding, highly sheared with shear bands. Contains zones of undeformed, possibly younger quartz	aqueous inclusions, possible primary origin	153 ±11 C (5)	-3.9°±0.6°C (5)
		B. younger, relatively undeformed, narrow, quartz-filled fractures (set 3?) at high angle to bedding.	no inclusions analyzed to date		
STRK01 4D (Ma, fossiliferous pelletal wackestone)	2	Calcite-cemented fracture, parallel to bedding (set 2). Fracture fill is relatively undeformed	Three different inclusion populations (oldest to youngest): •Coeval primary (?) aqueous two-phase and single-phase CH4-rich gas inclusions	223 ±4 C (4)	-3.4°±0.2°C (4)
			• single-phase inclusions, CH4-rich gas		
			• secondary aqueous, clathrate-rich two-phase inclusions	147 ±5.5 C (5)	>5°C (5)
STRK01 5A (Ma, crystalline dolomitic limestone)	2 and 3	2 generations of fractures: **A.** early, calcite-filled fractures (set 2); calcite cement is heavily twinned and deformed; syntectonic quartz with crack-seal and bent fiber textures replaces some calcite cement	2 generations of fluid inclusions in syntectonic quartz replacement: primary aqueous inclusions	194 ±7 C (7)	-2.2°±0.2°C (9)
			secondary inclusions	226 ±7 C (6)	-2.2°±0.1°C (6)
		B. younger, calcite- filled fractures (set 3) at a high angle to set 2 fractures; calcite cement is less deformed and less twinned; some quartz replacement	No inclusions analyzed to date		
STRK01 5E (Ma, fossiliferous wackestone, highly sheared)	2 and 3	2 generations of fractures: **A.** calcite-filled fracture (set 2) at low angle to bedding; calcite cement twinned and sheared during later deformation	•aqueous inclusions of unknown origin	273 ±4.4 C (n=7)	-3.7°±0.3°C (2)
			(Mean Th should be used with caution due to the considerable strain in set 2 fractures)		
		B. partially calcite-filled fractures (set 3) at high angle to set 2; has untwinned, undeformed calcite cement.	Thermometric analysis not successful due to stretching and leaking of inclusions. This behavior suggests, however, that the inclusions formed at <80°C.		

Table 2. Results of fluid inclusion analyses of fracture fill from selected samples of Carboniferous Lisburne Group and PermoTriassic Echooka Formation from the Fourth Range. Abbreviations: Th: aqueous homogenization temperature; Tmice: final ice melting temperature.

Fracture distribution and flow modeling in folded Lisburne Group

by Thang Din Bui and J. L. Jensen, Texas A&M University, College Station, Texas 77843-3116, and J. Brinton and C. L. Hanks, Geophysical Institute, University of Alaska, Fairbanks, Alaska, 99775-7320

Abstract

In exposed detachment-folded Lisburne Group carbonates, field evidence and statistical analysis suggest that a significant population of fractures formed either late during folding or after folding.

Both pre-fold fractures and penetrative strain associated with peak folding are overprinted by late-fold and post-fold fractures. The late-fold fractures strike EW parallel to the fold axes, are perpendicular to bedding, are commonly only partially filled with cement, and generally terminate at bedding planes. These and the earlier structures are consistently overprinted by pervasive late NS-striking extension fractures. These later fractures strike perpendicular to the fold axes, and are vertically extensive, evenly spaced, and unfilled. Both the late-fold and post-fold fracture sets have similar average and median spacing.

Statistical analysis of fold interlimb angle and fracture spacing indicates that, as the folds tighten, the spacing of both the EW- and NS-striking fracture sets increases by a factor of two or three and becomes slightly more variable. This behavior is opposite from that expected if the fractures were closely related to folding. It suggests that the two sets are similar to each other and are only weakly affected by the folding.

This weak genetic relationship between folding and formation of the most obvious and open fractures serves as an important example with major consequences for reservoir modelling. Complex genetic and timing relationships between fractures and folds may result in several fracture sets, each having different characteristics (e.g., size, amount of fill, and termination type). Unless recognized, genetically disparate fractures may be combined into one or a few sets to produce a reservoir model with fracture properties that do not apply to any of the sets. This could result in inappropriate wellbore placement or inaccurate productivity and recovery estimates.

Introduction

Understanding and quantifying the fracture distribution can be critical for the exploitation of a fractured reservoir. Unfortunately, surveying and measuring fractures in the subsurface is usually difficult and very costly. Examination of fractures in outcrops of the equivalent formation may be a useful means of studying the fracture properties and their distribution under the influence of different parameters. This research examines the fracture distributions within detachment-folded Carboniferous Lisburne Group carbonates, exposed in northeastern Brooks Range of Alaska.

The Carboniferous Lisburne Group in the northeastern Brooks Range is the closest exposed stratigraphic equivalent to the reservoir of the Lisburne oil field, located approximately 120 km to the northwest (Figure 1). A thrust front separates the subsurface Lisburne field from the Lisburne Group exposed in the northeastern Brook Range fold and thrust belt (Hanks *et al.*, 1997). The Lisburne Group has deformed primarily by detachment folding and thrusting

throughout most of the northeastern Brook Range (Homza and Wallace, 1997). In the Fourth Range and the Shublik Mountains, the Lisburne Group deformed into detachment folds over regional anticlinora (Figure 2). Detailed structural and stratigraphic aspects of the Lisburne Group and the northeastern Brooks Range are discussed by Homza and Wallace (1997), Wallace and Hanks (1990), and Hanks *et al.* (1997). The exposed detachment folds in this area serve as a target of the fracture study in this work.

Numerous studies have investigated the relationship between fracture properties and parameters related to the mechanical-stratigraphy parameters. Many suggest that the average fracture spacing is directly proportional to the formation bed thickness (McQuillan, 1973; Ladeira and Price, 1981; Huang and Angelier, 1989; Narr and Suppe, 1991; Ji and Saruwatari, 1998; Bai and Pollard, 2000). Fracture spacing also appears to be a function of rheology, with more competent rocks having more closely spaced fractures (Huang and Angelier, 1989). McQuillan (1973), for example, investigated the Asmari limestone outcrops over an extensive area of the Zagros Mountains and proposed that fracture density has an inverse logarithmic relation to bed thickness but is independent of structural setting.

Others have investigated the effect of the lithology on the fracture distribution. Hanks *et al.* (1997) showed that lithology is the primary controlling factor on fracture properties and characteristics in relatively undeformed sections of the upper Lisburne Group in the eastern Sadlerochit Mountains. In these undeformed carbonates, grainstones are the least fractured, with wider and more through-going individual fractures. Dolomitic mudstones are the most fractured, but have narrower fractures of limited vertical extent that generally terminate at bed boundaries. Homza and Wallace (1997) discussed the effect of the contrast between layers on the fracture distribution and termination.

Some other researchers have investigated the effects of the structural setting on the fracture distribution. Murray (1969) assumed that fracture aperture increased as the strain or the degree of the curvature of the bed increased. Several studies (Nelson and Serra, 1993; Lisle, 1994; Jamison, 1997; Henning, 2000) suggest that fracture density increases with increasing bed curvature. Since the fold can be developed under different scenarios, the fracture distribution within one fold can be highly variable. For example, Jamison (1997) suggested that the highest fracture density could be found in the mid-limb region instead of in the region of greatest curvature (the hinge).

Thus, the studies of the fracture distribution as a function of mechanical stratigraphy in folded bedded rocks have generally focused on 3 major parameters: bed thickness, degree of deformation, and lithology, including the contrast between layers in layered formations. The observations are that the average fracture spacing is linearly proportional to bed thickness, fracturing is enhancing by the degree of strata bending, and lithology controls the difference in fracture spacing in beds of equal thickness.

In contrast to these observations, our analysis of fracture data from detachment-folded Lisburne Group Carbonates in the northeastern Brooks Range, suggests that:

1. Stratigraphic bed thickness does not have a consistent effect on fracture spacing.
2. Fracture density does not increase with increasing curvature.

These observations and other field observations indicate a complex relationship between fracture and folds. Our observations suggest that bedded rocks in folded systems may experience multiple fracture generation episodes before, during and after folding. Complex genetic and timing relationships between fractures and folds may result in several fracture sets, each having different characteristics (e.g., size, amount of fill, and termination type). Unless recognized, the

genetically distinct fractures may be combined into one or a few sets to produce a reservoir model with fracture properties which do not apply to any of the sets.

Fracture data

A total 464 fractures were collected from 3 places: Fourth Range, North Shublik and South Shublik Mountains (Figures 1 and 2). The data represented 25 outcrop locations, from which 19 are on the limb of a fold, 2 are on synclinal hinges, and 4 are on anticline hinges, resulting in a total of 64 fracture sets. Outcrops to be studied were chosen based on proximity to or location on a detachment fold and accessibility to measurable fractures. Exposed bedding planes were chosen instead of outcrop face exposures whenever available, due to the greater ease and accuracy of measurement.

At each outcrop, general geologic data were collected, including bed thickness, orientation and lithology. Fracture data were collected using a "scan-line" technique. At each location, a nylon tape measure was laid out along a line perpendicular to the fracture set of interest. Each fracture encountered along the scan line was then counted and described and its distance from the beginning of the measuring tape was recorded. The following aspects of each fracture were described: the orientation (strike and dip); fracture height (the linear measurement of the fracture perpendicular to bedding); fracture length/depth (the linear measurement of the fracture parallel to bedding); and fracture aperture (as measured perpendicular to the fracture walls).

Lithologies sampled ranged from carbonate mudstone to grainstone with 57 fractures associated with mudstone, 87 with wackestone, 286 with packstone and 166 with grainstone. Stratigraphic bed thicknesses ranged from 0.1 m to 4 m. The interlimb angle of the surveyed folds ranged from 90° to 160°.

Data observations

General observations are as follows:

Orientation. Two major fracture orientations can be distinguished throughout the area of study. The fractures in the first set strike EW parallel to the fold axes and are mostly perpendicular to bedding. The later, NS-striking fractures are perpendicular to the fold axes, vertically extensive, and more evenly spaced. Figure 3 illustrates the range in fracture strike.

Filling. The majority of the fractures are partially filled with calcite, the rest are unfilled. The number of unfilled fractures varies depending on the fracture orientation and location on the fold. Generally, NS fractures are less filled than the EW fractures.

Fracture termination. In both hinge and limb zones, the fractures terminate primarily at bedding planes, and less frequently terminate at other fractures. In many locations, the age relationship between the two fracture sets (as determined by abutment patterns) is not clear. In general, the NS fractures are usually more through-going than the EW fractures.

As these observations show, the two fracture sets observed on detachment-folded Lisburne Group carbonates have distinctive differences in orientation, amount of fill and the nature of their termination. These differences could have a significant impact on the role of each fracture set in fluid flow within the reservoir.

Statistical analysis

At first glance, the NS and EW fracture sets have very similar spacing statistics: averages, medians, and standard deviations (Table 1). A plot (Figure 4) of fracture spacing versus bed thickness shows that, as bed thickness increases, fracture spacing and its variability in both sets increases. A plot (Figure 5) of fracture spacing versus interlimb angle shows a different trend: in each set, the average fracture spacing decreases and the spacing becomes more variable with decreasing interlimb angle. Thus, both sets appear to have similar behavior with respect to the effects of bed thickness and tightness of the fold. On closer inspection, however, there are differences.

In subsequent statistical analysis, the fracture spacings were divided into subsets according to the values of bed thickness and interlimb angle (Figures 6 and 7). The thickness threshold was 2.0 m and the interlimb angle threshold was 105°. The criterion for the thresholds was that they maximized the differences between the resulting subsets. Along with graphical comparison of the different subsets, we applied several statistical tests to quantify and to assess the relationships between fracture spacing and mechanical stratigraphical parameters. We used the t-test for the average fracture spacing, the Kolmogorov-Smirnov (KS) test for the general difference between distributions, and a bootstrapping technique for the median (Neave and Worthington, 1988; Mooney and Dulal, 1995).

Spacing, bed thickness, and interlimb angle. A box plot of fracture spacing for the interlimb angle and bed thickness subsets (Figure 6), shows that the fracture spacing is not affected by the value of bed thickness as it seems to be on Figure 4. Within each range of interlimb angle, fracture spacing remains relatively unchanged for variations in bed thickness. This effect contrasts with the often-reported relationship between fracture spacing and bed thickness (McQuillan, 1973; Ladeira and Price, 1981; Huang and Angelier, 1989; Narr and Suppe, 1991; Ji and Saruwatari, 1998; Bai and Pollard, 2000). On Figure 6, we also note that the fracture spacing increases for both subsets of bed thickness as the interlimb angle decreases. This relationship is contrary to the expectation that fracturing would be enhanced by folding, i.e., fracture spacing is expected to be smaller for the tighter folds or small interlimb angle (Nelson and Serra, 1993; Lisle, 1994; Jamison, 1997; Henning, 2000). The observed relationship between fracture spacing and interlimb angle in these detachment folds suggests that the fractures may not be closely or wholly related to the folding. At the 95% confidence level, all three statistical tests confirmed what we observed graphically, i.e.:

- Bed thickness does not have a significant effect on the fracture spacing distribution.
- As interlimb angle decreases, the fracture spacing increases and becomes more variable.

Spacing, interlimb angle, and orientation. As already noted, the results of comparing the two fracture sets indicated that both sets are statistically similar. When plotted against interlimb angle, fracture spacing in both fracture sets appears to behave similarly (Figure 7). Fracture spacing in both the NS and EW-striking fracture sets increases and becomes more variable as the interlimb angle decreases. A t-test confirms this. The KS and median test, however, reveal that the distribution and the median of the fracture spacing are significantly different for the two fracture orientations with high interlimb angle. As the fold tightens, the difference in fracture spacing between the two fracture sets decreases.

Spacing and structural position. The position of the sample location on the fold also has an effect on the fracture spacing distributions. Most of the differences in spacing distribution noted earlier are due to the fractures on the limbs of tight folds, with small interlimb angles (Figure 8). Fracture spacings for EW-striking fractures on the limbs of open folds, with large interlimb angles, are smaller than for the other sets (Figure 9), as also noted by Jamison (1997). This suggests that the local structural setting plays a role in the fracture spacing.

Fracture size analysis. The height distributions of the NS and EW-striking fracture sets are significantly different (Table 2). In particular,

- The average height distribution of the NS-striking set is twice the average of the EW-striking and the median height distribution of the NS-striking fracture set is 76% greater than the that of the EW set
- The 90^{th} percentile of the height distribution for the NS set is 114% greater than the 90^{th} percentile of the EW set.

These results agree with the visual assessment of fracture characteristics noted earlier. All statistical tests indicate significant height differences between the NS and EW sets.

The length distributions of NS and EW fractures are also significantly different (Table 3). While the median length distribution of the NS fractures is only 50% greater than the median length distribution of the EW fractures, the averages differ by 160%, and the 90^{th} percentiles differ by 233%. The average length of the largest 10% of NS fractures is 3.2 times the corresponding EW value.

Since the flow characteristics of fractured reservoirs can be controlled by a few large fractures, these differences in height and length between fracture sets can play an important role in the reservoir flow behavior.

Implications for reservoir performance

Based strictly on spacing, one could assume that the fracture flow properties for the EW and NS-striking fracture sets would be similar. For example, if one only had borehole observations of fracture spacing, these sets would appear similar. The differences in termination, size, and fill observed between these sets, however, could lead to significant differences in connectivity and wellbore placement. This was shown in a study by Karpov (2001), who modelled flow performance of the relatively undeformed Lisburne Group in the eastern Sadlerochit Mountains (Figure 1).

For the detachment-fold fractures studied here, it is clear that the larger NS fractures have a greater probability of interconnection than the EW set. However, the NS fracture density is sufficiently small that the NS connectivity could be also affected by the permeability of the EW fracture set. In Karpov's (2001) study, NS permeability dropped by half an order of magnitude for each order of magnitude reduction in EW fracture permeability. In this example, however, conductance in the EW direction was found to be less sensitive to the NS fracture properties.

The nature of termination of the EW and NS striking fractures also is expected to influence flow properties. In undeformed Lisburne, termination of the EW fractures on the NS set changed the dependence of the NS connectivity on the smaller fractures in the system. Assuming no termination (i.e., simultaneous development of both sets), the NS connectivity depended only upon the largest 10% of these fractures. Allowing for termination of EW fractures on the NS fractures increased that proportion to the largest 45% of the fractures. With termination, EW

connectivity dropped to zero. Thus, termination of EW fractures reduced connectivity in both the EW and NS directions.

Karpov's (2001) study showed that, due to the differences in size of the two fracture sets, orienting the wellbore to intersect the maximum number of EW fractures gives disappointing results; termination of the EW set against the NS fracture set changed the optimal wellbore orientation by 30° and reduced the area of matrix contacted by 50%. It is also probable that the optimum orientation for horizontal wellbores in detachment-folded Lisburne Group carbonates would be affected by fracture size and relationship.

Conclusions

Two distinct fracture sets were observed in detachment-folded examples of the Carboniferous Lisburne Group carbonates of northeastern Alaska: an EW-striking set that formed late during folding and a post-folding NS-striking set. Statistical analysis of outcrop fracture data shows that bed thickness does not have significant effect on the fracture spacing distribution of either set. Fracture density is only weakly related to the fold geometry, with fracture density greater on the limbs than in the hinge area. These results contradict the results of many other studies.

The weak effect of folding on the fracture spacing of each set suggests that both fracture sets are only weakly related to the folding process. This and the above observations suggest that detachment fold geometry cannot always be used as a reliable predictive tool for fracture distribution within the Lisburne Group.

This study clearly demonstrates that the local geological setting plays an important role in fracture spacing distribution. Determining the characteristics of the fractures, the relative age of the different fracture sets, and the relationship between the fractures and their local geologic setting can be an important factor in reservoir performance.

Acknowledgements

The data used in this paper were collected as part of a UAF M.S. geology thesis by J. Brinton. The work was supported by DOE contract DE-AC26-98BC15102. An expanded version of this work has been reported in SPE paper 76754, presented at the May, 2002 Western Regional Meeting in Anchorage. We wish to thank Golder & Associates for donation of Fracman software for this project.

References

Bai, T. and Pollard, D.D, 2000: "Fracture Spacing in Layered Rocks: A New Explanation Based on the Stress Transition," *J. of Structural Geology,* **22**, 43.

Hanks, C.L. *et al.*, 1997: "Lithologic and Structural Controls on Natural Fracture Distribution and Behavior Within the Lisburne Group, Northeastern Brooks Range and North Slope Subsurface, Alaska," *AAPG Bulletin,* **81**, No 10, 1700.

Henning, P.H., 2000: "Combining Outcrop Data and Three-Dimensional Structural Models to Characterize Fractured Reservoirs: An Example from Wyoming," *AAPG Bulletin*, **84**, No 6, 830.

Homza, T.X. and Wallace, W.K., 1997: "Detachment Folds With Fixed Hinges and Variable Detachment Depth, Northeastern Brooks Range, Alaska," *J. Struct. Geol.* **19**, 1700.

Huang, Q. and Angelier, J., 1989: "Fracture Spacing and its Relation to Bed Thickness," *Geol. Mag.*, **126**, 355.

Jamison, W. R., 1997: "Quantitative Evaluation of Fractures on Monshood Anticline, a Detachment Fold in the Foothills of Western Canada," *AAPG Bulletin,* **81**, No 7, 1110.

Ji, S. and Saruwatari, K., 1998: "A Revised Model for the Relationship Between Joint Spacing and Layer Thickness," *J. of Structural Geology,* **20**, 1495.

Karpov, V.A, 2001: Lisburne Formation Fracture Characterization and Flow Modeling, MS Thesis, Texas A&M U.

Ladeira, F.L. and Price, N.J., 1981: "Relationship between Fracture Spacing and Bed Thickness," *J. of Struct. Geol.,* **3**, 179.

Lisle, R.J., 1994: "Detection of Zones of Abnormal Strains in Structures Using Gausian Curvature Analysis," *AAPG Bulletin,* **78**, 1811.

McQuillan, H., 1973: "Small-Scale Fracture Density in Asmari Formation of Southwest Iran and its Relation to Bed Thickness and Structural Setting," *AAPG Bulletin,* **57**, 2367.

Mooney, C.Z., and Dulal, R.D., 1995: *Bootstrapping - A nonparametric approach to statistical inference*, SAGE publications, CA.

Murrays, G.H.Jr., 1968: "Quantitative Fracture Study – Spanish Pool, Mckenzie Co., North Dakota," *AAPG Bulletin,* **52**, 57.

Narr, W. and Suppe, J., 1991: "Joint Spacing in Sedimentary Rocks," *J. of Structural Geology,* **13**, 1037.

Neave, H. R. and Worthington, P. L. 1998: *Distribution Free Tests*, Unwin Hyman Ltd., London, UK.

Nelson, R.A. and Serra, S., 1993: "Vertical and Lateral Variations in Fracture Spacing in Folded Carbonate Sections and its Relation to Locating Horizontal Wells," *Proc.* Canadian SPE/CIM/CANMET International Conference on Recent Advances in Horizontal Well Applications, Canadian Society of Petroleum Engineers, Paper HWC94-41, 10.

Wallace, W.K. and Hanks, C.L., 1990: "Structural Provinces of the Northeastern Brooks Range, Arctic National Wildlife Refuge, Alaska," *AAPG Bulletin*, **74**, No 7, 1100.

Wu, H. and Pollard, D.D., 1995: "An Experimental Study of the Relationship Between Joint Spacing and Layer Thickness," *J. of Structural Geology,* **17**, 887.

TABLE 1 – FRACTURE SPACING SUMMARY

	EW fracture	NS fracture	Difference, %
Number of fractures	176	215	-
Average, m	0.26	0.28	6.7
Median, m	0.14	0.15	7.1
Standard deviation, m	0.455	0.370	-18.6
90th percentile, m	0.45	0.65	44.4

TABLE 2 – FRACTURE HEIGHT SUMMARY

	EW fracture	NS fracture	Difference, %
Number of fractures	203	250	-
Average, m	0.595	1.165	96
Median, m	0.34	0.6	76
Standard deviation, m	0.708	1.639	131
90th percentile, m	1.4	3.0	114

TABLE 3 – FRACTURE LENGTH SUMMARY

	EW fracture	NS fracture	Difference, %
Number of fractures	192	247	-
Average spacing, m	0.327	0.853	161
Median, m	0.2	0.3	50
Standard deviation, m	0.382	1.848	383
90th percentile, m	0.6	2.0	233

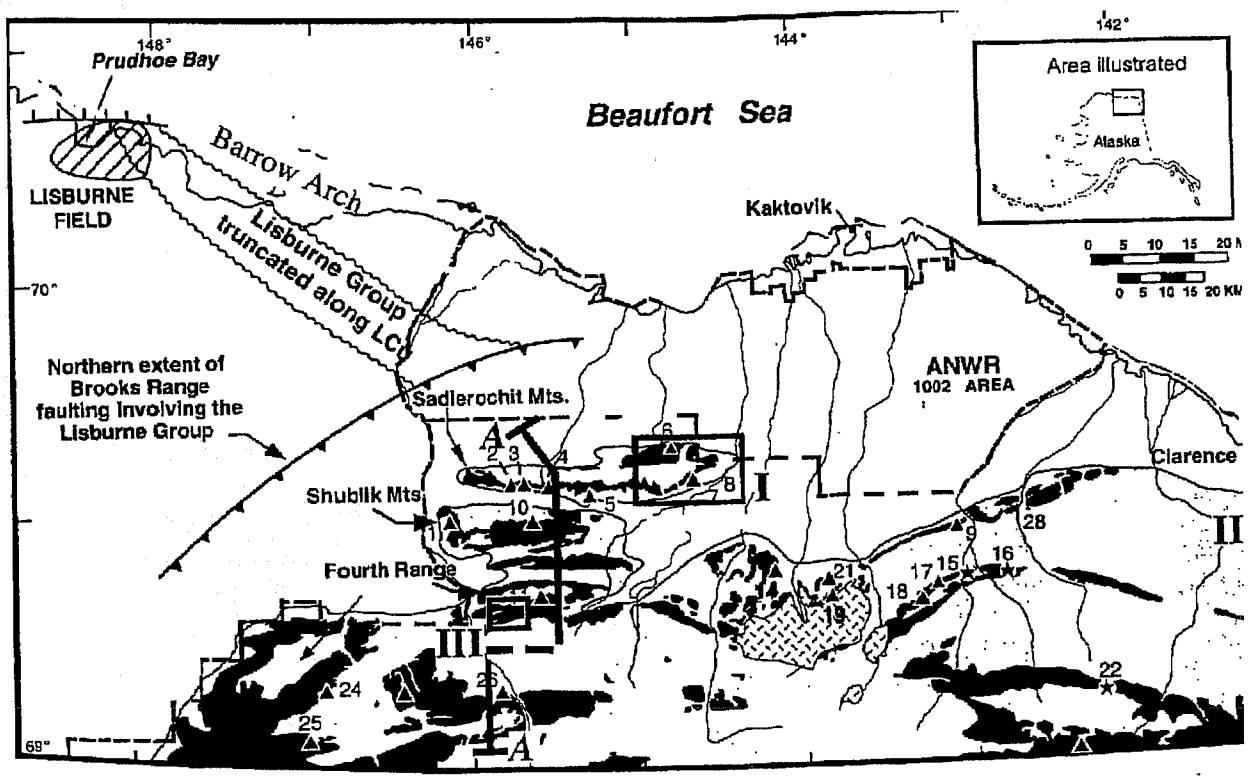

Figure 1 - Generalized geologic map of the northern part of the northeastern Brooks Range (from Hanks et al., 1997)

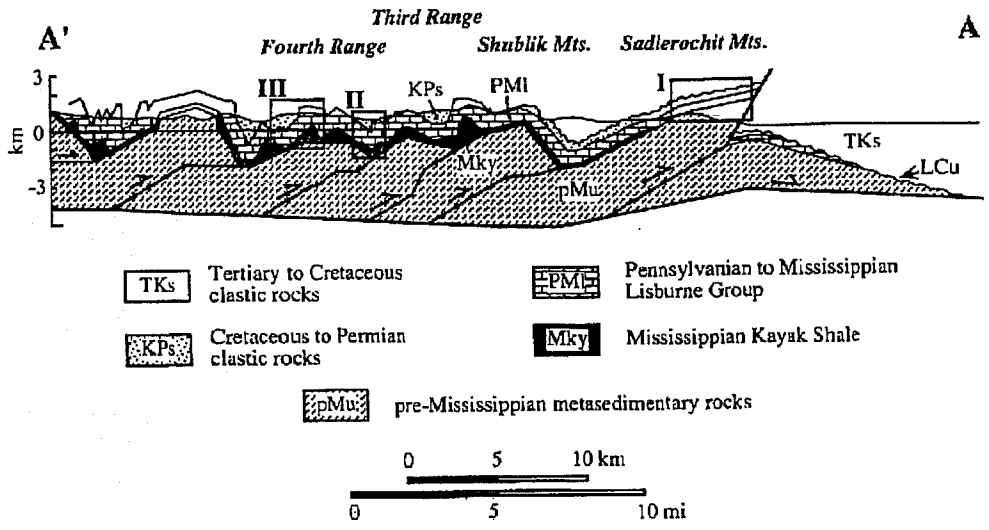

Figure 2 - Balanced cross section through the western part of the northeastern Brooks Range. (from Hanks et al., 1997)

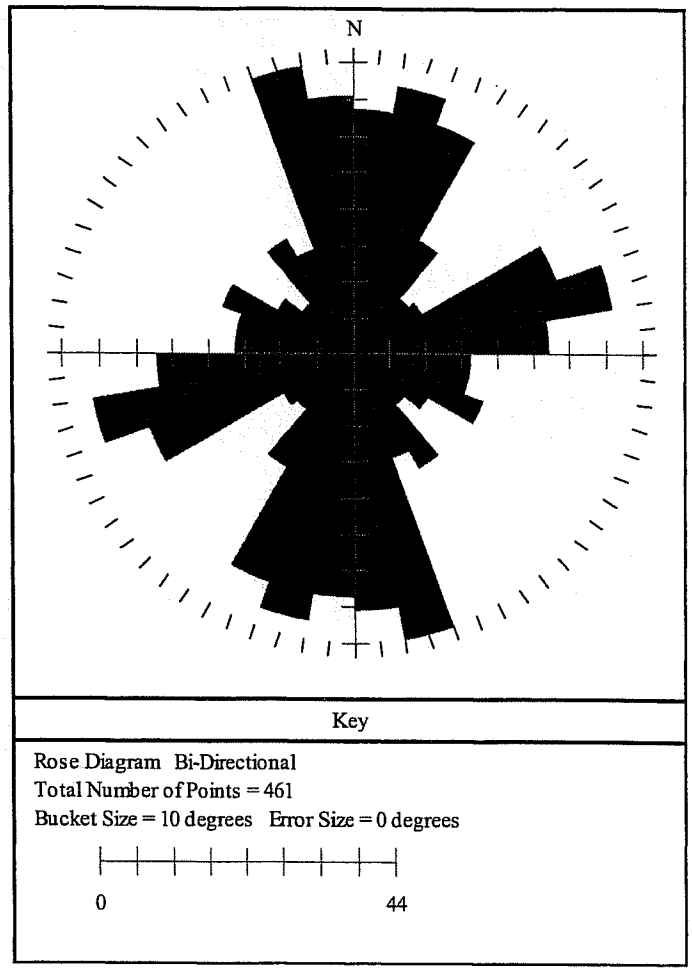

Figure 3 - Fracture orientation for all fracture data shows two major directions: East-West and North-South striking.

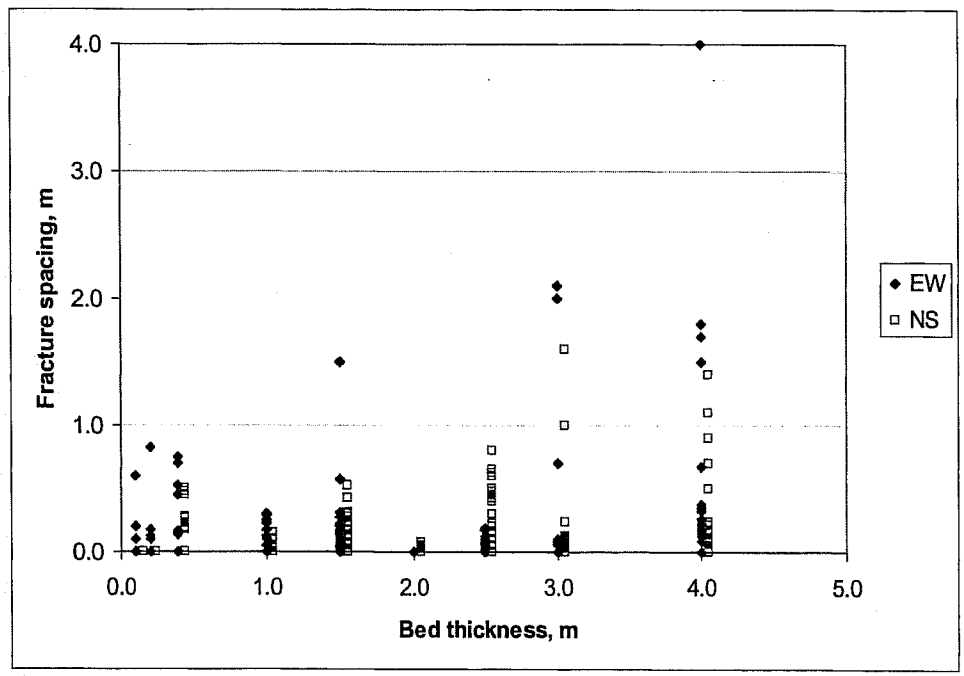

Figure 4 - Fracture spacing versus bed thickness for two orientations: the fracture spacing increases with the bed thickness.

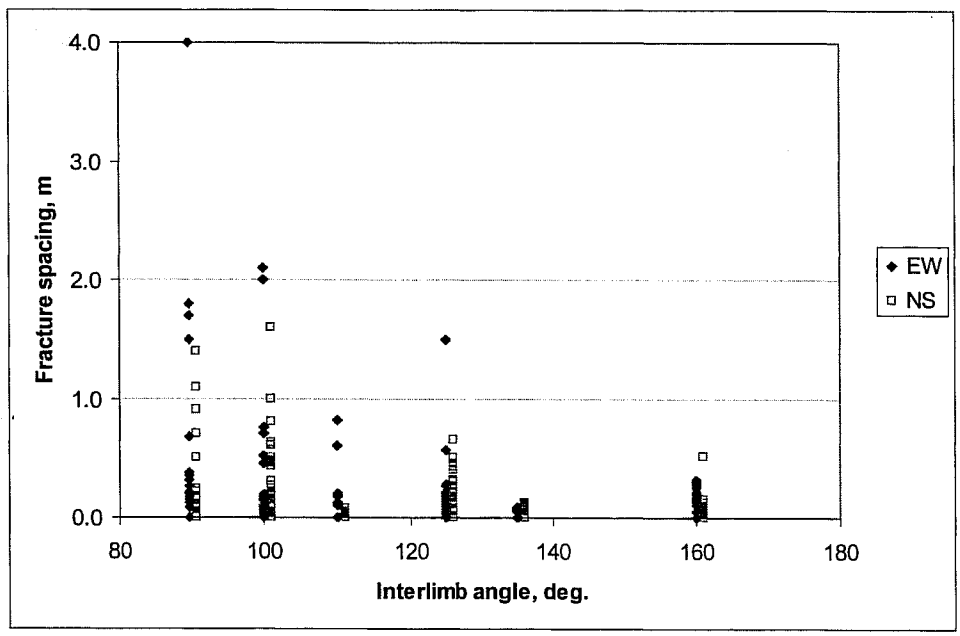

Figure 5 - Fracture spacing and interlimb angle for two orientations. As interlimb angle decreases, fracture spacing and its variability increases.

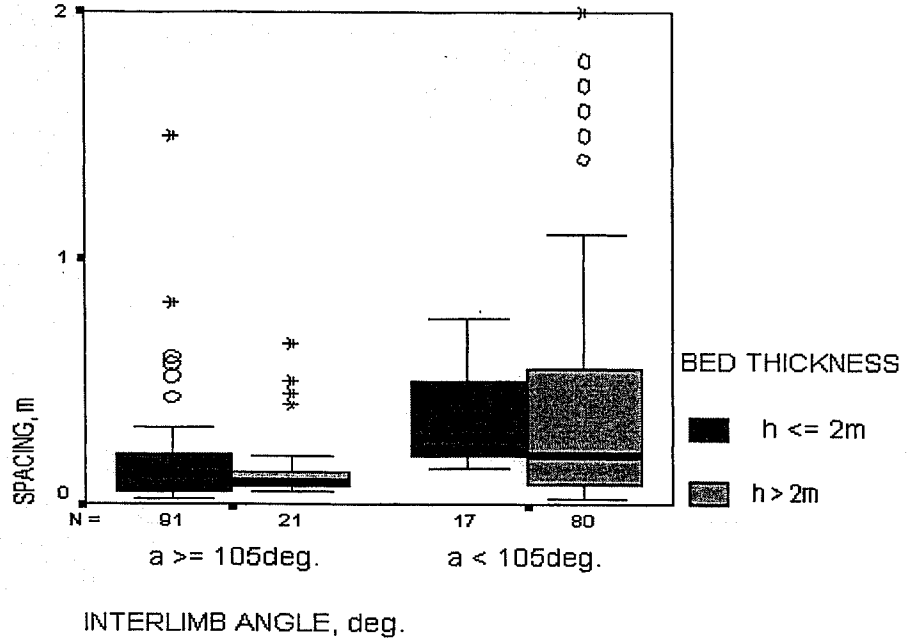

Figure 6 - Box plot of fracture spacing for two groups of interlimb angle. Fracture spacing and its variability increase as the interlimb angle decreases for both groups of bed thickness.

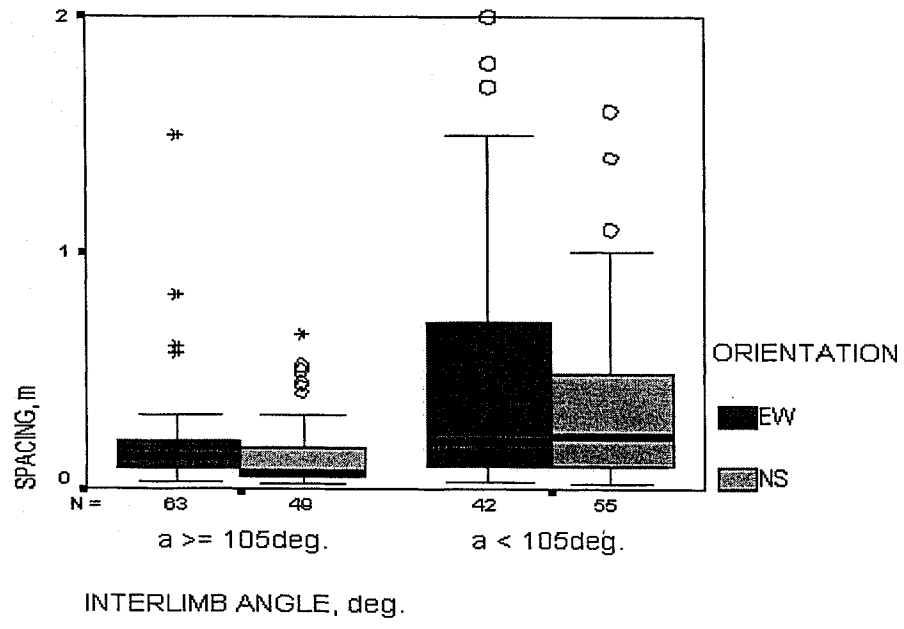

Figure 7 - Box plot of fracture spacing for different interlimb angles and orientations. As folding increases, fracture spacing and its variability increases in both directions.

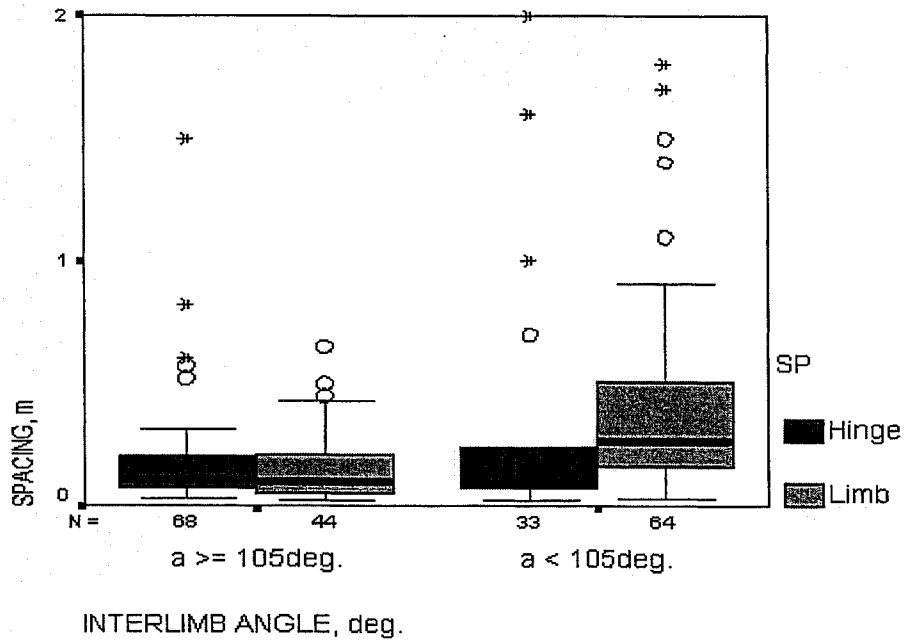

Figure 8 - Box plot of fracture spacing for different interlimb angle and structural position. As folding increases, fracture spacing and its variability increases in both limb and hinge, especially in limb.

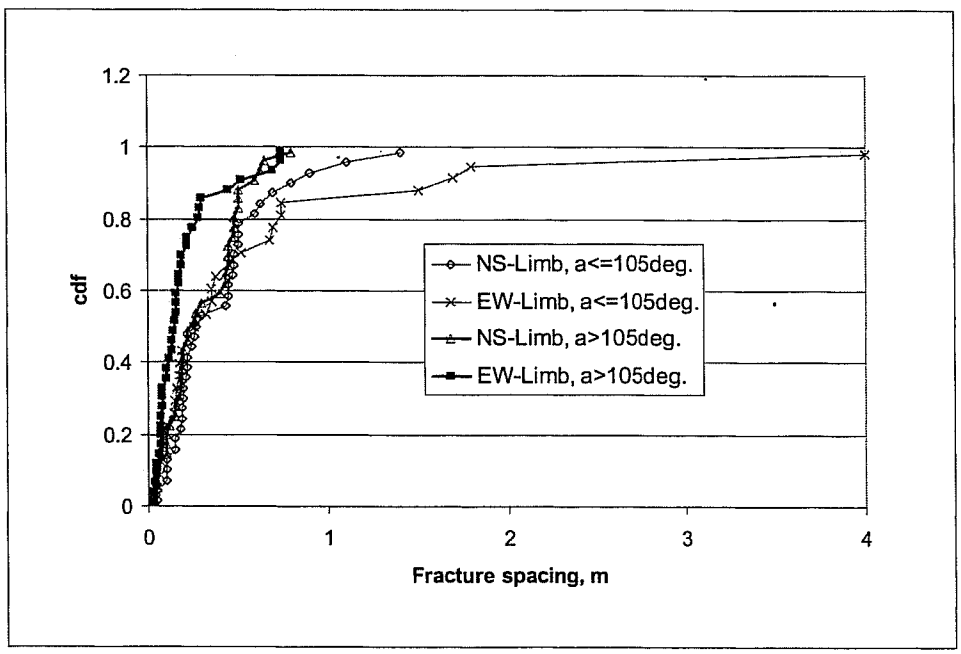

Figure 9 - Fracture spacing for two orientations in limbs of different folds. The fractures in folds with large interlimb angle are smaller than the others.